Functional and mechanistic analysis of microtubule network architecture in pancreatic beta cells

By

Kai Milton Bracey

Dissertation

Submitted to the Faculty of the

Graduate School of Vanderbilt University

in partial fulfillment of the requirements

for the degree of

DOCTOR OF PHILOSOPHY

In

Cell and Developmental Biology

May 12th, 2023

Nashville Tennessee

Approved:

David Miller III, Ph.D.

Irina Kaverina, Ph.D.

Marija Zanic Ph.D.

Maureen Gannon, Ph.D.

Wenbiao Chen, Ph.D.

To my wife, Courtney, for her love, patience, support, and faith

To my mom, Sonia, for always encouraging me, listening, and supporting me

To my dad, James, for always pushing me towards greatness

To my brother, Chazz, for always making me laugh even when times were dark

Acknowledgements

Thank you to my advisor, Irina Kaverina, for her support and guidance both for her support and guidance both in this body of work and in my personal development as a scientist. I would also like to thank my committee members: David Miller III, Marija Zanic, Maureen Gannon, and Wenbiao Chen, their advice, support, and patience.

This work would not have been possible without advice and help from all members of the Kaverina lab. Special thank you to Kung-Hsien Ho for training me when I first joined the lab. He inspired me to work hard and play harder. To Hamida for all her support, her eagerness to help out with anything, and her always taking care of my messes. To the “TIRF Princess” Maggie Fye since you joined the lab you have been my best friend and every moment with you no matter how mindless of a task is always better.

I am grateful to so many members of the Department of Cell and Developmental Biology, whom have offered advice and companionship. Notably, I would like to thank Anuj (AJ) for always bailing me out of equipment and technical problems, and Mark Wozniak for his tech savvy. Thank you to Lorie Franklin for all her administrative work and reminders of things that I needed to do (or things that were past due).

Research reported in this publication is from the National Institutes of health, (Grant # F31 DK122650).

I wish to thank IMSD, and all the friends I have made. Even if it was just a slice of pizza and a backyard somewhere thank you. To Roger and Linda, I will always be indebted to you for all your advice and your faith in me.

I would be remised if I did not thank the Fisk-Vanderbilt Bridge Program Masters to PhD. Especially my Masters advisor Brian Nelms, who really made science so much fun and made me want to continue down this path.

My close knit friends: The guys Jamal (JPEG), Isaiah (SPVIII), Jon, Nathan (Natedawgnash), Daniel(The_MLG_Junior), Vincent (Vinsanity), Logan, Josh N., Isom, Tolu, Sean, Stephen, Ryan, and of course my first friend in Nashville Bryan. We spent countless nights together, raiding, looting, clutching out W’s in a number of games, working out, playing basketball. You guys were always down to let off steam when things weren’t going our way. The gals: Kellie, Keyada, Maggie, Morgan, Mabel, Jasmine, Leah, Khamani, Breanna, Geena, Sabrina for being the most supportive group of women a guy like me could ask for.

My parents, words can’t explain how much I appreciate everything you have done for me over the course of my life.

My brother for being the best man I know. And even though you’re younger than me you still inspire me.

My squad for life Josh H., Fatima, and Courtney. We been through so much together and I look forward to the next chapter of life with you all. #WDN

Table of Contents

List of Tables

List of Figures

Chapter 1

Introduction

Cell structure and function are intricately linked. In biology, "structure" refers to the physical arrangement or organization of a biological entity, such as a cell, tissue, organ, or organism. For example, the structure of a protein molecule refers to the specific arrangement of its amino acid components. The structure of a leaf refers to the arrangement of its veins, stomata, and other cellular components.

"Function" refers to the specific role or purpose that a biological structure plays within an organism or system. For example, the function of the heart is to pump blood throughout the body, while the function of chloroplasts is to carry out photosynthesis in plant cells. In other words, the function of a structure is what it does and how it contributes to the overall functioning of an organism or system.

Overall, the structure and function of biological entities are intimately linked, as the specific structure of a biological entity determines its function and vice versa. Understanding the relationship between structure and function is fundamental to understanding the workings of living organisms. Understanding this link is necessary to gain insight into diseases that disrupt the homeostasis of a system and, ultimately help develop effective therapies in the future.

Diabetes

Diabetes Mellitus is a chronic metabolic disorder characterized by high blood sugar (glucose) levels due to an absolute or relative lack of insulin, a hormone produced by the pancreas. The disease has become a global health problem, affecting millions of people worldwide. In this article, we will discuss the various types of diabetes, its causes, symptoms, diagnosis, and treatment options, along with some preventive measures(Olokoba et al., 2012).

Types of Diabetes Mellitus

There are three main types of diabetes: Type 1, Type 2, and Gestational Diabetes.

Type 1 Diabetes: Formerly known as juvenile diabetes, this type of diabetes is caused by the destruction of the insulin-producing cells in the pancreas by the immune system. As a result, people with Type 1 diabetes are unable to produce insulin, and they require daily injections or

insulin pump therapy to regulate their blood sugar levels (American Diabetes Association, 2021).

Type 2 Diabetes (T2D): This is the most common form of diabetes, accounting for around 90-95% of all cases. In Type 2 diabetes, the body either does not produce enough insulin and/or becomes resistant to the insulin produced. This leads to high blood sugar levels, which can damage the blood vessels and nerves, leading to various complications (American Diabetes Association, 2021).

Gestational Diabetes: This type of diabetes occurs during pregnancy, and it affects around 2-10% of all pregnancies. Women with gestational diabetes have high blood sugar levels during pregnancy, which can affect their health as well as the health of their baby. However, gestational diabetes usually resolves after pregnancy, but women with gestational diabetes have a higher risk of developing T2D later in life (American Diabetes Association, 2021).

Causes of Diabetes Mellitus

The exact cause of diabetes is still unknown, but it is believed to be a combination of genetic and environmental factors. Some of the risk factors for developing diabetes include:

- Family history: If a person has a family history of diabetes, their risk of developing the disease increases.
- Obesity: People who are overweight or obese have a higher risk of developing Type 2 diabetes.
- Physical inactivity: Lack of physical activity is a major risk factor for developing Type 2 diabetes.
- Age: The risk of developing diabetes increases as a person ages.
- Ethnicity: People of certain ethnicities, such as African Americans, Hispanic Americans, American Indians, and some Asian Americans, are at a higher risk of developing diabetes (American Diabetes Association, 2021).

Symptoms of Diabetes Mellitus

The symptoms of diabetes can vary depending on the type of diabetes and the severity of the disease. Some of the common symptoms include:

- Increased thirst
- Frequent urination
- Increased hunger
- Fatigue
- Blurred vision
- Slow-healing cuts and bruises
- Tingling or numbness in the hands or feet
- Recurring infections

Diagnosis of Diabetes Mellitus

Diabetes can be diagnosed through various methods, including:

- Fasting Plasma Glucose Test (FPG): This test measures the blood glucose level after fasting for at least 8 hours.
- Oral Glucose Tolerance Test (OGTT): This test measures the blood sugar level after fasting for at least 8 hours and then again 2 hours after drinking a sugary drink.
- HbA1c Test: This test measures the average blood sugar level over the past 2-3 months (American Diabetes Association, 2021).

Treatment of Diabetes Mellitus

The treatment of diabetes depends on the type of diabetes and the severity of the disease. People with Type 1 diabetes require daily injections or insulin pump therapy to regulate their blood sugar levels. People with T2D may also require insulin therapy, particularly if their blood sugar levels are not well controlled with oral medications or lifestyle changes.

- Oral Medications: People with T2D may be prescribed oral medications, such as:
    - Metformin: Decreases the amount of blood sugar that the liver produces and that the intestines or stomach absorb(Nasri and Rafieian-Kopaei, 2014a; Nasri and Rafieian-Kopaei, 2014b). Metformin has no significant adverse effects; however, it may cause a serious condition called lactic acidosis.

- Sulfonylureas: Stimulate insulin secretion from pancreatic β-cells thereby lowering blood glucose concentration. They primarily act by binding to the SUR subunit of the ATP-sensitive potassium (K_{ATP}) channel and inducing channel closure(Proks et al., 2002).
- GLP-1 receptor agonists: These drugs mimic the action of a hormone called glucagon-like peptide 1. When blood sugar levels start to rise after someone eats, these drugs stimulate the body to produce more insulin(Hinnen, 2017).

- Lifestyle Changes: Lifestyle changes, such as healthy eating, regular physical activity, and weight management, are important for managing diabetes and reducing the risk of complications.
- Continuous Glucose Monitoring (CGM): CGMs are wearable devices that continuously monitor the blood sugar levels and provide real-time glucose readings. This can help people with diabetes to better manage their blood sugar levels and prevent severe low or high blood sugar events.
- Bariatric Surgery: In severe cases of obesity, bariatric surgery may be recommended for people with T2D as a treatment option. Bariatric surgery has been shown to improve blood sugar control and in some cases, lead to complete remission of the disease (American Diabetes Association, 2021).

According to the CDC, it is estimated that ~37 million people have T2D in the US. Because of the large number of individuals diagnosed with T2D, it is critical to study possible links between the structure and function of the cells that are involved in glucose homeostasis. The endocrine function of the pancreas involves the production and secretion of hormones, such as insulin and glucagon, which are essential in regulating blood sugar levels.

Pancreatic Beta Cell

The beta cells are specialized cells located in the Islets of Langerhans in the pancreas, and they are responsible for producing insulin. Insulin is a hormone that helps regulate glucose levels in the body by facilitating the uptake of glucose into cells for energy production. When blood glucose levels are high, beta cells release insulin into the bloodstream, which signals the body's cells to absorb glucose from the blood.

Insulin secretion is tightly regulated by a complex series of events that involve the biogenesis, storage, and secretion of insulin-containing granules. In the following section, we will discuss the processes involved in insulin biogenesis and secretion machinery in detail.

Insulin Biogenesis

Insulin is a critical hormone in regulating glucose metabolism in the body, and it is produced and secreted by beta cells in the pancreas. The structure of insulin is highly organized and consists of two polypeptide chains, the A chain and the B chain, which are linked together by disulfide bonds. The A chain contains 21 amino acids, while the B chain contains 30 amino acids, and both chains are highly conserved across species(Ghiasi et al., 2019; Omar-Hmeadi and Idevall-Hagren, 2021; Teitelman, 2019).

As preproinsulin mRNA is translated, the N-terminal signal peptide is recognized by signal recognition particles that direct the ribosome to the endoplasmic reticulum(ER) and facilitate preproinsulin translocation across the ER membrane where the signal peptide is removed. The signal peptide directs the nascent peptide to the ER lumen, where it undergoes post-translational modifications, including disulfide bond formation, glycosylation, and folding(Huang and Arvan, 1995). The correctly folded proinsulin is then transported to the Golgi apparatus, where it undergoes additional processing with the help of chaperones, including Glucose-regulated protein 94 (GRP94), and form stabile hexamers through interactions with zinc ions(Ghiasi et al., 2019). After passing the quality control checkpoint, proinsulin is transported to the cis-face of the Golgi apparatus via the ER-Golgi interface compartment(Omar-Hmeadi and Idevall-Hagren, 2021).

The cleavage of proinsulin occurs through the action of prohormone convertases (PCs), which are a family of proteolytic enzymes. Two members of the PC family, PC2 and PC3, are expressed in beta cells and are responsible for processing proinsulin. The first cleavage occurs at the junction between the B-chain and C-peptide, generating insulin and C-peptide. The insulin and C-peptide are then stored in secretory granules until they are released in response to a stimulus(Teitelman, 2019).

Insulin is stored in specialized granules called insulin granules, which are highly regulated and contain a variety of proteins and enzymes involved in insulin processing and secretion. These granules are composed of a lipid membrane that surrounds a matrix of proteins and enzymes, including insulin and zinc. Zinc plays a crucial role in the processing,

storage, and secretion of insulin, as zinc ions are coordinated with cysteine residues in the insulin molecule, forming a hexameric structure essential for the stability and function of insulin.

Several studies have explored the mechanisms involved in insulin biogenesis. For example, a study by Li et al. (Li et al., 2019) investigated the role of the translocon-associated protein (TRAP) complex in the biogenesis of insulin-containing granules. The authors found that the TRAP complex is required for the correct folding and assembly of insulin-containing granules in beta cells. Another study by Dai et al. (2015) identified a protein called TMEM24 that plays a critical role in the biogenesis of insulin-containing granules. The authors showed that TMEM24 is required for the formation of the proinsulin-containing vesicles that give rise to insulin-containing granules.

Insulin Secretion Machinery

The release of insulin from beta cells is tightly regulated by a complex series of events that involves the depolarization of the plasma membrane, the influx of calcium ions, and the exocytosis of insulin-containing granules. The secretion of insulin can be divided into three phases: the first phase, which is triggered by a rapid increase in glucose concentration; the second phase, which is sustained in response to sustained glucose stimulation; and the third phase, which is a slow release of insulin that occurs over several hours (Henquin, 2000).

The depolarization of the plasma membrane is the first step in insulin secretion. Glucose is transported into the beta cell by the glucose transporter 2 (GLUT2), which is expressed on the beta cell membrane. Once inside the cell, glucose is phosphorylated by glucokinase, and subsequently metabolized in the processes of glycolysis and the citric acid cycle, which both generate ATP. The increase in ATP levels leads to the closure of ATP-sensitive potassium channels, causing the membrane to depolarize(Huang et al., 2018; Mourad et al., 2011; Olofsson et al., 2002; Rorsman and Ashcroft, 2018; Zhao et al., 2010).

The depolarization of the membrane triggers the influx of calcium ions through voltage-gated calcium channels. The increase in calcium ion concentration triggers the exocytosis of insulin-containing granules. The exocytosis of the granules occurs through the fusion of the granule membrane with the plasma membrane, which leads to the release of insulin into the extracellular space.

The process of exocytosis is regulated by a complex machinery that involves several proteins, including SNARE proteins, synaptotagmin, and complexin. SNARE proteins are a

family of proteins that are involved in the fusion of vesicle membranes with target membranes. In pancreatic beta cells, the SNARE proteins syntaxin 1A, SNAP-25, and synaptobrevin 2 (also known as VAMP2) are expressed on the plasma membrane and insulin-containing granules (Spurlin and Thurmond, 2006; Yan et al., 2022). The interaction between these proteins leads to the fusion of the granule membrane with the plasma membrane, allowing the release of insulin.

Synaptotagmin is a calcium-binding protein that plays a critical role in the regulation of insulin secretion. Synaptotagmin is located on the surface of insulin-containing granules and senses the increase in calcium ion concentration that occurs during membrane depolarization. The binding of calcium ions to synaptotagmin triggers a conformational change in the protein that leads to the fusion of the granule membrane with the plasma membrane, allowing the release of insulin (Chang et al., 2018).

Complexin is another protein that regulates the process of exocytosis. Complexin binds to the SNARE complex and modulates its activity, allowing for the regulated release of insulin-containing granules(Abderrahmani et al., 2004).

In addition to these proteins, other factors regulate insulin secretion, including hormones, neurotransmitters, and nutrients.

Conclusion

In summary, insulin biogenesis and secretion are complex processes that involve a series of events that are tightly regulated by a complex machinery. The synthesis of insulin begins with the translation of preproinsulin in the ER of pancreatic beta cells, followed by its transport to the Golgi apparatus, where it is processed into mature insulin. The secretion of insulin is triggered by the depolarization of the plasma membrane, which leads to the influx of calcium ions and the exocytosis of insulin-containing granules. This process is regulated by a complex machinery that involves several proteins, including SNARE proteins, synaptotagmin, and complexin(Gaisano, 2017; Omar-Hmeadi and Idevall-Hagren, 2021; Thurmond and Gaisano, 2020; Verhage and Sorensen, 2008).

Understanding the mechanisms involved in insulin biogenesis and secretion is critical for the development of new treatments for diabetes. Many of the drugs today are quite effective in assisting people with T2D to manage their disease however many are expensive(Tseng et al., 2020). By advancing our understanding of beta cell structure and cell maintenance factors we can possibly identify molecular risk factors in order to prevent or delay the onset of T2D.

The pancreas plays a pivotal role in regulating blood sugar levels, with beta cells being a vital component of this process due to their insulin production. Despite significant advancements in comprehending the role of beta cells, their structure and its potential impact on function remain elusive. This dissertation offers a comprehensive collection of research aimed at shedding light on the cytoskeleton architecture of beta cells. The hope is that this work will provide a foundational framework to aid in the treatment of T2D.

Cytoskeleton

The cytoskeleton is a complex network of protein fibers that provide structural support, shape, and organization to cells. It is found in all types of cells, from bacteria to human cells. The cytoskeleton is composed of three main types of fibers: actin, intermediate filaments, and microtubule (Figure 1).

-Actin filaments are thin, flexible fibers made of the protein actin. They are responsible for cell movement, including muscle contraction and cell division.

-Intermediate filaments are made of various types of proteins such as lamins and vimentin, are responsible for providing mechanical strength and stability to cells(Herrmann and Aebi, 2016).

-Microtubules are hollow tubes made of the protein tubulin. They play important roles in cell division, intracellular transport, and maintaining cell shape.

Together, these three types of fibers form a dynamic network that allows cells to maintain their shape, move, and carry out their various functions. The cytoskeleton is also involved in many important cellular processes, including signaling, intracellular transport, and cell division. In the following section, we will provide a brief overview of each type of cytoskeletal fiber(Bouchet and Akhmanova, 2017; Dogterom and Surrey, 2013; Wang and Thurmond, 2009).

Actin

Actin is a globular protein and exists in two forms: monomeric (G-actin) and filamentous, also known as polymerized, actin (F-actin). G-actin is the globular, soluble form of actin that can bind to ATP and other proteins, while F-actin is the filamentous, insoluble form of actin that forms the backbone of microfilaments in the cytoskeleton. Actin filaments are dynamic

structures that can rapidly assemble and disassemble, allowing cells to quickly reorganize their shape and structure in response to various stimuli (Dominguez and Holmes, 2011).

Actin is a type of protein that forms a critical component of the cytoskeleton, along with microtubules and intermediate filaments. Actin is found in all eukaryotic cells and is a highly conserved protein, meaning that its basic structure is similar across different species.

Actin is involved in many cellular processes, including cell division, intracellular transport, and cell movement. One of the main functions of actin is to provide cells with shape and stability. Actin forms a network of fibers that give cells their structure and helps them resist mechanical stress(Dominguez and Holmes, 2011; Lappalainen et al., 2022).

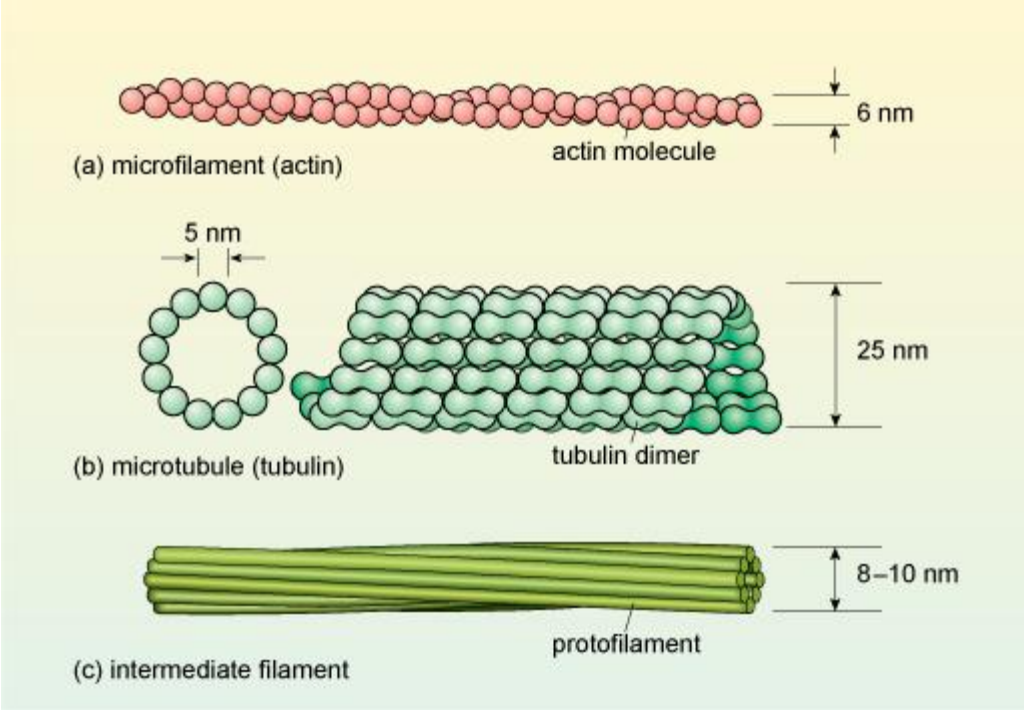

Figure 1. Cytoskeleton Components.

Simplified schematic diagrams showing the structure of (a) a microfilament; (b) a microtubule; and (c) an intermediate filament. In (a) the microfilament comprises two chains of actin monomers in a loose spiral structure the diameter of which is about 6 nanometers. Part (b) includes a schematic cross-section through a microtubule which is a ring of 13 tubulin monomers each of diameter about 5 nanometers; there is also a side-on view of part of a microtubule, showing the dumb-bells-shaped tubulin monomers arranged in a spiral structure to form the tubule. The external diameter of the tubule is about 25 nanometers. The intermediate filament shown in part (c) comprises about eight narrow protofilaments, which do not have a subunit structure. The protofilaments are wound around each other in a rope-like structure 8-10 nanometers in diameter. Illustration provided by Open Learn University

Actin also plays a role in cell movement. It is involved in the formation of contractile structures called actin-myosin filaments, which are responsible for muscle contraction. In non-muscle cells, actin filaments can also participate in cell movement, such as in the formation of filopodia, which are finger-like extensions that help cells move and explore their environment(Dominguez and Holmes, 2011).

Another important function of actin is to facilitate intracellular transport. Actin filaments help guide vesicles and organelles to their final destinations within the cell. This process is powered by molecular motors, such as myosin, which move along the actin filaments and transport vesicles and organelles to specific locations within the cell(Dominguez and Holmes, 2011).

In addition to its role in the cytoskeleton, actin also plays a role in cell signaling. Actin can interact with other proteins to regulate a variety of cellular processes, such as gene expression, cell growth, and differentiation.

It is worth mentioning that actin is also a target of a number of drugs and toxins. For example, some drugs target actin to disrupt the formation of actin-myosin filaments and prevent proper cell movement(Yarmola et al., 2000). Other drugs target actin to disrupt the cytoskeleton and cause cell death.

In conclusion, actin is an essential component of the cytoskeleton and plays a critical role in a variety of cellular processes. It provides cells with shape and stability, participates in cell movement and intracellular transport, and is involved in cell signaling. The importance of actin in cellular function is reflected in its highly conserved structure and presence in all eukaryotic cells (Lappalainen et al., 2022).

Intermediate Filaments

Intermediate filaments (IFs) are a class of cytoskeletal proteins that are essential for maintaining the structural integrity of cells. They are so named because they have a diameter intermediate to that of microfilaments and microtubules, which are the other two major components of the cytoskeleton. IFs are expressed in a tissue-specific manner and have diverse functions that include mechanical support, cell signaling, and regulation of cell differentiation.

IFs are found in all eukaryotic cells and are made up of a family of proteins called intermediate filament proteins (IFPs). The IFP family includes over 70 members in humans,

which are classified into six major types based on their sequence homology and tissue-specific expression patterns. These types are Type I acidic keratins, Type II basic keratins, Type III vimentin-like proteins, Type IV neurofilament-like proteins, Type V nuclear lamins, and Type VI lens-specific proteins.

The structure of IFs is characterized by a central alpha-helical rod domain that is flanked by non-helical N- and C-terminal domains. The rod domain is made up of heptad repeats of amino acids that form a coiled-coil structure, which is stabilized by hydrophobic interactions and hydrogen bonds. The coiled-coil structure of the rod domain allows IFs to form long, flexible filaments that can withstand mechanical stress(Herrmann and Aebi, 2016).

IFs are involved in a variety of cellular processes, including cell migration, cell division, and apoptosis. They also play a role in the maintenance of tissue architecture and have been implicated in several diseases, including cancer and neurodegenerative disorders.

Microtubules

Microtubules are dynamic, filamentous structures in eukaryotic cells. They are made up of tubulin protein subunits and play a critical role in cell division, intracellular transport, and cell shape and motility. They form a framework that gives cells their structure and helps resist mechanical stress. When cells are subjected to mechanical stress, microtubules can change their shape and orientation to help the cell resist the stress.

Microtubules are assembled from alpha- and beta-tubulin heterodimers, which combine to form protofilaments. The protofilaments then align side by side to form a hollow tube-like structure with a diameter of approximately 25 nm. Microtubules are typically organized into arrays with distinct orientations and functions in the cell.

One of the defining features of microtubules is their polarity. They have a "plus" end and a "minus" end, with the plus end being more dynamic and prone to growth, while the minus end is more stable. This polarity allows microtubules to participate in a variety of cellular processes.

Additionally, microtubules undergo dynamic instability, which is a phenomenon in where microtubules constantly switch between periods of growth and shrinkage. During growth, tubulin subunits are added to the "plus" end of the microtubule, while during shrinkage, tubulin subunits are removed from the same end. The growth and shrinkage of microtubules occur primarily at the plus end, which is regulated by the binding and hydrolysis of GTP (guanosine triphosphate) on the tubulin subunits. When the tubulin subunits at the plus end are bound to GTP, the

microtubule grows rapidly. However, as the GTP on the subunits is hydrolyzed to GDP, the microtubule growth rate slows down, and eventually, the microtubule may begin to shrink from the plus end. This dynamic instability is due to the intrinsic properties of microtubules, which allow them to switch between phases of growth and shrinkage in response to changes in the cellular environment (Kliuchnikov et al., 2022; Mitchison and Kirschner, 1984).

Microtubule Organizing Center

The organization of microtubule networks is crucial in regulating various aspects of cell architecture and function. Microtubules can arise from multiple sources within the cell, including the centrosome, which serves as the primary microtubule organizing center in most animal cells. Additionally, the Golgi apparatus is a well-established microtubule organizing center that plays a significant role in organizing and maintaining the Golgi structure and function. The centrosome contains a pair of centrioles that serve as a template for microtubule assembly, while the Golgi apparatus functions as the second major mammalian microtubule organizing center, both for nucleation and anchoring of microtubules (Rios, 2014; Zhu and Kaverina, 2013).

It is commonly accepted that γ-tubulin is the primary component responsible for microtubule nucleation (Wu and Akhmanova, 2017). In budding yeast, γ-tubulin is a constituent of the γ-tubulin small complex (γ-TuSC), whereas in other organisms, it forms part of the larger γ-tubulin ring complex (γ-TuRC). However, the microtubule-nucleating activity of γ-TuRC is significantly modulated by various additional factors, many of which are typically located in microtubule-organizing centers (MTOCs) (Petry and Vale, 2015). Certain factors directly bind to γ-TuRC and can recruit this complex to particular sites (Lin et al., 2015), while others can interact with tubulin dimers or nascent microtubule plus ends, stimulating microtubule growth from existing templates (Wieczorek et al., 2015).

Even in cells with a seemingly radial microtubule system, such as fibroblasts, a significant proportion of microtubules do not converge in a single ∼1-μm-large site, indicating that they are not attached to the centrosome. In certain types of mammalian cells, such as retinal pigment epithelium cells (RPE1 cells), nearly half of all cellular microtubules initiate at the Golgi apparatus (Efimov et al., 2007). The ability of the Golgi apparatus to organize microtubules is functionally important for several reasons. First, in mammalian cells, Golgi membranes are positioned close to the centrosome by dynein-mediated transport (Corthesy-Theulaz et al., 1992), and Golgi-anchored microtubules help to assemble dispersed Golgi stacks into the Golgi ribbon after mitosis (Rios, 2014; Zhu and Kaverina, 2013). Second, in

contrast to the centrosome, which forms a symmetric array, Golgi-derived microtubule networks are polarized and can thus drive asymmetric vesicle transport and promote overall cell polarity (Vinogradova et al., 2009). Recent work showed that in mesenchymal cells, the presence of Golgi-attached microtubules accelerates reorientation of the whole microtubule network, including the centrosome, in the direction of migration (Wu et al., 2016). This suggests that the centrosome may be the passenger and not the driver during cell polarization. Golgi-derived microtubules become particularly important when mesenchymal-type migration of cancer cells is examined in a soft three-dimensional matrix (Wu et al., 2016), which represents a more natural substrate for these cells than the conventional hard two-dimensional substrates, such as coverslips. This finding supports the idea that microtubule organization and dynamics are much more important for cell migration in soft 3D substrates than on hard 2D surfaces (Bouchet and Akhmanova, 2017). Furthermore, Golgi membranes control formation of noncentrosomal microtubule arrays in differentiated cells, including pancreatic beta cells and muscle cells (Oddoux et al., 2013; Wu and Akhmanova, 2017; Zhu et al., 2015).

Overall, the formation and regulation of microtubules are complex processes that involve a variety of proteins and cellular structures. The origin of microtubules depends on the specific cellular context and function, and their assembly and disassembly are tightly regulated to ensure proper cellular function. In many types of differentiated animal cells, such as epithelial cells or neurons, microtubule networks are not radial but instead form parallel or antiparallel arrays (Sanchez and Feldman, 2017).

Microtubule Function

One of the main functions of microtubules is to help organize the division of cells. During cell division, microtubules play a role in separating the chromosomes and pulling them towards opposite poles of the cell. This process is known as mitosis. The microtubules form the "spindle apparatus," a structure that helps separate the chromosomes and ensures their equal distribution to the daughter cells.

Microtubules are also involved in the formation of cilia and flagella, specialized structures that allow cells to move. Cilia and flagella are made up of microtubules that are arranged in a specific pattern. By coordinated beating or waving, they provide the propulsion needed for cells to move through liquids or over surfaces.

Microtubules also play a role in intracellular transport. They provide a “highway” for vesicles and organelles to move from one part of the cell to another. This movement is powered by molecular motors, such as kinesin and dynein, which move along microtubules in opposite directions. Kinesin moves towards the plus end of the microtubule, while dynein moves towards the minus end. This allows for the directed transport of vesicles and organelles to specific locations within the cell.

It is worth mentioning that microtubules are also a target of a number of drugs and toxins. For example, the drug paclitaxel, commonly used to treat cancer, works by stabilizing microtubules and preventing them from breaking down. This leads to the formation of microtubule bundles that prevent proper cell division, ultimately leading to cell death(Pellegrini and Budman, 2005).

In conclusion, microtubules are an essential component of the cytoskeleton and play a critical role in a variety of cellular processes. They help organize cell division, support intracellular transport, maintain cell shape, and play a role in the formation of cilia and flagella. Through their dynamic behavior, microtubules are able to participate in a variety of processes that allow cells to carry out their functions (Brouhard and Rice, 2018).

Microtubule-associated proteins (MAPs)

Microtubule-associated proteins (MAPs) are a diverse group of proteins that interact with microtubules. MAPs play important roles in regulating the structure, dynamics, and functions of microtubules in cells.

There are several classes of MAPs, including:

1. Structural MAPs: These proteins help to stabilize microtubules and regulate their length, orientation, and distribution within cells. Examples include tau and MAP2(Barbier et al., 2019).
2. Motor MAPs: These proteins interact with microtubules and help to move vesicles, organelles, and other cellular components along microtubules. Examples include kinesins and dyneins.
3. Regulatory MAPs: These proteins bind to microtubules and help to control their dynamic behavior, including nucleation, polymerization, and depolymerization. Examples include stathmin and Op18.

4. Crosslinking MAPs: These proteins crosslink microtubules to each other or to other cellular structures, creating a stable network. Examples include MAP1B and MAP4(Bonnet et al., 2001).

Overall, MAPs are essential for the proper organization and function of the microtubule cytoskeleton, which is important for many cellular processes, including cell division, intracellular transport, and cell morphology(Barbier et al., 2019; Bonnet et al., 2001; Goodson and Jonasson, 2018; Monroy et al., 2018; Wieczorek et al., 2015).

Post Translational Modifications

Tubulins are highly conserved proteins across various species, possessing nearly identical structures as observed through studies on several organisms. These proteins assemble into microtubules in all eukaryotic organisms, which are essentially hollow tubes made up of 13 α–beta-tubulin dimer chains, also known as protofilaments. Despite their evolutionary conservation, microtubules exhibit diverse properties, behaviors, or even structures within single cells or between different species and cell types due to the incorporation of various tubulin isotypes and their post-translational modifications(Hammond et al., 2008).

Tubulin undergoes various post-translational modifications (PTMs) that affect its function and stability(Akimoto et al., 2007; Gundersen et al., 1987; Song and Brady, 2015; Wloga et al., 2017). Some of these modifications, such as phosphorylation, acetylation, methylation, palmitoylation, ubiquitylation, and polyamination, are found on many different proteins. Other modifications were initially identified on tubulin, such as the addition of tyrosine (tyrosination), glutamate (glutamylation and polyglutamylation), and glycine (glycylation and polyglycylation) to specific amino acid residues. Tubulin is also subject to enzymatic removal of amino acids, such as tyrosine from the C-terminus of α-tubulin (detyrosination) or glutamate residues from the detyrosinated α-tubulin C-terminus to generate Δ2-tubulin or Δ3-tubulin (Janke and Magiera, 2020).

Acetylation and Detyrosination of Tubulin: Acetylation and detyrosination have been reported to attenuate microtubule stability and function. Acetylation occurs on lysine 40 of α-tubulin, and is associated with increased microtubule stability, resistance to depolymerization, and interactions with motor proteins. Detyrosination, on the other hand, involves the removal of the C-terminal tyrosine residue from α-tubulin, and is associated with decreased microtubule stability and increased interactions with MAPs (Nekooki-Machida and Hagiwara, 2020).

Polyglutamylation and Polyglycylation of Tubulin: Polyglutamylation and polyglycylation of tubulin, involve the addition of glutamate or glycine residues to the C-terminus of tubulin subunits. This results in the creation of multiple negative charges in the regions of the tubulin dimer that face the microtubule surface. As a result, it has the potential to regulate the interaction between microtubules and other proteins, including MAPs that affect microtubule stability and function, as well as molecular motors that use microtubules as tracks. In the nervous system, polyglutamylation has been associated with the differential binding of MAPs like MAP2, which might affect neurite outgrowth (Bonnet et al., 2001). Additionally, a mutation in mice, called ROSA22, alters patterns of alpha tubulin polyglutamylation and selectively inhibits neuronal vesicle transport by KIF1A kinesin. Removing tubulin C-termini via subtilisin digestion in vitro reduces the processivity of both cytoplasmic dynein and kinesin motors, creating another potential connection between polyglutamylation and motor function.

These PTMs of tubulin differentiate microtubules into subpopulations in cells, which could potentially program these microtubules for specific functions, prime them for specific cargoes or designate them for specific fates. These modifications play important roles in regulating microtubule dynamics, stability, and organization, as well as in modulating the binding properties of MAPs. The various combinations and cell specific examples are vastly too numerous to depict here however numerous reviews and reports have been written to substantiate these observations (Janke and Magiera, 2020; Song and Brady, 2015; Wloga et al., 2017).

Motor Proteins

Molecular motors that use cytoskeletal fibers as a track are well-studied, and there are three known classes of cytoskeletal motors: myosin, which interacts with actin filaments (not discussed here), and two types of microtubule motors, dynein and kinesin. All cytoskeletal motors possess a motor domain, also known as the "head," which contains two binding sites: one for ATP and one for the track. Interestingly, the kinesin motor domain is relatively small (about 350 amino acids), while the myosin motor domain is of intermediate size (about 800 amino acids), and the dynein motor domain is large (over 4,000 amino acids). In addition, the non-motor domains of the three classes of motors differ significantly, suggesting that functional diversity is partly determined by these regions (Woehlke and Schliwa, 2000).

Dynein

Dynein is a large molecular motor protein that is essential for a wide range of biological processes, including cell division, intracellular transport, and ciliary and flagellar beating. The protein belongs to the family of cytoplasmic dynein, which is responsible for the movement of various cellular components along microtubules. In this essay, we will explore the structure, function, and significance of dynein in the context of cellular processes.

Structure of Dynein

Dynein is a multi-subunit protein complex that is composed of two heavy chains (also known as dynein heavy chains or DHCs), several intermediate chains (ICs), several light intermediate chains (LICs), and several light chains (LCs). The heavy chains are the largest and most conserved components of the dynein complex and contain the ATPase activity required for movement. Each heavy chain has a globular head domain at its N-terminus, which binds to microtubules, and a tail domain at its C-terminus, which interacts with the intermediate and light chains. The intermediate and light chains are involved in binding cargo and regulating dynein activity (Figure 2).

The dynein complex has two identical heavy chains, each of which contains six AAA+ (ATPases Associated with various cellular Activities) domains, which are arranged in a ring-like structure that encircles the microtubule. The AAA+ domains are responsible for hydrolyzing ATP to provide the energy needed for movement. The N-terminal end of the heavy chain binds to microtubules, while the C-terminal end interacts with the intermediate and light chains.

Dynein moves through the ATP-dependent movement of its two heads, which are connected by a stalk domain. The leading head of the dynein molecule attaches to the microtubule and undergoes ATP hydrolysis, leading to a conformational change that allows the trailing head to bind to the microtubule. The leading head subsequently releases from the microtubule and swings backward towards the trailing head, causing the dynein complex to move along the microtubule towards the minus end. The trailing head then undergoes ATP hydrolysis, and the process repeats itself(Ananthanarayanan, 2016; Canty and Yildiz, 2020; Harada et al., 1998; Lu and Gelfand, 2017; Reck-Peterson et al., 2018a; Reck-Peterson et al., 2018b).

Function of Dynein

The primary function of dynein is to move cellular components along microtubules. Microtubules are one of the three types of cytoskeletal filaments in eukaryotic cells, the others being actin

filaments and intermediate filaments. Microtubules are composed of α- and beta-tubulin heterodimers, which form a hollow tube-like structure. Dynein moves along the microtubules by hydrolyzing ATP to produce mechanical force. Dynein can move towards the minus end of microtubules, which is usually located near the center of the cell(Ananthanarayanan, 2016; Canty and Yildiz, 2020; Harada et al., 1998).

One of the most important functions of dynein is in mitosis, the process of cell division. During cell division, dynein plays a crucial role in the separation of chromosomes by pulling them towards the minus end of microtubules. This movement is essential for the formation of the spindle apparatus, which is responsible for organizing and separating chromosomes during cell division.

Dynein is also involved in intracellular transport. It is responsible for the movement of vesicles, organelles, and other cellular components along microtubules. This movement is essential for the delivery of proteins and other molecules to various parts of the cell, as well as the removal of waste and other cellular debris(Harada et al., 1998; Varadi et al., 2003).

Dynein is also responsible for the beating of cilia and flagella. Cilia and flagella are motile structures that extend from the surface of many eukaryotic cells. They are composed of microtubules that are arranged in a specific pattern, with dynein located along the length of each microtubule. Dynein moves along the microtubules to generate the force required for the beating of cilia and flagella (Canty and Yildiz, 2020; Grabham et al., 2007; Lu and Gelfand, 2017; Reck-Peterson et al., 2018a).

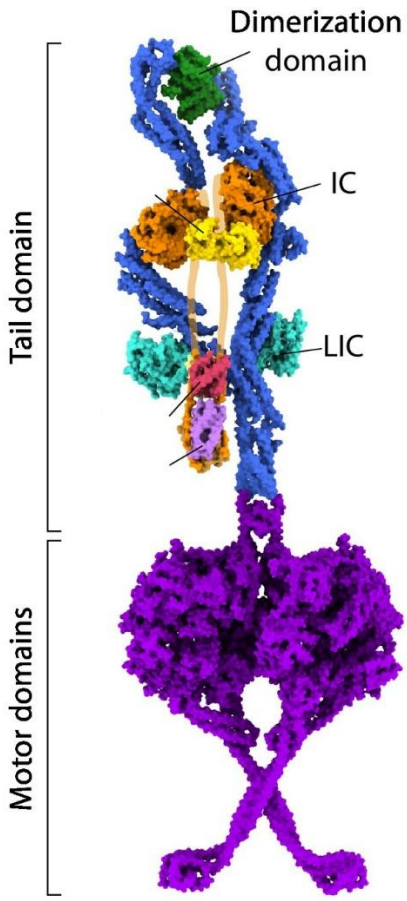

Figure 2. Dynein Motor Structure

Architecture of the dynein complex in the autoinhibited conformation (PDB accession: 5NVU). The N-terminal dimerization domain links the two dynein heavy chains (blue) together. The intermediate chains (ICs) are held together through an N-terminal unstructured region (purported location shown in orange outline). The light intermediate chains (LICs, cyan) bind midway along the tail domain. The motor domains (purple) form a stacked structure with the coiled-coil stalks crossed. Image adapted from John Canty (Canty and Yildiz, 2020).

Significance of Dynein

Dynein is an essential protein that is required for many fundamental cellular processes. Defects in dynein function have been implicated in a range of human diseases, including neurodegenerative disorders, cancer, and developmental defects. For example, mutations in dynein have been linked to various neurological disorders, such as motor neuron disease and Perry syndrome, which are characterized by the degeneration of motor neurons in the brain and spinal cord. These conditions result in a range of symptoms, including muscle weakness, difficulty walking, and impaired speech (Tsuboi et al., 2021). Dynein is also important in the transport of mitochondria, which are the energy-producing organelles in cells. Defects in dynein-mediated transport of mitochondria have been linked to various neurodegenerative disorders, including Alzheimer's disease and Parkinson's disease(Ananthanarayanan, 2016; Canty and Yildiz, 2020; Harada et al., 1998).

Dynein has also been linked to cancer. Studies have shown that dynein is involved in the movement of proteins that regulate cell division and cell growth. Dysregulation of these processes can lead to uncontrolled cell growth and the development of cancer. In addition, dynein has been found to be overexpressed in certain types of cancer, such as breast cancer and pancreatic cancer, and may contribute to the invasiveness of cancer cells.

In addition to its biological significance, dynein has also been of interest to researchers due to its mechanical properties. Dynein is one of the largest and most complex molecular motors known, and its movements and interactions with microtubules have been the subject of extensive research. Understanding the mechanics of dynein has important implications for the design of synthetic motors and other nanoscale devices.

Conclusion

Dynein is a complex and versatile protein that plays a critical role in a wide range of biological processes, from cell division and intracellular transport to the beating of cilia and flagella. The protein is composed of multiple subunits that work together to generate mechanical force and move along microtubules. Defects in dynein function have been linked to a range of human diseases, including neurodegenerative disorders and cancer, highlighting the importance of this protein in maintaining cellular health. Studying dynein has provided valuable insights into the mechanics of molecular motors and has important implications for the development of new nanoscale devices.

Kinesin Family

Kinesin superfamily proteins (KIFs) comprise a subset of motor protein that have major roles in intracellular transport across different cell types(Marx et al., 2009). Presently, there are believed to be more than 45 mammalian KIF genes, but there could be more than twice as many KIF proteins due to alternative mRNA splicing. The KIFs can be classified into 15 families, numbered kinesin 1 through kinesin 14B, according to phylogenetic analyses. These families are broadly grouped into three types based on the location of their motor domain in the molecule: N-kinesins have a motor domain in the amino-terminal region, M-kinesins have a motor domain in the middle, and C-kinesins have a motor domain in the carboxy-terminal region. In this thesis we will discuss conventional kinesin, and a kinesin-1 (KIF5B)(Hirokawa et al., 2009).

Kinesin-1 (KIF5B)

Kinesin-1 is a motor protein that plays a crucial role in intracellular transport in eukaryotic cells. It is responsible for the movement of various cargoes, including organelles, vesicles, and protein complexes, along microtubules. Kinesin-1 belongs to the kinesin family of proteins, which are characterized by their ability to move along microtubules using energy derived from ATP hydrolysis. In this article, we will explore the structure, function, and regulation of kinesin-1, as well as its involvement in various biological processes and diseases(Hirokawa et al., 2009).

Structure of Kinesin-1

The motor domain of kinesin-1 is located at the N-terminus of each heavy chain and is responsible for the ATP-dependent movement of the protein along microtubules. It contains a highly conserved core consisting of an alpha-helical bundle, a beta-sheet, and a microtubule-binding loop, which interacts with tubulin subunits in the microtubule lattice. The motor domain also contains an ATP-binding site, which is responsible for powering the movement of the protein along microtubules (Rice et al., 1999; Shang et al., 2014).

The stalk domain of kinesin-1 connects the motor domain to the tail domain and contains coiled-coil regions that allow for the dimerization of the heavy chains. The stalk domain also contains binding sites for the light chains and other regulatory proteins.

The tail domain of kinesin-1 is located at the C-terminus of each heavy chain and is responsible for cargo binding. It contains multiple domains, including a cargo-binding domain, a lipid-binding

domain, and a protein-binding domain, that allow for the specific recognition and binding of different types of cargoes.

The light chains of kinesin-1 are small, globular proteins that bind to the tail domain and are involved in cargo binding. They also regulate the activity of the motor domain by interacting with the stalk domain and the heavy chain(Hirokawa et al., 2009).

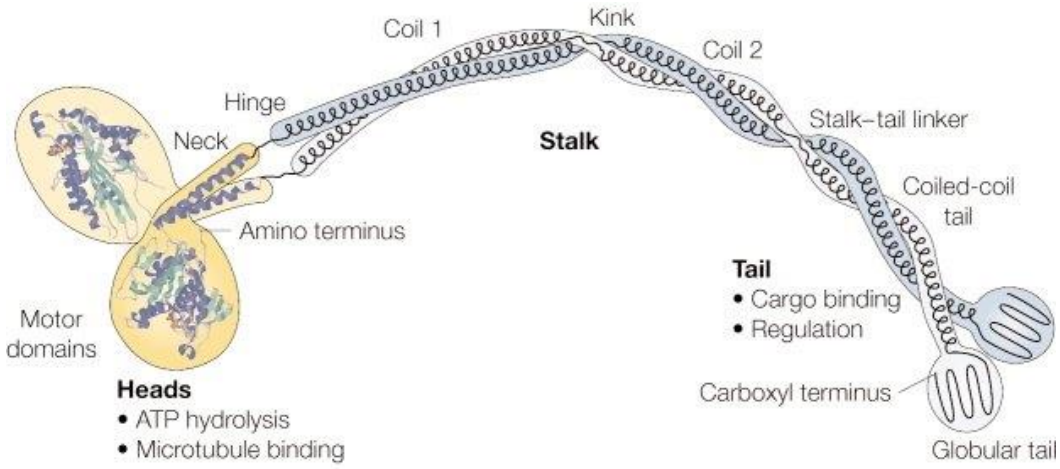

Figure 3. Structure of Kinesin-1

Structure of kinesin-1. Kinesin-1 is a homodimer consisting of two heavy chains (KHCs). The KHCs contain a motor domain (heads) that binds to microtubules and hydrolyzes ATP to generate movement, as well as a coiled-coil stalk that dimerizes with the other KHC to form the protein complex. The stalk domain is full of sites that can be post translationally modified to gate the activity of kinesin. The Kinesin Light Chains (KLCs) bind to the KHCs and act as adapters for many of the various cargoes that are transported by kinesin-1.

The globular head domain of the KHCs is composed of four distinct regions: The N-terminal motor domain, the neck linker, the central stalk, and the tail domain. The motor domain contains a microtubule-binding site and an ATP-binding site, and it hydrolyzes ATP to generate movement along the microtubule. The neck linker is a flexible region that connects the motor domain to the central stalk and undergoes a conformational change upon ATP hydrolysis that results in movement of the motor domain along the microtubule. The central stalk is a coiled-coil structure that forms a rigid rod that spans the distance between the two motor domains of the KHC dimer. The tail domain is a flexible region that extends from the central stalk and binds to the KLCs.

The KLCs are composed of an N-terminal domain and a C-terminal domain, which are connected by a coiled-coil region. The N-terminal domain binds to the KHCs and contains a tetratricopeptide repeat (TPR) domain, which is thought to play a role in regulating the activity of the motor protein. The C-terminal domain contains a cargo-binding domain that binds to various cargoes, including membrane-bound organelles, vesicles, and protein complexes.

Kinesin uses a hand-over-hand mechanism to walk along microtubules. This involves the two heads of the kinesin molecule being out of phase with each other, with one head always attached to the microtubule while the other head is free to move to a new binding site. Once the free head binds to the microtubule, the previous head undergoes ATP hydrolysis and releases from the microtubule. The released head then swings forward and attaches to the microtubule at a new site, repeating the cycle(Hirokawa et al., 2009).

Function of Kinesin-1

Kinesin-1 is involved in the transport of various cargoes along microtubules in eukaryotic cells. It is responsible for anterograde transport, which is movement of cargoes away from the microtubule organizing center (MTOC) towards the cell periphery. Kinesin-1 is responsible for the movement of organelles, such as mitochondria and lysosomes, as well as vesicles containing neurotransmitters, proteins, and lipids.

Kinesin-1 has also been shown to be involved in the regulation of microtubule dynamics. It can bind to and stabilize microtubules, as well as promote microtubule growth by transporting MAPs and tubulin to the plus end of the microtubule (Hirokawa et al., 2009).

Regulation of Kinesin-1

The activity of kinesin-1 is regulated by several mechanisms, including post-translational modifications, interactions with other proteins such as MAPs, and changes in cellular signaling pathways.

1. PTMs: Kinesin-1 can be regulated by PTMs, including phosphorylation, acetylation, and ubiquitination. Phosphorylation of kinesin-1 by kinases such as GSK3β, MAPK, and PKA can modulate its activity and affect its interaction with other proteins. Acetylation of kinesin-1 by histone acetyltransferases has been shown to enhance its motility along microtubules. Phosphorylation of the KHCs and KLCs can modulate the activity of the motor protein, and several kinases and phosphatases have been identified that can phosphorylate or dephosphorylate kinesin-1 subunits(Donelan et al., 2002).
2. Interactions with other proteins: Ensconsin, also known as MAP7 (Microtubule-Associated Protein 7), is a protein that interacts with microtubules and plays a role in regulating the activity of kinesin motor proteins. Studies have shown that ensconsin can directly interact with kinesin motor proteins and modulate their activity, affecting microtubule-based transport in cells(Barlan et al., 2013). By modulating the activity of kinesin-1, ensconsin can influence the transport of key cellular components, such as vesicles and mitochondria, along the microtubule network. Overall, ensconsin plays an important role in regulating microtubule-based transport in cells, and its interaction with kinesin motor proteins is one mechanism by which it exerts its effects (Barlan et al., 2013).
3. Cellular signaling pathways: Kinesin-1 activity can also be regulated by changes in cellular signaling pathways. For example, the activity of kinesin-1 in neurons is regulated by the protein BDNF (brain-derived neurotrophic factor), which activates the TrkB receptor and downstream signaling pathways, leading to the phosphorylation of kinesin-1 and its activation.
4. As discussed in the section above PTMs on the microtubule lattice also can “gate” kinesin-1 activity.

Biological Processes Involving Kinesin-1

Kinesin-1 is involved in various biological processes in eukaryotic cells, including the following:

1. Neuronal transport: Kinesin-1 plays a critical role in the transport of neurotransmitter-containing vesicles along axons in neurons. Defects in kinesin-1 function have been linked to various neurological disorders, including Alzheimer's disease, Parkinson's disease, and amyotrophic lateral sclerosis (ALS).
2. Mitochondrial transport: Kinesin-1 is responsible for the movement of mitochondria along microtubules in cells. Disruption of kinesin-1 function can lead to defects in mitochondrial transport and dysfunction, which have been implicated in various diseases, including neurodegenerative disorders and cancer(Glater et al., 2006).
3. Golgi transport: Kinesin-1 is involved in the transport of Golgi stacks along microtubules in cells. Defects in kinesin-1 function can lead to defects in Golgi organization and secretion, which have been implicated in various diseases, including cancer and congenital disorders of glycosylation(Harada et al., 1998; Luini et al., 2008; Sanders and Kaverina, 2015).
4. Cytokinesis: Kinesin-1 is involved in the final stages of cell division, where it plays a role in the separation of the two daughter cells. Disruption of kinesin-1 function can lead to defects in cytokinesis, which have been implicated in various diseases, including cancer.

Kinesin and dynein are two motor proteins that operate in opposite directions to transport cargos along microtubules. In mice, three KHC genes have been identified: Kif5a, Kif5b, and Kif5c. Kif5b is the mouse equivalent of the human ubiquitous KHC and was initially characterized in pancreatic beta-cells. While the role and molecular mechanism of kinesin transportation have been extensively studied in neuronal cells and tissues, only a few reports have examined its function in nonneuronal mammalian cells. Meng et al. reported that inhibiting Kif5b through the use of antisense oligonucleotides inhibited both basal and glucose-stimulated insulin secretion in primary mouse pancreatic beta-cells. Immunocytochemistry studies demonstrated that Kif5b is colocalized with insulin-containing vesicles in the immortalized rodent beta-cell lines MIN6 and INS-1. Furthermore, expression of a dominant-negative KHC motor domain (KHCmut) significantly inhibited sustained insulin secretion in response to glucose challenge, but not acute insulin secretion.

Microtubule Sliding

Dynamic microtubules can form various typical intracellular structures that are linked to specific cellular tasks. For instance, in non-dividing mammalian fibroblasts, microtubules generally emanate from a centrosome with their plus ends oriented outward, forming a radial pattern that extends toward the cell periphery to facilitate intracellular trafficking driven by molecular motors. On the other hand, in dividing animal cells, two radial arrays nucleated by centrosomes merge with an antiparallel overlap region to create a mitotic spindle that ensures the accurate separation of chromosomes (Dogterom and Surrey, 2013). Microtubule sliding is an underappreciated, yet essential mechanism that plays a vital role in establishing, organizing, preserving, and modifying microtubule arrays. This process involves the movement of microtubules relative to other microtubules or non-microtubule structures such as the actin cytoskeleton, and is powered by molecular motor proteins and regulated, in part, by static crosslinker proteins(Jolly and Gelfand, 2010; Lu et al., 2013; Lu et al., 2016). Microtubule sliding is particularly crucial for establishing and maintaining microtubule polarity patterns in various parts of the cell, among other essential functions. Here we focus specifically on Kinesin-1, highlighting major milestones in our understanding of kinesin-1 mediated microtubule sliding.

The conventional role of kinesin-1, is to transport cargo along microtubules towards the plus-ends. However, recent studies, including our own (see Chapter 4), have identified a new function of kinesin-1 in sliding cytoplasmic microtubules against each other, during the interphase of a cell. This is made possible by the presence of a microtubule-binding site at the C-terminus of the kinesin-1 heavy chain, which can bind to an acidic E-hook at the tubulin C-terminus through electrostatic interactions. Unlike the N-terminal motor domain, this C-terminal binding site is ATP-independent (Seeger and Rice, 2010). By using both the N-terminal motor domain and the C-terminal binding site, kinesin-1 can cross-bridge two microtubules and slide them against each other. In this process, one microtubule acts as the cargo while the other serves as the track. Examples of microtubule sliding has been observed for decades.

In 2006, Straube and colleagues discovered the phenomenon of microtubule sliding in the fungus Ustilago maydis. Through live-cell observations and analysis of various Kin1 (the fungus nomenclature for Kinesin-1) mutants, the researchers found that the Kinesin-1 motor protein plays a critical role in efficient microtubule bundling and contributes to microtubule bending in living organisms. The presence of high levels of Kin1 resulted in increased microtubule bending, whereas a rigor mutation in the motor domain hindered all microtubule

movement and caused strong microtubule bundling. The finding suggested that kinesin-1 could form cross-bridges between microtubules in living cells. The conserved region in the C terminus of Kin1 was also shown to bind microtubules in vitro, emphasizing its role in microtubule bundling (Straube et al., 2006).

Subsequently, studies followed by Barlan and colleagues sought to directly visualize microtubule sliding, the group fused a photoconvertible protein tag to tubulin and imaged microtubule movement in interphase cells. The photoconversion of this probe allowed them to apply fiduciary marks on microtubules. Following these marks (photoconverted microtubule segments) the authors visualized microtubule movements in live cells (Jolly and Gelfand, 2010; Jolly et al., 2010).

Additionally, a 2013 study utilized a similar technique to identify essential cofactors for kinesin-1-mediated microtubule sliding in Drosophila S2 cells. Kinesin-1 typically exists in an inactive, autoinhibited state, and motor activation is believed to occur upon binding to cargo through the C terminus(Friedman and Vale, 1999). By using RNAi-mediated depletion in Drosophila S2 cells, the researchers demonstrated that kinesin-1 relies on ensconsin (MAP7), a ubiquitous microtubule-associated protein, for its primary function of organelle transport(Barlan et al., 2013).

Kinesin-1 is known for its cargo transport and now microtubule sliding functions, both of which are highly conserved. One theory proposes that some cargoes can be transported by simply riding on sliding microtubules within cells. This hypothesis was initially based on the observation of organelles moving with sliding microtubules in amoeba Reticulomyxa. Recently, the movement of peroxisomes in Drosophila S2 cells was also thought to be due to their attachment to a moving microtubule (Barlan and Gelfand, 2017; Barlan et al., 2013). A study on Drosophila ooplasmic streaming suggested that kinesin-1 driven microtubule sliding is crucial for cytoplasmic streaming in oocytes, where microtubule sliding occurs between the anchored and free microtubules, generating unidirectional cytoplasmic movement. Inhibition of sliding resulted in a diffuse pattern of posterior determinants in the oocyte (Lu et al., 2016). This suggests that cytoplasmic streaming helps refine the posterior determination by transporting determinants that are attached to moving microtubules to the posterior pole for proper anchorage. This mode of transport, known as "ride-on-microtubules," can be a rapid and efficient way of redistributing organelles and mRNAs/proteins parallel to microtubule reorganization, particularly in large cells such as oocytes(Lu and Gelfand, 2017; Lu et al., 2016).

In higher organisms, microtubule sliding has predominantly been shown in neuronal culture to promote neurite outgrowth. Due to inadequate tubulin synthesis in the axon and insufficient diffusion from the cell body to deliver sufficient amounts of tubulin down the axon, an active transport mechanism must be present to carry tubulin. Initially, early leaders in axonal transport suggested that microtubules, rather than free tubulin subunits, are transported down the axon. This theory was supported by indirect evidence from radiolabel analyses of newly assembled proteins in the neuron (Galbraith et al., 1999). However, during that time, very little was known about the transport machinery, and live imaging of microtubule behaviors in living cells was only just becoming possible. Biochemical approaches revealed that the transport of tubulin as polymers occurred at much slower rates than those observed in later studies on molecular motor proteins. The idea of entirely stationary microtubules failed to explain how tubulin could be actively transported down the axon, except as microtubule polymers.

Transporting tubulin as polymers also provided an explanation for the need to organize microtubules in the axon with a plus-end-out polarity orientation (Baas and Ahmad, 1993). By transporting microtubules with their plus end leading into the axon and anterograde down its length, this mechanism could accomplish the organization. Although structural factors such as nucleation sites may also contribute to the neuron's microtubule polarity patterns, transporting the polymers offers a powerful and flexible method of generating, preserving, and re-establishing these patterns after insult.

It is important to note that although this section has focused on microtubule sliding during interphase. The microtubule sliding mechanism is most notably utilized by the cell during mitosis(Forth and Kapoor, 2017). During cell division the cell alters its microtubule network to form two opposing poles with the microtubules plus end are oriented towards the midline. For the sake of brevity, these poles orchestrate dynamic changes where populations of microtubules are slid apart by a number of mitotic motor proteins, such as kinesin-5 and kinesin-8. For a holistic review see, *The mechanics of microtubule networks in cell division*, by Scott Forth and Tarun Kapoor.

In conclusion, the cell’s ability to change its cytoskeleton allows for diverse functions. The ATP independent microtubule binding domain enables motors such as kinesin-1 to slide microtubules relative to one another. In subsequent chapters we will attempt to lay the framework of how the beta cell organizes its microtubule and how its unique function requires a unique structure that is derived from this mechanism(Jolly et al., 2010; Lu et al., 2015).

Chapter 2
Microtubules in Pancreatic Beta Cells: Convoluted Roadways Toward Precision

This chapter has been adapted from Bracey KM, Gu G, Kaverina I. Microtubules in Pancreatic Beta Cells: Convoluted Roadways Toward Precision. Front Cell Dev Biol. 2022 Jul 8;10:915206. doi: 10.3389/fcell.2022.915206. PMID: 35874834; PMCID: PMC9305484.

Introduction

Pancreatic islet beta cells regulate glucose homeostasis in vertebrates *via* glucose-stimulated insulin secretion (GSIS). This function is of critical importance to human health, because excessive GSIS causes hyperinsulinemic hypoglycemia that damages the brain and other tissues (Nessa et al., 2016), while insufficient secretion causes diabetes (Alejandro et al., 2015; Hudish et al., 2019). To avoid these pathological effects, the correct number of secretion-competent insulin granules (IGs) has to be prepared prior to a glucose stimulus. Moreover, these IGs must be positioned to the exocytosis sites at the plasma membrane at the right moment (Gandasi et al., 2018; Gao et al., 2007; Kasai et al., 2008; Verhage and Sorensen, 2008; Wang and Thurmond, 2009; Zhao et al., 2010) Several studies over the years have established that microtubules (MTs), which serve as tracks for IG transport, precisely regulate IG positioning over time (Bracey et al., 2020; Heaslip et al., 2014; Ho et al., 2020; Hoboth et al., 2015; Trogden et al., 2021; Zhu et al., 2015)

Our surprising findings are that the beta-cell MTs serve two functions. In the long-term, they promote endocrine function *via* facilitating IG biosynthesis, which relies on the growth of new MTs (Trogden et al., 2019). In the short-term, they acutely attenuate GSIS by restricting the number of readily-releasable IGs at the secretion sites, depending on microtubule stabilization (Bracey et al., 2020; Ho et al., 2020; Trogden et al., 2021; Zhu et al., 2015). In this perspective, we will provide our current views on how microtubule networks in beta cells are designed at the cellular and sub-cellular scales to precisely tune IG-transport and GSIS. Our current model is that beta-cell MTs are built, modulated, and utilized by such intracellular factors as MAPs and molecular motors to regulate IG transport and secretion.

Challenge of Insulin Granule Transport for Correct Secretion Levels

The task of correctly positioning secretory vesicles for acute stimulated secretion is a complicated process. On one hand, IGs are produced from the trans-Golgi network in the inner cytoplasm (Hou et al., 2009). They must then be transported to underneath the plasma

membrane for regulated release (Gandasi et al., 2018; Gao et al., 2007; Kasai et al., 2008; Verhage and Sorensen, 2008; Wang and Thurmond, 2009; Zhao et al., 2010). Since most of the IG transport in a beta cell is MT-dependent (Heaslip et al., 2014; Tabei et al., 2013a; Varadi and Rutter, 2002; Zhu et al., 2015), overall IG distribution in the cytoplasm including the cell periphery is a result of such active transport.

On the other hand, insulin secretion occurs within minutes after high glucose treatment, while it takes hours for newly synthesized IGs to mature and reach the cell membrane (Hou et al., 2009). To provide a timely response, a large number of pre-processed secretion-competent IGs is awaiting the signal. In a resting beta cell, several thousand IGs fill the entire cytoplasm, and only ~1% of those are secreted at a given stimulus (Dean, 1973; Fu et al., 2013; Olofsson et al., 2002; Rorsman and Renstrom, 2003). This scenario dramatically differs from constitutive secretion when secretory vesicles are constantly produced and readily transported for immediate secretion.

Not surprisingly, numerous secretion-restricting mechanisms have evolved to prevent over-secretion *via* the occasional release of pre-stored IGs (Chatterjee Bhowmick et al., 2021). These mechanisms act in concert as a combination of locks on a door or filters in a pipe. Broadly defined, these “filters” include any cellular tool preventing uncontrollable secretion. For example, restricting calcium levels in the cytoplasm can be considered a filter, because calcium influx is needed for priming of docked IGs for secretion (Idevall-Hagren and Tengholm, 2020; Omar-Hmeadi and Idevall-Hagren, 2021). Actin cytoskeleton provides another set of filters: actin remodeling and activity of myosins are thought to remove steric hindrance between IGs and the plasma membrane, drive short-distance IG transport to the secretion site, and provide mechanical force for the exocytic event itself (Arous and Halban, 2015; Kalwat and Thurmond, 2013; Varadi et al., 2005; Veluthakal and Thurmond, 2021). When we discuss MT-dependent positioning and transport of IGs in the cytoplasm, we must take the over-crowding of beta-cell cytoplasm into account and consider that removal of IG from the secretion sites can act as one of those “filters”. Our findings over the last few years support this model (Bracey et al., 2020; Ho et al., 2020; Trogden et al., 2021; Zhu et al., 2015). All the “filters” that prevent secretion at steady-state (basal) conditions must be adjusted upon each stimulus to allow a proper number of IGs to be secreted (Idevall-Hagren and Tengholm, 2020; Omar-Hmeadi and Idevall-Hagren, 2021). Being one of the filters, the microtubule network and transport must be modified downstream of glucose in a precise and reversible manner. Indeed, emerging evidence indicates that both microtubule network itself and MT-dependent motor activity are regulated by

glucose signaling in beta cells (Donelan et al., 2002; Heaslip et al., 2014; Ho et al., 2020; McDonald et al., 2009; Trogden et al., 2021; Trogden et al., 2019; Zhu et al., 2015).

Organization and Origin of Microtubule Network in beta Cells

Early work has assumed that microtubule networks in beta cells resemble radial microtubule organization in other cells (Byers et al., 1980), and serve for directional delivery of IGs to the cell periphery (Lacy, 1972). Such a view emerged, in part, due to technical inability, at that time, to distinguish which microtubule networks belonged to functional beta cells vs. other cell types in pancreatic primary cell cultures (Boyd et al., 1982). This view has been challenged by the demonstration of a complex microtubule network in Min6 cells (Varadi et al., 2003), followed by a series of data in primary functional beta cells uncovering a dense non-radial interlocking mesh of MTs in mouse and human islet beta cells (Figure 4) (Bracey et al., 2020; Ho et al., 2020; Muller et al., 2021; Trogden et al., 2019; Zhu et al., 2015). Identification of the sites of microtubule origin (nucleation) has shown that the vast majority of beta-cell MTs nucleate at the Golgi complex membrane (Figure 4) (Trogden et al., 2019; Zhu et al., 2015). Such MTs, in contrast to those nucleated at the conventional MT-organizing centers (MTOCs), the centrosomes, are called Golgi-derived MTs, or GDMTs (Sanders and Kaverina, 2015; Zhu and Kaverina, 2013). More recently, a thorough analysis of three-dimensional confocal (Bracey et al., 2020) and electron microscopy (Muller et al., 2021) data has shown that in addition to inner meshwork, the islet beta-cell microtubule network features a prominent array of peripheral MTs parallel to the plasma membrane (Figure 4). We found that this sub-membrane microtubule bundle is locally stabilized by a MAP called tau (Ho et al., 2020).

What could possibly produce a microtubule network so drastically different from the classic radial microtubule array? Switching microtubule nucleation to the Golgi can, in part, explain the non-radial microtubule pattern in the beta-cell interior: because the Golgi in beta cells is relatively large, GDMTs minus ends are intrinsically distributed over a significant volume, contributing to the network complexity. In addition, irregular microtubule organization might result from their extended lifetimes: beta-cell MTs are extraordinarily stable with a half-life of hours at basal glucose compared with minutes to tens of minutes in other cell types (Ho et al., 2020; Zhu et al., 2015). This increases their flexibility (Portran et al., 2017) and the probability of bending and buckling by intracellular forces over time (Bicek et al., 2009; Odde et al., 1999; Straube et al., 2006).

The origin of the sub-membrane microtubule bundle is, so far, a matter of speculation. GDMTs might extend from the Golgi to the cell periphery and bend to elongate along the plasma

membrane (Figure 4), however such long GDMTs have not yet been detected in beta cells (Muller et al., 2021). Nevertheless, MTs do not nucleate anew at beta-cell locations other than the Golgi, and, to a much lesser extent, the centrosome (Trogden et al., 2019), meaning that GDMTs must serve as precursors of most components of the microtubule network in a long run. In principle, microtubule polymer mass can increase without new nucleation, *via* using small fragments of existing MTs as seeds (Roll-Mecak and Vale, 2006). Interestingly, FIB-SEM studies found multiple small microtubule fragments at the beta-cell periphery (Muller et al., 2021), which might serve as such seeds. These fragments were suggested to potentially arise from microtubule severing by katanin-family proteins directly in the sub-membrane area (Muller et al., 2021). Alternatively, these fragments could be short MTs nucleated elsewhere (most likely, at the Golgi) and transported to the cell periphery by a motor-dependent microtubule sliding, as described in other cell types (Jolly and Gelfand, 2010; Jolly et al., 2010).

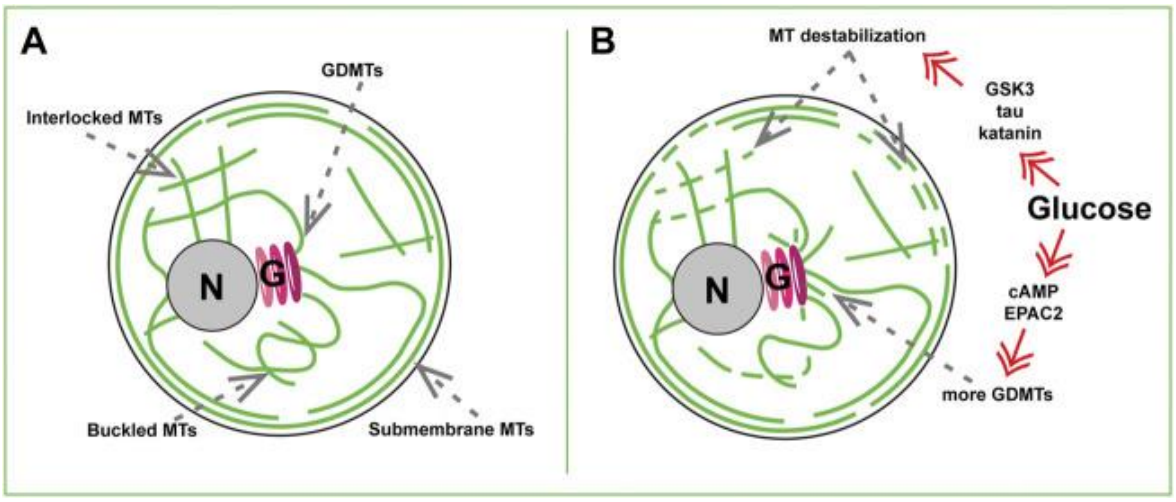

Figure 4. Microtubule sub-populations in a beta cell

(A) Steady-state basal glucose conditions. Newly nucleated GDMTs and the Golgi (G), Inner microtubule mesh formed by interlocked and buckled MTs, and submembrane microtubule array are shown. **(B)** High-glucose triggered microtubule remodeling *via* two signaling axes. Top: Kinase- (e.g. GSK3), tau phosphorylation-, and katanin severing-dependent microtubule destabilization. Bottom: cAMP and EPAC2- dependent enhancement of GDMT nucleation. Nucleus, N.

On an additional note, it is important to keep in mind that everything said above assumes that every beta cell has a similar microtubule organization. This, however, is not the case. beta cells are known to be extremely heterogeneous in their granularity, Ca^{2+} response, metabolic activity, GSIS level, and gene expression (Avrahami et al., 2017; Benninger and Kravets, 2022; Miranda et al., 2021; Nasteska and Hodson, 2018). Not an exception, MTs also vary significantly from one beta cell to another, as obvious from the dramatic differences in the amount of long-lived MTs, detected by the detyrosinated tubulin immunostaining (Trogden et al., 2021). This means that certain beta cells have stable, unchanging microtubule networks, while others have more labile, dynamic networks. Thus, some important subtypes of beta-cell microtubule networks might potentially differ from the generalized picture described here. Moreover, specific local microtubule features within individual cells might have yet escaped averaged analyses (Bracey et al., 2020) or studies unavoidably restricted to a small sample number [e.g., FIB-SEM, (Muller et al., 2021)], and may be functionally very important. Thus, the heterogeneity of MTs within the beta-cell population and their fine functional features remain an intriguing area of research.

Beta-Cell Microtubule Network Regulation by Glucose

The critical features of beta cells are to be able to respond to postprandial glucose stimulus properly and rapidly and to be able to revert to a steady-state condition after the glucose levels have been reduced. Like other important beta-cellular systems, the microtubule network readily reacts to stimulation. Combined evidence (Heaslip et al., 2014; Zhu et al., 2015; Trogden et al., 2019; Ho et al., 2020; Muller et al., 2021) indicates that being very stable at basal, low-glucose, conditions, MTs undergo a significant turnover in high glucose: both destabilization/depolymerization of pre-existing MTs and simultaneous polymerization of new MTs (Figure 4).

Live imaging assays indicate that microtubule depolymerization is triggered already 5 min after the high glucose application (Ho et al., 2020). This response relies on hyper-phosphorylation of microtubule stabilizer tau *via* glucose-responsive kinases GSK3, PKA, PKC, and CDK5 (Ho et al., 2020), which promotes tau detachment from MTs (Lindwall and Cole, 1984). While dynamics of the whole microtubule network is facilitated upon tau removal, this effect is especially manifested at the submembrane MTs (Figure 4), which initially contain a higher concentration of tau (Ho et al., 2020). This glucose-dependent microtubule destabilization coincides with a substantial fragmentation of MTs into small “seeds” (Muller et al., 2021), which may be potentially used to rebuild the submembrane bundle after glucose is

cleared from the extracellular environment. It is tempting to suggest that tau hyper-phosphorylation and detachment from MTs is a priming step for submembrane microtubule severing by katanin [as suggested in (Muller et al., 2021)], considering that tau is known to protect MTs from such severing in neurons or *in vitro* (Barbier et al., 2019).

In parallel with destabilization, glucose stimulation also leads to an increase in microtubule polymerization. This includes facilitated microtubule nucleation at the Golgi [Figure 4, (Trogden et al., 2019)] and faster polymerization at peripheral microtubule plus ends (Heaslip et al., 2014). Such responses likely compensate for microtubule loss, so that the whole microtubule polymer mass is affected by glucose only to a slight (Zhu et al., 2015) or non-detectable level (Muller et al., 2021). At the same time, the amount of detyrosinated tubulin (Glu-tubulin) within MTs, a post-translational modification used as a readout for microtubule lifetime (Gundersen et al., 1987; Khawaja et al., 1988), is significantly decreased (Zhu et al., 2015; Ho et al., 2020; Trogden et al., 2021), which is a direct indication of high microtubule polymer turnover.

Intriguingly, signaling pathways downstream of glucose that trigger the processes of microtubule depolymerization versus repolymerization in beta cells are distinct from one another. While microtubule destabilization is ATP-production and kinase-dependent (Ho et al., 2020), microtubule nucleation at the beta-cell Golgi requires cAMP and cAMP effector EPAC2 (Trogden et al., 2019), another metabolic signaling axis involved in GSIS (Ramos et al., 2008; Renstrom et al., 1997). This suggests that the amount of microtubule polymer can be fine-tuned by relative inputs of those two pathways. In addition, microtubule subsets predominantly affected by those pathways are also distinct, meaning that while the microtubule polymer mass is mostly sustained, the balance between different microtubule subsets is likely tilted at the time of secretion stimulation. We will next discuss how changing specific microtubule subsets and their relative representation within a cell affects beta-cell function and fitness.

Functions of Distinct Subpopulations of Beta-Cell Microtubule Network

Complete depolymerization of MTs by nocodazole leads to enhanced GSIS (Zhu et al., 2015; Trogden et al., 2021), laying a base for our model that MTs serve as one of the “filters” for regulated, dosed secretion levels. What are the functions of distinct microtubule subsets and how do they affect secretion?

The net movement of insulin granules is non-directional and has characteristics of sub-diffusion, or random walk (Tabei et al., 2013; Zhu et al., 2015). This is, however, not true diffusion: the beta-cell cytoplasm is too crowded for IG to move unless they are forcefully

transported by molecular motors. Non-directional transport likely arises from a convoluted configuration of microtubule tracks in the beta-cell interior (Varadi et al., 2003; Zhu et al., 2015), where IGs frequently switch tracks and/or follow buckled microtubule loops (Figure 5). In addition, IGs likely often get restrained by the dense microtubule meshwork and other components of the crowded cytoplasm.

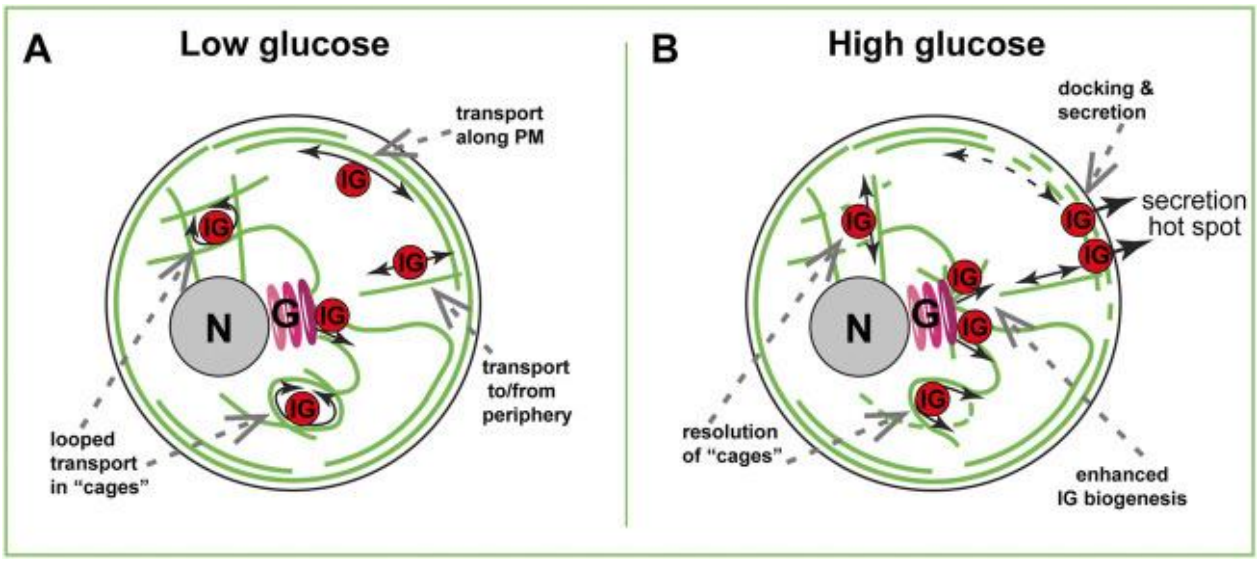

Figure 5. MT-dependent IG transport in a beta cell

MT-dependent IG transport in a beta cell. **(A)** Steady-state basal glucose conditions. Low number of nascent IGs are formed at the Golgi (G) in a GDMTs-dependent manner. In the inner cytoplasm, many IGs are trapped in microtubule cages and undergo looped transport. At the cell periphery, sub-membrane and randomly oriented MTs serve for bi-directional IG transport. **(B)** High-glucose triggered IG transport. Partial destabilization of inner meshwork allows for the resolution of "cages" and rare directional transport events. Local destabilization of submembrane MTs allows for interruption of IG withdrawal from the hot spots, leading to docking and secretion. Facilitated GDMT formation supports new IG biogenesis to replenish the IG population. Golgi, (G). Nucleus, N. Plasma membrane, PM.

In the absence of other factors, sub-diffusive transport should move IGs down the concentration gradient: from the areas of high IG abundance to the areas of low IG abundance. Under conditions of IG depletion at the periphery after an extreme secretion wave (degranulation), this would deliver IGs from the cell interior to the cell periphery [positive microtubule regulation of secretion, as proposed in (Boyd et al., 1982; Lacy, 1972; Rorsman and Renstrom, 2003). Net IG transport in a healthy beta cell does not enrich IG concentration at the cell periphery (Zhu et al., 2015), probably due to an ample IG abundance at that location (the lack of IG gradient). However, instances of direct IG movement along MTs (Figure 5) have been reported (Varadi et al., 2002; Heaslip et al., 2014; Hoboth et al., 2015). Such rare events deliver recently produced (young) insulin granules toward the periphery for secretion regardless of the gradient and have been proposed to serve as a positive microtubule regulation of secretion in functional beta cells (Hoboth et al., 2015).

Instances of direct IG movement along MTs were also reported when observing IG transport by TIRF microscopy, which by design visualizes only peripheral, submembrane IGs (Varadi et al., 2003; Zhu et al., 2015). Such movements are consistent with utilizing peripheral MTs parallel to the membrane (Figure 5), (Bracey et al., 2020). Those submembrane MTs get destabilized and fragmented upon glucose stimulation (Ho et al., 2020; Muller et al., 2021), prompting a hypothesis that this microtubule array must be interrupted for secretion to occur (Figure 5B). Indeed, preventing microtubule destabilization by taxol treatment inhibits GSIS (Howell et al., 1982; Zhu et al., 2015). Our computational model predicts that submembrane MTs, as long as they are connected with the inner microtubule network and serve as tracks for bi-directional IG transport, will promote the removal of IGs from the periphery, acting like a “sponge” (Bracey et al., 2020).

Interestingly, both computational (Bracey et al., 2020) and experimental (Hu et al., 2021; Zhu et al., 2015) data indicate that destabilization of submembrane MTs in the absence of glucose trigger does not strongly influence the amount of IGs at the periphery. Accordingly, at basal glucose levels, effects of microtubule destabilization on secretion are not detectable (Zhu et al., 2015; Trogden et al., 2021) unless the accumulated effects over several days are evaluated (Ho et al., 2020). However, destabilization under conditions of active IG retention [glucose-activated IG-plasma membrane association, or docking (Nagamatsu, 2006; Nagamatsu and Ohara-Imaizumi, 2008)], leads to a dramatic IG accumulation at the plasma membrane (Zhu et al., 2015; Hu et al., 2021). We speculate that microtubule destabilization promotes docking by eliminating fast IG movement and allowing for longer IG

dwelling in the proximity of docking molecular machinery (Figure 5B). It is also possible that active transport physically breaks emerging protein interactions and rips some already docked IGs away from the secretion sites. Importantly, IG docking and secretion do not occur randomly across the plasma membrane. Rather, it is allowed only at so-called secretion “hot spots”, cortical/plasma membrane locations where clustered exocytic machinery targets secretion into the bloodstream (Fu et al., 2017; Ohara-Imaizumi et al., 2019; Yuan et al., 2015b). MT-dependent mechanisms restrict functioning of those hot spots: microtubule destabilization by nocodazole increases the number of actively secreting hot spots per cell (Trogden et al., 2021). In part, the hot spots are activated in otherwise dormant, non-secreting beta cell subpopulation. This suggests that the differences in microtubule stability observed over beta cell population in an islet might be one of the mechanisms of functional beta-cell heterogeneity, reviewed in (Miranda et al., 2021). microtubule presence also restricted the number of IGs secreted at each hot-spot location. This implies that if MTs act *via* removal of IGs from the docking sites, they remove all IGs from some secretion loci, and only a percent from others. Exact microtubule organization and dynamics at secretion hot spots are unknown, and whether it is differential between hot spots, is yet to be understood. It also cannot be excluded that MTs regulate secretion hot-spot machinery through a different, non-IG-transport-dependent mechanism. For example, the turnover of hot-spot structural elements could be regulated by MTs similar to integrin and membrane receptor recycling (Balasubramanian et al., 2007; Pellinen et al., 2006; Yoon et al., 2005). Along these lines, MTs were shown to promote the localization of clathrin pits to the vicinity of insulin secretion sites, which is necessary for compensatory endocytosis, and, potentially, molecular component turnover during secretion responses (Yuan et al., 2015a).

Considering microtubules roles in various trafficking processes in a beta cell besides IG transport and positioning, it is important to consider functions of MT-dependent transport at earlier stages of insulin biogenesis. MTs are known to promote every stage of protein production and trafficking in the cytoplasm, including mRNA transport, ER shaping, ER-to-Golgi and Golgi-to-ER trafficking, and exit of secretory vesicles from the trans-Golgi network (TGN) (Luini et al., 2008; Palmer et al., 2005; Suter, 2018). It is plausible that all same steps are regulated in beta cells and influence insulin production, as suggested by early studies (Malaisse-Lagae et al., 1979). It is indeed true for efficient budding on nascent IGs off the TGN (Figure 5B): under high glucose conditions when IG biogenesis must be intensified, without efficient microtubule nucleation at the Golgi IG biogenesis fails (Trogden et al., 2019). This means that GDMTs are critical in replenishing IG population after each secretion cycle and maintaining beta-cell fitness. This function, likely similar to what was described for post-Golgi

carrier formation during constitutive secretion (Polishchuk et al., 2003), indicates an important microtubule contribution to the positive regulation of insulin secretion at the IG biogenesis stage.

Thus, the microtubule network in beta cells promotes IG availability in the long-term (*via* biogenesis and distribution in the cytoplasm) but restricts IG secretion in the short-term (by withdrawing IGs from secretion sites).

Microtubule-Dependent Molecular Motors and Their Role in Glucose-Stimulated Insulin Secretion

As summarized above, we are starting to understand how microtubule networks are organized and metabolically tuned in beta cells. Besides rearranging the microtubule geometry, IG transport can be tuned by activation of molecular motors or by changing the capacity of MTs to serve as tracks for specific motors (Figure 6 A,B) (Monroy et al., 2018; Yu et al., 2015). MT-dependent motors are recognized by their capacity to move toward the plus- or minus- end of a MT. In a non-differentiated cell with a radial microtubule network plus-end directed motors drive center-to-periphery (anterograde) transport, while minus-end directed motors drive periphery-to-interior (retrograde) transport. At this point, we do not have a good understanding of MT plus and minus end distributions within complex beta-cell microtubule networks. With largely non-centrosomal long-lived MTs, a significant microtubule population being parallel to the plasma membrane, and many short microtubule fragments, it is difficult to predict their polarity. Thus, it is elusive whether plus- or minus-end directed transport will be more efficient in taking IGs to or from the cell border and even less clear, to or from secretion hot spots. To understand specific motor functions, it is important to gather more knowledge on microtubule polarity and the regulation and function of specific motors in beta cells.

The major molecular motor that is thought to drive insulin transport is conventional kinesin, or kinesin-1 (KHC, KIF5b) (Balczon et al., 1992; Monroy et al., 2018; Varadi and Rutter, 2002; Varadi et al., 2003; Yu et al., 2015). It is robustly present at isolated IGs (Balczon et al., 1992), and colocalized with insulin-containing vesicles in beta-cell lines (MIN6 & INS-1) (Varadi and Rutter, 2002). Inactivation of kinesin-1 in MIN6 cells results in seized IG movement (Varadi et al., 2003). Moreover, a variety of kinesin-1 loss-of-function approaches in cell lines and in mice lead to decreased GSIS levels (Meng et al., 1997; Varadi et al., 2003).

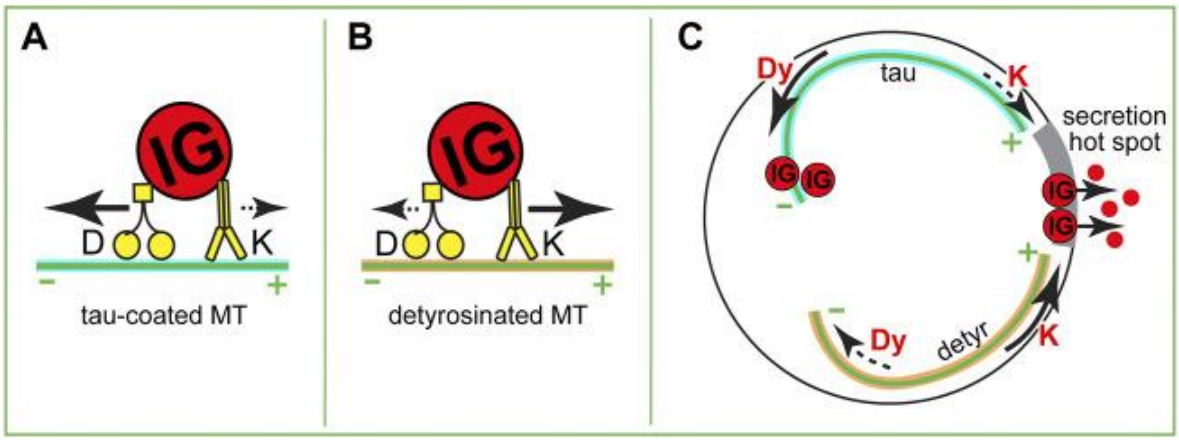

Figure 6. Hypothetical roles of MT-dependent molecular motors in IG transport

(A, B) Variants of a tug-of-war between dynein and kinesin-1. **(A)** On a tau-coated MT, dynein overcomes kinesin-1 and transports an IG toward the minus end. **(B)** On a detyrosinated MT, kinesin-1 overcomes dynein and transports an IG toward the plus end. **(C)** A variant of IG delivery-withdrawn regulation. If in high glucose submembrane MTs are partially depolymerized so that the plus ends of remaining MTs are oriented toward a secretion hot spot (gray), different microtubule modifications could result in either withdrawal (dynein-dependent transport on a tau-coated MT) or delivery (kinesin-1-dependent transport on a detyrosinated MT) of IGs to the secretion sites.

The importance of kinesin-1 for GSIS is consistent with the glucose-dependent regulation of kinesin-1 activity. Interestingly, kinesin-1 heavy chain is heavily phosphorylated at basal (low glucose) conditions (Donelan et al., 2002). Kinesin-1 phosphorylation by a variety of kinases has been associated with inhibited motor activity, data accumulated mostly *in vitro* and in neurons (Morfini et al., 2016). Kinesin-1 becomes dephosphorylated upon high glucose stimulation (Donelan et al., 2002), which is correlated with faster insulin granule movement (McDonald et al., 2009; Zhu et al., 2015).

Collectively, these data strongly indicated that kinesin-1 positively regulated insulin secretion, either *via* promoting the steady-state distribution of IG in the cytoplasm, or by specifically targeting IGs to secretion hot spots. The first option would result from the already described non-directional sub-diffusive transport (Tabei et al., 2013a; Zhu et al., 2015). The second option assumes the existence of a microtubule subset that has an accumulation of microtubule plus ends at secretion hot spots and favors kinesin-1 movement toward those spots (Figure 6C). Such a subset is yet to be detected in beta cells, but it could be created *via* such mechanisms as detyrosination (Figure 6B), MAP7 accumulation, or other MAP/tubulin PTM variations (Barlan et al., 2013; Monroy et al., 2018; Yu et al., 2015).

Very little is known about the role of other MT-dependent motors in insulin transport. Retrograde transport of granules was implicated in the retrieval of granules away from the secretion sites during kiss-and-run exocytosis (Varadi et al., 2003), however, because of the lack of clarity in microtubule organization and polarity at those sites, it is yet unclear whether it is dynein or another motor that drives such retrieval. It is tempting to extrapolate the role of dynein as a “brake” that slows down plus-end directed movement [tug-of-war mechanism reported for other cell types (Bryantseva and Zhapparova, 2012)] to beta cells (Figure 6A,B), however this hypothesis has not been tested yet. Interestingly, dynein activity is dramatically decreased on detyrosinated MTs (McKenney et al., 2016), which would lead to the release of a brake on kinesin-1 movement and make detyrosinated MTs strongly preferred tracks for plus end-directed IG transport (Figure 4). Another extrapolation from the neuronal scenario calls for testing whether a local accumulation of specific MAPs [e.g. tau enrichment at the peripheral microtubule bundle: tau regulates the efficiency of several motors, restricting kinesin-1 but not dynein movement (Chaudhary et al., 2018; Dixit et al., 2008; Tan et al., 2019; Vershinin et al., 2007)] defines which motor takes advantage for the movement of IG in a certain direction or to a certain location (Figure 6A). Additionally, a variety of other MT-dependent motors that are expressed in beta cells at lower levels might be important for fine-tuning IG transport.

Finally, it is important to consider the role of MTs and microtubule motors in the transport of other beta-cell components, positioning of which can have indirect yet very important effects on insulin secretion. For example, the scaffolding of transcription factor SP1 at MTs by kinesin KIF12 promotes GSIS and glucose homeostasis in mice *via* regulating the oxidative stress (Yang et al., 2014). It is known from other cell models that kinesin-1 can reconfigure the microtubule network *via* transport and intracellular positioning of microtubule fragments (Jolly and Gelfand, 2010). The main glucose-processing stations in cells, mitochondria, are positioned at the sites of energy consumption by microtubule motor-dependent transport [e.g., (Wang and Schwarz, 2009)]. An important process of insulin degradation/turnover could also be dependent on microtubule transport, since in other cell types, lysosome movement is mediated by both kinesin-1 (Hollenbeck and Swanson, 1990) and dynein motors (Harada et al., 1998; Jordens et al., 2001). MT-motor-dependent transport is also crucial for the organization of many other cellular features which could contribute to beta-cell fitness.

Conclusion

To conclude, we are currently at an exciting nucleation point where increased understanding of microtubule organization and regulation will inform how GSIS is precisely tuned in endocrine islet beta cells. Specifically, we now know that the beta-cell microtubule network is built in a unique configuration. This configuration, surely the microtubule stability and possibly also the 3D precise arrangement, is varied within the cell population to contribute to beta-cell functional heterogeneity. We also know that the microtubule network is remodeled downstream of glucose in such a way that both MT-dependent insulin biogenesis and secretion are allowed. Yet, mere microtubule presence serves as a negative regulator, adding to other "filter" mechanisms that prevent insulin over-secretion. Kinesin-1 is specifically activated by glucose to support GSIS, and there is still an intriguing possibility that other MT-dependent motors act in concert with kinesin-1 for the precision and restriction of the response. Thus, future studies to illustrate how MT-regulators and motor proteins interact are essential for a better understanding of beta-cell function.

Another intriguing area of future research is dissecting the cooperation and hierarchy of the secretion-restricting "filters". To this end, depolymerization of the actin cytoskeleton, which strongly promotes GSIS (Li et al., 1994; Thurmond et al., 2003; van Obberghen et al., 1973), also leads to a partial microtubule network disruption and eliminates MT-dependent regulation of secretion (Zhu et al., 2015). Furthermore, microtubule depolymerization affects neither glucose-induced calcium influx nor secretion enforced by membrane depolarization (Mourad et

al., 2011; Trogden et al., 2021), suggesting that the calcium-dependent component of GSIS is not controlled by MTs. At the same time, the intriguing question whether and how calcium-independent mechanisms downstream of glucose are affected by microtubule presence has received some mixed answers (Mourad et al., 2011; Trogden et al., 2021), indicating a potential for yet-unknown, condition-dependent, cooperation of those pathways. Studies on actin-microtubule cross-regulation in IG localization and Ca^{2+}-dependent vesicle-plasma membrane fusion should not only help with our understanding of diabetes, but also serve as a prototype in understanding how different cell types leverage the regulation and configuration of MTs to serve distinct physiological functions.

Chapter 3
Microtubules Regulate Localization and Availability of Insulin Granules in Pancreatic Beta Cells

This chapter has been adapted from Bracey KM, Ho KH, Yampolsky D, Gu G, Kaverina I, Holmes WR. Microtubules Regulate Localization and Availability of Insulin Granules in Pancreatic Beta Cells. Biophys J. 2020 Jan 7;118(1):193-206. doi: 10.1016/j.bpj.2019.10.031. Epub 2019 Oct 31. PMID: 31839261; PMCID: PMC6950633.

Introduction

Deregulated GSIS results in diabetes, a disease that afflicts ~9% of the population in the USA (DeFronzo et al., 2015; Kahn et al., 2014; Stokes and Preston, 2017; Swisa et al., 2017). Thus, elucidating how GSIS is regulated is of fundamental importance in understanding glucose homeostasis at both the cellular and systemic level. Pancreatic islet beta cells are the insulin factories in the body. Here, insulin is produced and sorted through the endoplasmic reticulum and the Golgi (Fu et al., 2013). Secretory insulin vesicles are generated at the *trans*-Golgi network, and those vesicles mature into hard-core granules that are distributed through the cell's cytoplasm for regulated secretion.

The major stimulant for insulin secretion is high glucose, whose entry into and subsequent metabolism in beta cells increases the ATP/ADP ratio, triggering insulin secretion (Rorsman and Ashcroft, 2018). The amount of secreted insulin is of critical importance for metabolism and health because over- or under secretion leads to hypo- or hyperglycemia in patients, respectively. A main determinant of insulin secretion dosage at given stimuli is the number of readily-releasable insulin vesicles. These vesicles are biochemically capable of anchoring at the secretion sites and are close enough to the plasma membrane to do so (Wang et al., 2009). Here, we investigate how cells use the cytoskeleton to regulate this readily releasable pool by controlling the number of granules near the plasma membrane as well as their availability for anchoring.

Although numerous intracellular factors regulate the localization and availability of insulin granules, it has long been thought that the cytoskeleton has a critical role (Arous and Halban, 2015; Lacy, 1975; Roux et al., 2016). Microtubules (MTs) and MT-dependent molecular motors are the major transport system in mammalian cells (Barlan and Gelfand, 2017; Vale, 2003). In many cell types, MTs extend toward the cell periphery in radial (mesenchymal cells) or parallel (neurons, columnar epithelia) arrays, allowing them to serve as long-distance transport highways, for example, for delivery of secretory vesicles, among other functions (Baas and Lin,

2011; Kapitein and Hoogenraad, 2011; Muroyama and Lechler, 2017; Vinogradova et al., 2009). In pancreatic *beta* cells, MTs also serve intracellular transport roles (Donelan et al., 2002; McDonald et al., 2009; Varadi and Rutter, 2002), but microtubule function in secretion is complex and incompletely understood. A number of observations indicate that prolonged insulin secretion is attenuated in the absence of MTs (Boyd et al., 1982; Lacy, 1972). In the long term, MT depletion inhibits new insulin granule formation by interfering with insulin transport through the endoplasmic reticulum and the Golgi ((Malaisse-Lagae et al., 1979) and our unpublished data). Reduced secretion could, however, be explained by lack of new granule production or delivery (Hoboth et al., 2015). Without MTs, the net movement of existing secretory insulin granule movement is significantly slowed (Zhu et al., 2015), potentially influencing delivery. Interestingly, in our recent finding, short-term depletion of MTs resulted in immediate facilitation of exocytosis and, as a result, increased GSIS, which is consistent with earlier findings (Devis et al., 1974; Somers et al., 1974). Commensurately, microtubule enrichment in *beta* cells both in taxol-treated islets and in diabetic mice (Zhu et al., 2015) was associated with decreased secretion. Thus, although all studies agree that MT-dependent transport is needed for new insulin granule production, it is not readily apparent how or why MTs regulate secretion of the readily releasable pool or how transport of existing granules is linked to GSIS. Here, we test the hypothesis that this link between MT-based transport and insulin secretion is a consequence of the cytoplasmic architecture of *beta* cells.

One important feature of *beta* cell cytoplasm is the abundance of premade insulin granules in a resting cell. Estimates indicate individual *beta* cells contain on the order of 10,000 insulin granules (Dean, 1973) of 100–300 nm in diameter (Rorsman and Renstrom, 2003), which are tightly packed in the cytoplasm. At any stimulation, only a small portion of these vesicles was secreted (~1% within an hour of high glucose stimulation (Rorsman and Renstrom, 2003)). This raises the question of why these abundant vesicles should be transported for GSIS. Additionally, granule motions analyzed in *beta* cell culture models (Tabei et al., 2013a) and in intact pancreatic islets (Zhu et al., 2015) were found to be random and undirected. This is not surprising, given that super-resolution imaging of the microtubule cytoskeleton in intact islets has indicated that *beta* cell MTs form a spaghetti-like random meshwork (Zhu et al., 2015), which is very different from directed microtubule arrays in cells that use MTs for directional long-distance transport. Thus, even if transport were important for GSIS, what random transport on an unstructured microtubule meshwork would accomplish and how it would influence GSIS is unclear.

Our prior data provide a clue to how MTs influence GSIS. In the absence of MTs, high glucose stimulation leads to accumulation of granules at the cell periphery (Zhu et al., 2015), possibly due to the stimulation of glucose-dependent priming or docking (Gandasi et al., 2018). Interestingly, the presence of MTs prevents this excess accumulation, suggesting MT-based transport may regulate granule localization even when effective motions (the motion resulting from multiple motors potentially interacting with multiple MTs) are random and undirected. Total internal reflection fluorescence (TIRF) microscopy data point to two possible mechanisms for this regulation. First, quantification of delivery and withdrawal of granules from the cell periphery demonstrates that MT-dependent transport is required to maintain the proper balance between delivery and removal (Zhu et al., 2015). Second, the motions of granules near the membrane (in the TIRF field, within ~200 nm of the plasma membrane) are predominantly parallel to it (Varadi and Rutter, 2002), indicating there may be organization to the microtubule network near the membrane and that insulin granule motions may not be random there. To clarify how MTs influence insulin localization and availability, we utilize super-resolution microscopy to image the structure of the microtubule meshwork near the plasma membrane and computational modeling to assess how the interactions between granules, the meshwork, and the plasma membrane influence GSIS.

There are generally two populations of MTs in cells: dynamic MTs that are undergoing "dynamic instability" (Brouhard and Rice, 2018; Mitchison and Kirschner, 1984) and stable MTs, characterized by the presence of detyrosinated tubulin (Glu-tubulin) among other modifications (Garnham and Roll-Mecak, 2012; Hammond et al., 2008; Roll-Mecak, 2019). Glucose alters the microtubule network in potentially important ways. Glucose stimulation destabilizes and depolymerizes stable MTs and increases microtubule nucleation and growth rates. This makes the microtubule network significantly more dynamic, whereas microtubule density is only modestly altered. Glucose is also well known to activate docking molecules, which are necessary for GSIS. This body of work thus suggests that glucose stimulation influences granule transport, which in turn alters GSIS.

We hypothesize that MTs have a dual role in negatively regulating GSIS: MTs 1) enhance withdrawal of granules from the periphery to the interior and 2) prevent anchoring and subsequent secretion of those at the periphery (e.g., by preventing the formation of or breaking bonds between granules and the anchoring machinery). This is a compelling hypothesis, but our understanding of microtubule control on cytoplasmic distribution of insulin granules remains fragmented and insufficient. In particular, the abundance of insulin, the apparently random

nature of the microtubule network, and the seemingly random but complex nature of granule motions (Tabei et al., 2013a) make it difficult to deduce how MTs influence GSIS. To test this hypothesis, we developed a computational model of intracellular insulin granule dynamics to investigate how microtubule dynamics influence insulin granule localization and availability. The basic elements of this model (e.g., transport rates and MT-binding rates) were calibrated to data and then tested against independent results, including TIRF observations of peripheral granule densities, along with quantification of GSIS under different conditions, to determine the conditions in which the model matched observations. In this way, the model and experimental observations were jointly used to infer how interactions between microtubule dynamics, granule dynamics, and membrane anchoring influence GSIS.

In this study, we investigated two specific questions, both of which are important to understanding GSIS: how MT-based transport influences the density of insulin granules near the plasma membrane and how the binding of granules to the microtubule cytoskeleton influences their membrane anchoring, both of which are a prerequisite to exocytosis. Given our focus on the dynamics of granules near the plasma membrane, we quantified the structural characteristics of the microtubule network near the membrane (directionality in particular) in pancreatic *beta* cells. These data were used in conjunction with prior three-dimensional tracking of granule motions (Zhu et al., 2015) to develop and simulate a discrete, two-dimensional (2D) computational model of insulin granule dynamics within a single cell. Results of this modeling support the aforementioned hypothesis that MT-based transport negatively regulates GSIS in two important ways: by 1) increasing the rate of transport of granules away from the plasma membrane and 2) reducing the ability of those that are near the membrane to stably anchor to it.

Materials and Methods

Discrete model description

This discrete model accounts for four essential features that impact the transport of granules: 1) transport along MTs, 2) transport independent of MTs, 3) binding and unbinding of granules to MTs, and 4) tethering of granules (that are sufficiently close) to the cell membrane, which renders them immobile (illustrated in Figure 7 *B*). We briefly discuss how each of these features is encoded into the model and how aspects of it are calibrated to data.

Modeling microtubule independent transport

We approximately modeled the cell as a 5 μm radius circle with a 1 μm hole cut out (representing the nucleus). A regular 2D grid is constructed on this cellular domain, and the motion of granules on this lattice is modeled as a subdiffusive (anomalous diffusion with a mean-square displacement (MSD) scaling exponent <1) random walk. Granule motion is assumed to obey the equation of motion for overdamped fractional Langevin equation (FLE) representing viscoelastic subdiffusion:

$$\gamma\int_{-\infty}^{t}K(t-s)\vec{v}(s)ds=F_{st},$$

(1)

where v is the velocity of the granule, γ is the drag coefficient for the granule, $\boldsymbol{K}$ is a memory kernel encoding history dependent viscoelastic effects, and F_{st} is the stochastic forcing obeying the appropriate fluctuation dissipation theorem. Here, the drag coefficient satisfies $\gamma = 2k_BT/(\Gamma(1+\alpha)D)$, where k_BT is the standard thermal noise constant and D, α are estimated from data (see (Lutz, 2001) for further details of the FLE). The kinetic lattice Monte Carlo method for simulating the overdamped FLE from (Fritsch and Langowski, 2012) is used to simulate motion.

Constructing the microtubule network and modeling MT-mediated transport

To simulate MT-mediated motion, we first populated the in silico cell with a microtubule network. We did so by essentially growing a network of 500 discrete, independent, and noninteracting MTs. Of these, 250 are short (mean length 2 μm) and 250 long (mean 5 μm). Short MTs are included to account for possible dynamically unstable MTs, whereas long ones are thought of as stable (similar results are found if all MTs are the same length, though). We specify a start point and initial growth direction for each MT. The microtubule is then elongated in a straight line until it interacts with the cell periphery (if it does so at all). If the growing microtubule interacts with the cell border, it either terminates with probability p or bends and grows parallel to the cell periphery with probability $1 - p$. Note that those MTs that terminate do not depolymerize. Thus, all probabilities (p) lead to the same interior microtubule densities. It is only the peripheral microtubule densities that will differ as a function of p. We also note that other potential mechanisms could lead to the formation of peripheral microtubule arrays aligned with the plasma membrane. For example, membrane-associated MT-binding proteins could potentially bring them into proximity. Our purpose here is to not investigate the formation of this structure, but rather, its consequences. We thus use this method of constructing the microtubule network only as a means to generate microtubule meshes with different properties near the boundary.

For most simulations, a value of $p = 0$ is chosen, corresponding to a peripherally aligned population of MTs forming. However, in **Error! Reference source not found.**, the effect of this microtubule structure parameter is considered. For simplicity, we assume the MTs are fixed in place once grown and thus do not model the detailed dynamics of remodeling of the microtubule cytoskeleton by motors themselves (Hillen et al., 2017; White et al., 2015). The model does incorporate dynamic instability (Goodson and Jonasson, 2018) of MTs through removal and replacement of MTs with a specified rate. We fix the average microtubule lifetime at 1000 s, though we also consider the effects of short microtubule lifetimes. As removal and replacement of MTs has much the same effect on granule motility as microtubule binding and unbinding, which are considered in somewhat more detail, we do not exhaustively explore the effect of microtubule catastrophe dynamics.

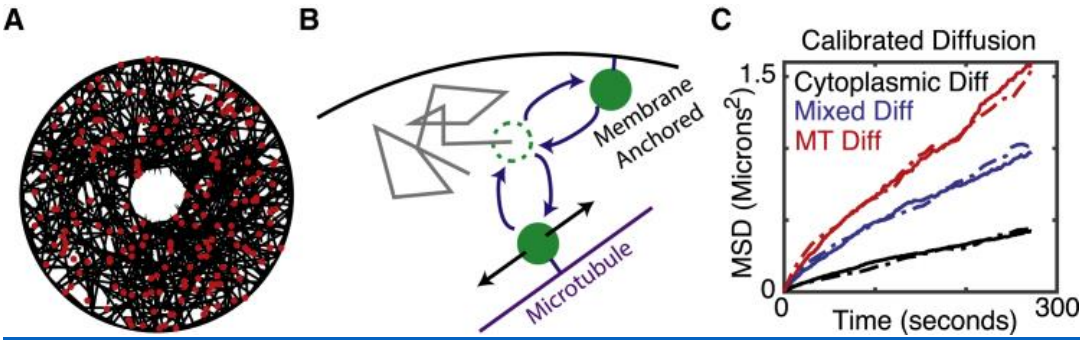

Figure 7. Description of model

Description of model. (*A*) A snapshot of a simulation with 500 microtubules and 200 insulin granules is shown. (*B*) A schematic of the basic model elements—including free diffusion, binding of granules to MTs, diffusion along MTs, and membrane anchoring—is given. The dashed green circle indicates the present state of a granule. The gray line indicates a possible diffusive path. The filled green circles depict potential MT-binding and membrane-binding events. (*C*) An illustration of calibrated diffusion is given. Dashed curves are data, and solid curves are simulated. Cytoplasmic and MT-bound diffusion coefficients were calibrated based on the red and black curves, and the relative fraction of time a granule spends in these two modes of motion was calibrated based on the blue curve.

Motion of granules is strongly subdiffusive even in the absence of actin, suggesting that individual microtubule motors are not moving granules along MTs in a directed fashion (this

would be superdiffusion). To be clear, we are not suggesting that microtubule motions are motor independent, only that they are not “ballistic” or directed, as is commonly the case with motor-driven motions. How might motor-driven motions, which typically generate near-ballistic motion, give rise to random motion? It is possible that each granule has a number of motors bound to it at any given time that are constantly competing to be the driver of motility. In this scenario, motions could be directed on very short timescales while appearing random on observed timescales because of the action of multiple motors. This is, however, beyond the scope of this article, and we only model the motions on observed timescales (as subdiffusive) rather than model the actions of large numbers of motors, for which we do not have constraining data. We thus do not model the dynamics of individual motors. Rather, MT-mediated granule motion is modeled as a one-dimensional subdiffusive random walk on the microtubule to which the granule is bound. The same FLE equation of motion (Eq. 1 above) describes this motion, and the same method of simulation is used.

Granule binding, unbinding, and tethering

It is highly likely that granules bind and unbind from the microtubule lattice, and thus, their aggregate motion is in some sense an interpolation of motion in those two forms. We assume that an unbound granule can bind to any microtubule within 250 nm of its center (assuming a 150 nm granule radius along with an additional ∼100 nm reach of the motor head) with a per microtubule rate of binding k_{on}. Similarly, granules are assumed to unbind from MTs with a rate of k_{off}. These two rate constants are not individually accessible because we do not know what specific motors are involved or how granules interact with the dense network of MTs. As discussed, however, we can calibrate their ratio based on data to ensure that the relative fraction of time each granule spends undergoing (un)bound motility is appropriate. We thus fix the rate k_{off} = 1:30 to represent a roughly 30 s bound lifetime, which is in the same range found for the kinesin Kip2 ((Brissova et al., 2002)), and calibrate k_{on} accordingly. Doubling or halving this bound lifetime leads to similar results. Switching of granules from one microtubule to another is not directly modeled. However, when a granule unbinds from an MT, it can rebind to any other nearby MT. All simulations were carried out with k_{off} = 1:15, 1:60, yielding similar results.

Anchoring of granules to the cell membrane is modeled similarly, with granules within 250 nm of the cell border binding with a rate constant k_T and unbinding with a rate k_U. We do not have estimates for these rate constants or any way to constrain them directly. However, in this study, we vary the affinity by fixing the unbinding rate and modulating the magnitude of k_T to

determine how the relative strength of anchoring (i.e., the relative fraction of time an unbound granule spends tethered to the membrane) influences insulin granule dynamics (see Figure 10). We further consider two possibilities for which granules can or cannot tether: 1) that all granules can tether or 2) that only unbound granules can tether.

Calibrating motility and binding and unbinding parameters

Many of the parameters in this model are directly estimable from data. In particular, using granule motility data, we can extract the values of the subdiffusive exponent (α), the diffusion coefficients for bound and unbound granule motion (D for each), and the relative fraction of time the granule spends in the bound and unbound states.

The data we use for this are derived from (Zhu et al., 2015), in which the MSD of granule motion was measured in control cells, cells with the microtubule cytoskeleton removed, and cells with the actin cytoskeleton removed. First, from (Tabei et al., 2013a), it was determined that $\alpha = 0.75$. To calibrate the diffusion constants, we will rely on MSD data. For simplicity, we will assume that in the absence of actin, all motion is microtubule mediated, and in the absence of MTs, all motion is actin mediated. We can thus use the data in which actin is removed to calibrate the diffusion constant for microtubule motion and the data in which MTs are removed to calibrate the diffusion constant for non- microtubule motion. See Figure 7 *C* (*black* and *red curves*) for calibration results.

We can additionally use the control MSD data to calibrate the relative time each granule spends in bound and unbound states; the more time a granule spends in the MT-bound state, the higher its MSD will be and vice versa. We fix the value of k_{off} and vary the value of k_{on} until the MSD data of the amalgamated diffusion match that of control data (*blue curve* in Figure 7 *C*). For a list of all parameters for the discrete model, see Table 1.

Table 1. Synopsis of the Discrete Model Parameters

Parameter Name	**Value**	**Units**
Number of MTs	500	Number
Number of granules	1000	Number
Cell radius	5	μm
Nucleus radius	1	μm
Granule radius	0.3	μm
Subdiffusion exponent (α)	0.75	None
MT-bound diffusion constant (D_1)	0.015	$\mu m^2/s$
2D grid diffusion constant (D_2)	0.005	$\mu m^2/s$
Microtubule mean length (short, long)	2, 5	μm
Microtubule length standard deviation	2	μm
Microtubule catastrophe rate	1/1000	1/sec
Granule/MT-binding rate (k_{on})	1/8	$1/(s \cdot MT)$
Granule/ Microtubule unbinding rate (k_{off})	1/30	1/s
Granule/MT-binding radius	0.25	μm
Granule tethering rate (k_T)	0	1/s
Granule untethering rate	1/30	1/s
Granule tethering radius	0.25	μm

Simulation protocol

All simulations begin with each of the 1000 granules randomly placed in the cell for a pseudouniform distribution. The time step for simulations granule motions is chosen to be ΔT = 10 ms, with simulations running nominally for 300 s to achieve a steady state. The kinetic lattice Monte Carlo method requires that the spatial grid size be chosen appropriately so that $\Delta x = (2D\Delta T^{\alpha})^{0.5}$. Because the diffusion constant for the MT- and non-MT-mediated motions are different, this yields spatial step sizes of 18 nm for the 2D lattice motions and 30 nm for the one-dimensional motions on MTs. In select simulations, decreasing the time step to ΔT = 5 ms did not alter results. In all results presented, averages of 50 independent simulations are presented unless otherwise stated.

Mice

Mouse usage and handling followed the protocol approved by the Vanderbilt Institutional Animal Care and Usage Committee for Dr. Gu. Wild type CD-1 (ICR) mice were purchased from Charles River (Wilmington, MA). All mice were bred and handled following protocols approved by the Vanderbilt Institutional Animal Care and Use Committee. All mice used were males 8–10 weeks of age.

Islet isolation

Islet isolation followed the previously described procedure (Brissova et al., 2002). Briefly, mouse pancreata were distended by injecting 3 mL 0.8 mg/mL collagenase P (Sigma-Aldrich, St. Louis, MO) through the bile duct and digested at 37°C for 20 min. Islets were hand-picked and cultured to recover in Gibco RPMI 1640 Medium (Thermo Fisher Scientific, Waltham, MA) containing 11 mM glucose, 10% heat-inactivated fetal bovine serum (Atlanta Biologicals, Flowery Branch, GA), 100 IU/mL penicillin, and 100 μg/mL streptomycin.

Immunofluorescence

Isolated mouse islets were treated with 2.8 mM (low) or 20 mM (high) glucose in RPMI media for 2 h and fixed with 4% paraformaldehyde in phosphate-buffered saline with 0.1% saponin (Sigma-Aldrich). Immunofluorescence followed the described procedure (Zhu et al., 2015). Briefly, fixed islets were stained with primary antibodies at 4°C overnight, followed by another staining with fluorophore-conjugated secondary antibodies. After each antibody incubation, islets were washed three times using phosphate-buffered saline with 0.1% saponin. After staining, islets were mounted with Vectashield mounting media (Vector Labs, Burlingame,

CA) for microscopy. Primary antibodies used are rabbit anti-*beta*-tubulin (Abcam, Cambridge, MA), guinea pig anti-insulin (DAKO, Houston, TX), rabbit anti-detyrosinated tubulin (Millipore, Burlington, MA), and mouse anti-E-cadherin (BD Biosciences, San Jose, CA). Secondary antibodies used are goat anti-rabbit IgG-Alexa Fluor 488 (Abcam), goat anti-mouse IgG-Alexa Fluor 488 (Invitrogen, Grand Island, NY), and goat anti-guinea pig IgG-Alexa Fluor 650 (Thermo Fisher Scientific).

Microscopy and image processing

All images were captured using a Nikon Eclipse A1R laser scanning confocal microscope equipped with a CFI Apochromat TIRF 100×/1.45 oil objective (Nikon, Tokyo, Japan). The microscope is driven by Nikon Elements software. For directionality analysis, oversampled image stacks (50 nm^3 voxels) were acquired and thereafter deconvolved by NIS Elements Software using the Richardson and Lucy algorithm (15 iterations). All images presented in figures were single-slice confocal images, for which the brightness and contrast were adjusted consistently across every image to better present small structural features. MTs were thresholded using the variation Isodata Algorithm default in ImageJ. All values between 55 and 280 were considered positive and used for this analysis.

Image analysis

An image-analysis algorithm was developed to determine the alignment of each point on a microtubule with the nearest region of the cell border based on tubulin images. *beta* cells within an islet were selected based on their ability to express insulin. Single slices from a deconvoluted confocal stack were used for analysis. Taking into consideration that microtubule width is below the resolution limit of light microscopy techniques, neighborhood block size was approximated to the pixel size of the oversampled confocal image (50 nm^2). Analysis was applied within a mask based on thresholded tubulin images. The local orientation at each pixel of the tubulin image was derived using the method described in multiscale principal components analysis. The cell outline curve, manually constructed based on the E-cadherin staining, was smoothed and used to estimate orientation of the cell border. Each pixel in the tubulin image was associated with the nearest pixel of the boundary curve. After applying cell border and tubulin threshold masks, the angle difference between local orientation and boundary orientation at the nearest pixel was calculated per pixel of microtubule area (with zero indicating perfect parallel alignment). Results were weighed according to variance of local orientation to avoid data from lumps of tubulin bands of excessive density and microtubule crossings with

ambiguous configuration in the results. All pixels were manually sorted according to their distance from the cell border into 0.5 μm bins.

Results

Peripheral MTs in islet *beta* cells are coaligned with the cell border

Prior imaging of intact islets (Zhu et al., 2015) indicated that the microtubule network in *beta* cells appears to lack previously assumed radial directionality characteristic commonly seen in mesenchymal cells in culture and instead resembles an undirected random mesh. However, the directionality of MTs in *beta* cells has not been quantitatively characterized, and the functional consequences of variable directionality have not been computationally assessed. Here, we analyze the directionality of MTs in *beta* cells using a custom image-analysis algorithm. In subsequent sections, we use computational modeling to assess the consequences of the type of microtubule organization near the plasma membrane.

Intact mouse pancreatic islets were isolated and equilibrated according to a standard protocol. After a pretreatment in low and high glucose conditions, islets were fixed and immunostained for insulin to distinguish *beta* cells, E-cadherin for cell border identification, and tubulin for microtubule network identification. Confocal stacks of whole-mount islets were deconvolved for increased resolution (Figure 8, *A* and *B*). Single 2D slices of microtubule images were subjected to thresholding (Figure 8, *A* and *B*, *second from the right*), and the directionality of MTs was determined in respect to the cell border (Figure 8, *A* and *B*, *right*). Every pixel of the image was analyzed, with inconclusive pixels disregarded. Subsequently, microtubule directionality was quantified as a function of the distance from the cell border (Figure 8, *C* and *D*).

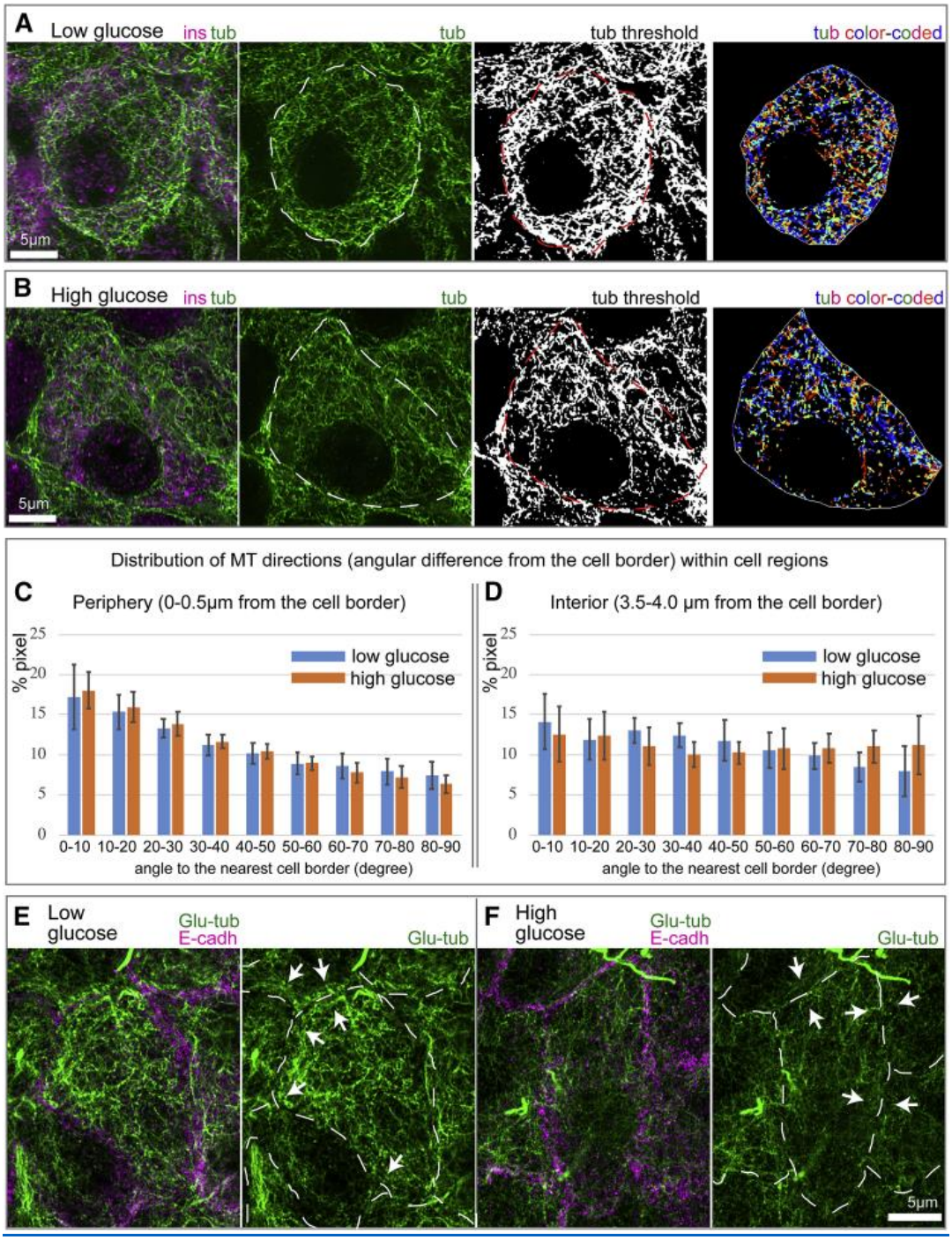
A
Low glucose
ins tub
tub
tub threshold
tub color-coded
5μm
B
High glucose
ins tub
tub
tub threshold
tub color-coded
5μm
Distribution of MT directions (angular difference from the cell border) within cell regions
C
Periphery (0-0.5μm from the cell border)
% pixel
low glucose
high glucose
0-10 10-20 20-30 30-40 40-50 50-60 60-70 70-80 80-90
angle to the nearest cell border (degree)
D
Interior (3.5-4.0 μm from the cell border)
% pixel
low glucose
high glucose
0-10 10-20 20-30 30-40 40-50 50-60 60-70 70-80 80-90
angle to the nearest cell border (degree)
E
Low glucose
Glu-tub
E-cadh
Glu-tub
F
High glucose
Glu-tub
E-cadh
Glu-tub
5μm

Figure 8.MTs parallel to the cell edge in beta cells are destabilized in high glucose.

MTs parallel to the cell edge in *beta* cells are destabilized in high glucose. (*A* and *B*) Examples of microtubule directionality quantification in low (*A*) and high (*B*) glucose are shown. Tubulin, green. Insulin (*beta* cell marker), magenta. Cell outline, as detected by E-cadherin staining, is shown as a dotted line on tubulin and thresholded images. The image on the right shows color-coded microtubule directions: parallel to the cell edge, blue; perpendicular to the cell edge, red. (*C* and *D*) Histograms of microtubule directionality within two cell regions are shown: periphery (*C*) and interior (*D*). Percentage of tubulin-positive pixels in the analyzed cell population is shown. MTs at the periphery tend to be parallel to the edge. Low and high glucose do not differ. Bars indicate averages over N = 12 and 11 cells for low and high glucose, respectively, and error bars indicate standard deviations. Pixel numbers in the analysis: 71,759 (low, periphery); 9622 (low, interior); 43,747 (high, periphery); 5833 (high, interior). Note that a lower number of pixels were identified in high glucose, consistent with the fact that MTs are destabilized under this condition. (*E* and *F*) Stable microtubule marker detyrosinated (Glu-)tubulin (*green*) in low (*E*) and high (*F*) glucose is shown. Cell-cell adhesions are stained for E-cadherin (*magenta*) in left-hand panels and outlined (*dashed line*) in right-hand panels. Note multiple Glu-tubulin-positive MTs parallel to the cell border (*arrows*) in low glucose (*E*). Glu-tubulin content is decreased in high glucose (*F*), indicating microtubule destabilization both across the cell and at the cell border (*arrows*). To see this figure in color, go online.

Our results indicate that in low glucose conditions, the distribution of microtubule angles in the cell interior and cell periphery are significantly different ($p < 0.05$ Kolmogorov-Smirnov (K-S) test, $D = 0.09 > D_{crit} = 0.01$). In the cell interior, the microtubule network lacks directionality and resembles a random interlocked mesh (Figure 8, *C* and *D*, *right*). However, MTs within a narrow peripheral region exhibit a significant coalignment with the cell border (Figure 8, *C* and *D*, *left*). Similar structural differences were seen in high glucose conditions ($p < 0.05$ K-S test, $D = 0.057 > D_{crit} = 0.017$). The fraction of MTs that were border aligned were similar in low and high glucose, although the number of detectable pixels was lower in high glucose, consistent with our previous finding of partial microtubule destabilization under high glucose conditions (Zhu et al., 2015). When the interior angular distributions of low glucose and high glucose are compared, the K-S test indicates the internal and peripheral distributions are not

statistically different between the two glucose conditions. Interestingly, visualization of long-lived (stable) MTs by detyrosinated (Glu-)tubulin staining detected many Glu-MTs coaligned with the cell periphery in low (Figure 8 *E*), but not in high (Figure 8 *F*), glucose. Because MTs parallel to the cell border are still observed in high glucose (Figure 8 *C*), we conclude that stability of this peripheral array is significantly diminished by glucose-triggered microtubule destabilization.

MTs generate counterpropagating density gradients that differentially deliver and remove granules from the cell periphery

In the remainder of this study, we develop and utilize computational modeling to assess how the microtubule organization features described above, along with MT- and non-MT-dependent transport processes, influence insulin granule localization. For specific model and implementation details, as well as a discussion of how parameters for the model were calibrated to data or chosen, see the Materials and Methods. Briefly, the model used here is composed of a discrete, 2D network of noninteracting MTs, along with a population of granules that undergo MT-dependent and independent motion. These granules are assumed to both bind and unbind to the microtubule network and to anchor to the plasma membrane when glucose is present.

Based on the above analysis, we consider a range of assumptions for how MTs interact with the plasma membrane. Computationally, we generate the microtubule network by growing individual MTs from a random seed location. We do not incorporate cyclical growing and shrinking phases of individual MTs (dynamic instability). However, we do allow for the random destruction and replacement of individual MTs (see Materials and Methods for further detail). We consider two assumptions for how MTs interact when they reach the border: they either terminate or bend and grow parallel to the periphery. By varying the likelihood of each in silico microtubule doing one or the other, we can vary the net orientation of the resulting peripheral network from being highly aligned to having no alignment. Because we do not know a priori the significance of this orientation on insulin granule dynamics, we explore the influence of this and the other model factors (e.g., docking rates) on peripheral granule density.

Granules are assumed to move randomly while on a given MT. Although granules can unbind from a given microtubule and subsequently bind to a new one, direct transitioning from one microtubule to another and competitive binding of a single granule to multiple MTs are not considered for simplicity. Granules that are anchored to the membrane are considered immobile. Finally, those granules that are neither anchored nor microtubule bound are assumed

to move randomly within the 2D cell. For further details and model calibration, see Materials and Methods.

We quantified (*Figure 9*, *A*–*C*) the simulated steady-state number of granules (total, microtubule bound, and unbound) near the cell border as a function of both the total number of cellular MTs and the peripheral alignment of MTs. Results indicate both influence granule densities. Here, “peripheral alignment” of MTs refers to the fraction of MTs that interact with the boundary and bend and grow parallel to it.

The presence of MTs always leads to an enrichment of granules near the cell periphery relative to densities when the microtubule network is completely removed (*Figure 9 A*). This is true for all microtubule densities and peripheral microtubule alignment conditions tested. In this study, we assumed that motors carrying granules stall at the tip of MTs. To ensure this is not the source of these results, we carried out identical simulations in which motors are assumed to disassociate at the tip and find similar results. Similar simulations were also performed in which granule motions are purely diffusive rather than subdiffusive, again with similar results, see (Bracey et al., 2020). This suggests that the microtubule network serves as a sponge that enriches granule densities near the cell border, which is likely the result of the increased density of microtubule tips near the cell periphery.

Interestingly, this enrichment effect appears to be weakened when the microtubule network is more aligned at the cell periphery. Specifically, when the microtubule network at the periphery is more aligned, fewer granules localize to the boundary. Further, when the network is highly aligned, peripheral granule density becomes essentially independent of total microtubule density. Further inspection of the peripheral densities of bound and unbound granules as a function of peripheral alignment (*Figure 9*, *B* and *C*) provides a clue to the cause of this observation. Increasing peripheral alignment has little influence on the number of bound peripheral granules but leads to a substantial reduction in the density of unbound peripheral granules. On net, this yields the observed inverse relationship between total peripheral granule density and peripheral microtubule alignment.

This suggest that an enrichment of peripherally oriented MTs would serve to 1) increase the total binding of peripheral granules to the microtubule network (thus reducing unbound granule numbers) and 2) transport those excess granules toward the cell interior (thus leaving the fraction of bound granules relatively unchanged). Critically, this transport of bound granules away from the periphery in the model is not due to directional motions of kinesin or dynein

motors because all granule motions are random and undirected. This raises an important question. If, at steady state, peripherally aligned MTs serve to soak up and transport granules away from the periphery, what counterbalances that net transport? To answer this, we quantified the density of bound and unbound granules as a function of radial distance from the cell center in simulations at steady state (*Figure 9*, *D* and *E*) for the two extreme cases of low and high alignment of peripheral MTs. In the highly aligned case (*Figure 9 E*), bound and unbound granule densities exhibit opposing density gradients, with unbound granules exhibiting a peripheral deficit and bound granules a peripheral enrichment. When peripheral MTs exhibit low alignment (*Figure 9 D*), these opposing gradients are not present. Thus, when there is a substantial number of peripherally aligned MTs, bound and unbound granules form counterpropagating gradients, with unbound granules flowing from the interior to the periphery and bound granules flowing from the periphery to the interior.

This counterpropagating gradient theory is consistent with our prior observations. We found, using TIRF microscopy, that the application of nocodazole (NOC) and glucose led to a ∼25% reduction in granule delivery but a ∼43% reduction in granule withdrawal (Zhu et al., 2015). Thus, removal of granules was more substantially impacted by removal of MTs than delivery, consistent with the counterpropagating gradient hypothesis in which MTs generate a net flow of granules from the periphery to the cell interior. In combination, these results suggest that the peripherally aligned network of MTs maintains a balance between delivery and withdrawal of granules and prevents excess accumulation near the plasma membrane.

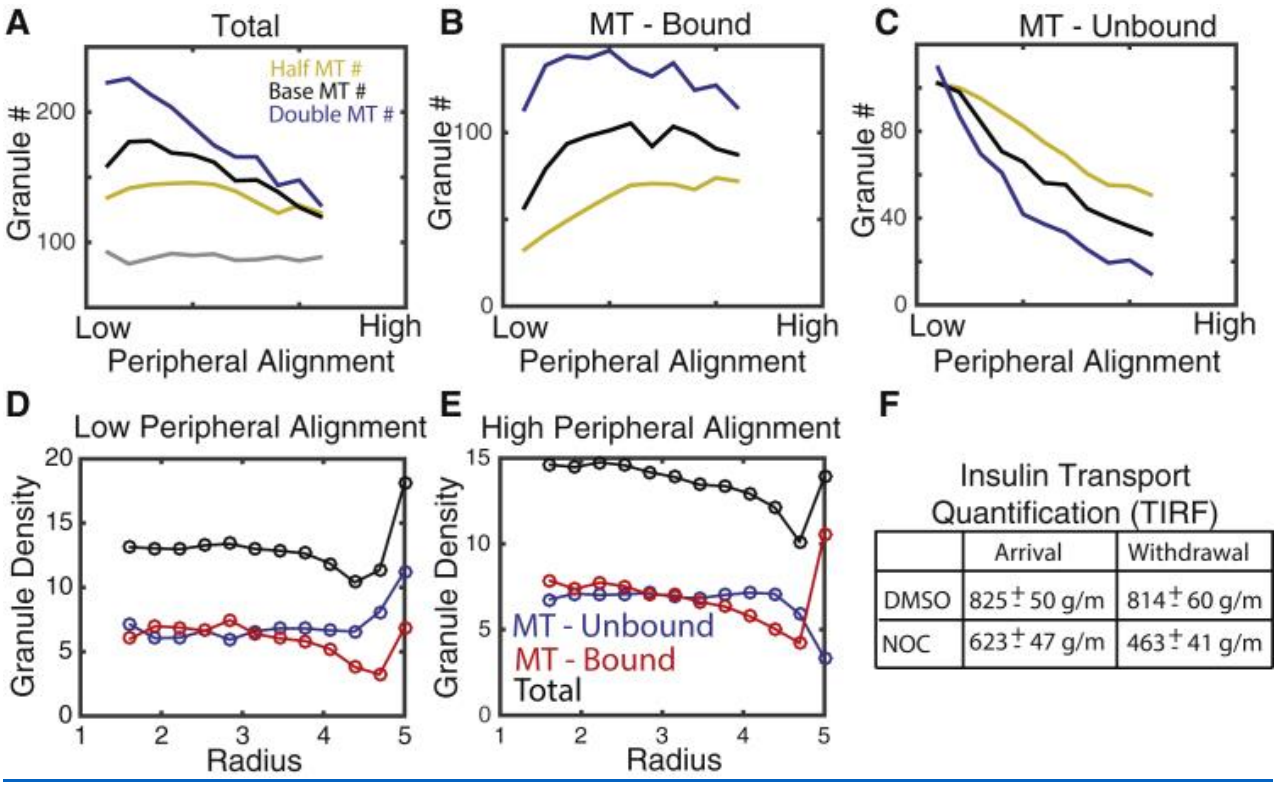

Figure 9. Effect of MTs on peripheral localization of insulin granules.

Effect of MTs on peripheral localization of insulin granules. (*A*) The total number of granules located within 250 nm of the cell membrane as a function of the peripheral density of MTs as well as the total density of MTs is shown. “Base MT#” refers to simulations with 500 total MTs, and “Half” and “Double” refer to 250 and 1000 MTs, respectively. The gray line depicts the number of peripheral granules when the microtubule network is removed and the density distribution achieves steady state. (*B*) The number of MT-bound granules is shown. (*C*) The number of unbound granules is shown. (*D* and *E*) The radial distribution of bound, unbound, and total granules in low and high peripheral density cases is shown. (*F*) A table depicting change in granule arrival delivery to the cell periphery in cells from experiments in our previous publication is given (data reproduced from (Zhu et al., 2015)). “Arrival” and “Withdrawal” indicate the rate of appearance and disappearance of granules in the TIRF field in control and NOC conditions. To see this figure in color, go online.

Changes in radial diffusion due to microtubule alignment are the source of counterpropagating gradients

We investigated two potential effects of peripheral microtubule alignment on insulin localization. Enrichment of these peripherally aligned MTs could serve to either 1) increase binding of granules to MTs or 2) restrict the radial motility of bound granules. In the discrete model, it is impossible to separate these effects; increased peripherally aligned density will necessarily influence both. To assess the relative importance of these effects in potentially generating counterpropagating gradients, we construct a simplified continuum model of granule dynamics where the two can be separately modulated.

For this continuum model, we consider concentrations of granules rather than individual granules and use partial differential equations to describe the time evolution of the spatial concentrations. Because the presence of the counterpropagating gradients in the prior study was not the result of subdiffusion, we consider the motions of both bound and unbound granules to be purely diffusive. This greatly simplifies the model, allowing it to be described by standard reaction diffusion partial differential equations. For simplicity, the cell is considered to be a radially symmetric circle, and we model only the dynamics in the radial direction because steady-state distributions in the discrete model depend on radius, but not angular position in the cell. This reduces the model to a one-dimensional, radially symmetric system that further simplifies calculations while allowing us to assess the influence of these factors on radial density.

This model encodes three essential components of the discrete model: 1) the ability of granules to bind and unbind from MT-bound to unbound states, 2) diffusion of unbound granules, and 3) diffusion of bound granules. It does not, however, explicitly include discrete MTs. Rather, bound and unbound forms are assumed to move with different rates of diffusion (faster for bound). We assess how increases in the rate of microtubule binding and decreases in the rate of radial diffusion at the cell periphery (due to microtubule enrichment) influence distributions of bound and unbound granules. To quantify this, we define a 250 nm zone near the cell border where MT-binding rates (k_{on}) and the speed of bound granule radial diffusion (D_r) are selectively modulated. The benefit of this continuum approach is that we can separately and selectively change these two parameters near the cell border to assess their influence in isolation.

The model was simulated for a range of different fold increases in the binding rate and fold decreases in the rate of bound granule radial diffusion near or at the periphery. Changes in

binding and radial diffusion rates have different roles in setting up these counterpropagating gradients (Figure 10). An increase in the binding rate is sufficient to induce a depletion of unbound peripheral granules, but not sufficient to induce a significant gradient in bound granules. A reduction in the rate of radial diffusion (in combination with the increase in binding rate) leads to a substantial enrichment of bound granules at the periphery. Thus, a moderate increase in the MT-binding rate in combination with a substantial decrease in the rate of bound granule radial diffusion is required to explain the counterpropagating gradients seen in the discrete model. Both would be expected to occur if MTs are enriched at the cell periphery.

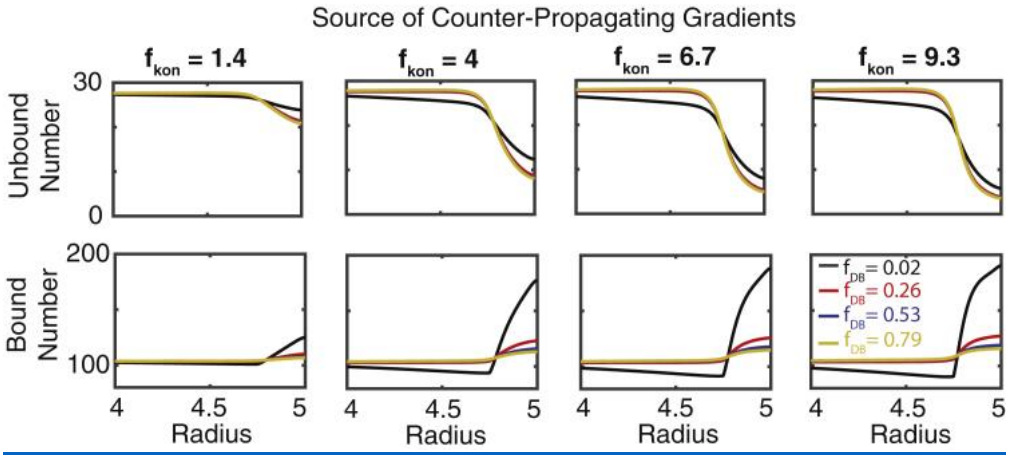

Figure 10. Effect of MT-binding propensity and reduction in radial diffusivity on granule densities

Effect of MT-binding propensity and reduction in radial diffusivity on granule densities. Simulations of the radially symmetric continuum model in which the rate of microtubule binding is increased by a factor (f_{kon}) and rate of radial diffusivity is decreased by a factor of (f_{DB}) within 250 nm of the cell membrane are shown. Top (*bottom*) panels show the steady-state insulin densities as a function of radius in different conditions. The notation f_{DB} = 0.02 and so forth indicates the base value of the relevant parameter is multiplied by the given value in the peripheral region (DB → 0.02 × DB, in this case).

The anomalous nature of granule motion alters localization of granules near the cell membrane in an MT-dependent fashion

It is well established that insulin granule motion (like the motion of many entities within the cell) is subdiffusive (Zhu et al., 2015). It is characterized by *MSD* curves obeying $MSD = Dt^{\alpha}$, where "*D*" is the generalized diffusion coefficient and "α" is the diffusive exponent: $\alpha = 1$ corresponds to regular diffusion, whereas $\alpha < 1$ indicates subdiffusion. For insulin granules, it has previously been found that $\alpha \sim 0.75$ (Tabei et al., 2013a), indicating significant anomalousness of diffusion. It has been further found that insulin granule motions exhibit characteristics of fractional Brownian motion (Tabei et al., 2013a), which is often associated with viscoelastic drag effects arising from the complex and crowded nature of the cell cytoplasm. Although numerous studies have investigated the anomalous nature of random particle motion in cellular environments (see (Hofling and Franosch, 2013) for a comprehensive review), to our knowledge, the effect of viscoelastic subdiffusion on the spatial distribution of particles (granules) at steady state has not been investigated. Here, we assess how this feature of motion and its changes due to alterations in the microtubule cytoskeleton affect steady-state spatial densities of granules within the cell.

It is well established that when particles obey standard random or Brownian motion, spatial distributions of particles tend to homogenize within a spatial domain. To determine whether this is the case when motions are more complex and governed by viscoelastic subdiffusion, we simulated the spatial distribution of 1000 noninteracting granules over time for different values of the *D* and α parameters (*Figure 11*). To independently assess the influence of anomalous motions, we initially consider only the 2D motions of granules independent of MTs. There is a significant depletion of granules at both the cellular and nuclear borders when granule motions are subdiffusive (*Figure 11 D*). Furthermore, as motions become more subdiffusive (smaller α) or faster (larger *D*), this depletion near the cell border becomes more substantial (*Figure 11A*, *D*, and *F*).

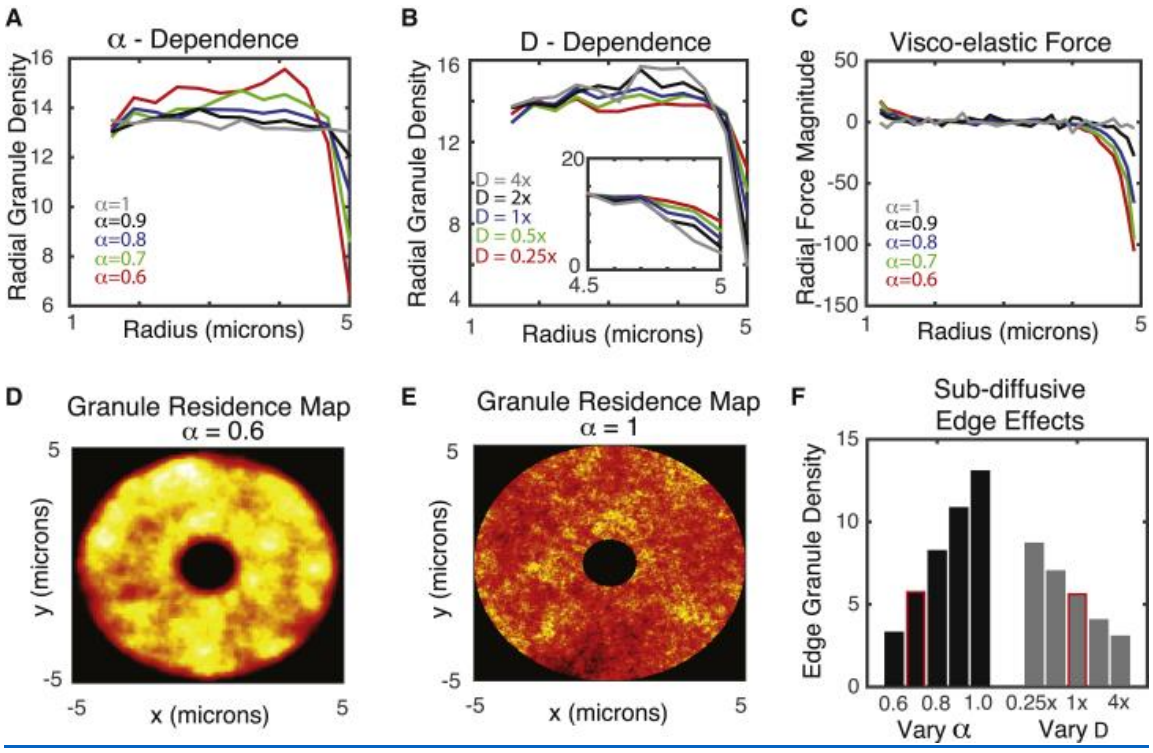

Figure 11. Influence of viscoelastic subdiffusive effects on peripheral granule density
Influence of viscoelastic subdiffusive effects on peripheral granule density. (*A*) Granule density as a function or radius for different values of the subdiffusion exponent *α* is shown. The rate of diffusion *D* is set to its base value here. (*B*) Radial granule density as a function of diffusion speed (*D*) for *α* = 0.7 is shown. (*C*) Net radial viscoelastic force as a function of radius for different values of *α*, with *D* fixed at its base value, is shown. Negative values near the periphery indicate a net inward force. (*D* and *E*) A granule residency map showing the distribution of granules over time for two values of *α* (note the depletion zones near the inner and outer radii) is given. Yellow indicates high density and red low density. (*F*) Effect of subdiffusive exponent (*α*) and diffusive strength (*D*) on the peripheral density of MTs is shown. In the "Vary *α*" case, the *D*-value corresponds to 1× (e.g., the base value). Similarly, for the "Vary *D*" case, *α* = 0.7. The highlighted bars most closely correspond to the calibrated *D*- and *α*-values used to model MT-based diffusion for all other simulations to follow. To see this figure in color, go online.

The explanation for this is subtle but follows readily from the basic assumptions of generalized Langevin dynamics. The physical mechanism often associated with viscoelastic subdiffusion is that as a particle moves in a given direction, resistive forces on that particle build up because of interactions with the crowded, filamentous cellular environment; the more a particle moves in a given direction, the larger the resistive force becomes. If a particle is observed near a cell border, it is more likely that the particle was transported from more interior regions of the cell rather than more exterior regions. This would lead to an expected resistive force that would tend to move the particle back to the interior of the cell, introducing a bias not present in standard diffusion.

To confirm this explanation, we quantified the average radial component of the viscoelastic force as a function of radius within the simulated cell at steady state to generate a force (*Figure 11 C*). This force map quantifies the average, expected resistive force that a granule would be subject to as a function of radial location within the cell. When diffusion is close to normal ($\alpha = 0.99$), that force is effectively zero everywhere. However, as diffusion becomes more anomalous, we begin to see a negative expected radial force near the cell border, suggesting a particle near the boundary would be expected to move inward rather than closer to the periphery. This is the source of the peripheral depletion of granules when motions are governed by viscoelastic subdiffusion.

Although this would be a general phenomenon in any system in which viscoelastic subdiffusion is present (Holmes, 2019), it is specifically relevant here because of the dependence of this depletion effect on the speed of motion. The gray bars in *Figure 11 F,* show that when the speed of motion is reduced by a factor of 1/4, peripheral densities increase by roughly 50%. Interestingly, when MTs are completely removed from *beta* cells via application of glucose + NOC, a roughly 1/4–1/3 reduction in *D* is observed (Figure 8 *C*, with data reproduced from (Zhu et al., 2015)), along with a roughly 50% increase in peripheral granule density.

Other mechanisms may influence insulin granule accumulation near the periphery. Glucose stimulation of *beta* cells influences cells in many ways, including activating docking proteins that bind granules to the membrane. Additionally, the dynamics of MTs significantly influence peripheral granule densities in other ways, independent of augmenting transport speed. Nonetheless, it is expected based on this analysis that the net slowdown in motion would contribute to the peripheral enrichment observed experimentally when glucose and NOC are jointly applied to cells.

Competition between membrane anchoring and microtubule binding regulates availability of peripheral granules

Here, we consider how the dynamics of MT-mediated motions influence granule localization and availability for membrane anchoring. A set of prior observations will allow us to assess what factors are important in understanding granule localization and constrain aspects of the computational model. In (Zhu et al., 2015), the authors quantified how granule density at the cell periphery changes when glucose, NOC, and glucose + NOC are applied to beta cells. Briefly, they found that the application of either factor alone had relatively little influence on granule densities. However, when they were jointly applied, peripheral densities increased by 50%.

When initially studying peripheral granule accumulation without considering membrane anchoring, we found the model unable to account for these observations. We thus consider the joint effects of membrane anchoring and MT-mediated transport, both of which are altered by glucose stimulation. To study how microtubule motion might influence membrane anchoring, we consider two possibilities for how granules anchor: 1) that any granule close enough to the periphery can anchor or 2) that only granules not bound to MTs can anchor. The latter possibility is motivated by the hypothesis that motions and forces subjected to granules by MT-associated motors either prevent anchoring or substantially reduce anchoring affinity. Because we do not have anchoring protein affinity data, we consider the effects of low, medium, and high affinity (high not shown in data), as well as the absence of anchoring (relevant for NOC-only treatment), on granule dynamics.

To understand the effect of MTs on the localization and availability of granules, we simulated the full model to steady state, performed both partial and complete removal of MTs in different anchoring scenarios, and quantified changes in peripheral granule density. In the absence of anchoring, neither partial nor complete removal of MTs alone has a significant effect on granule density, and thus, removal of MTs alone is not sufficient to explain granule enrichment when glucose + NOC is applied (Figure 12, *B* and *C*). The inclusion of anchoring can lead to the enrichment of peripheral densities; however, those enrichment dynamics are only consistent with observations when MT-unbound granules anchor to the membrane with low affinity. In this scenario, peripheral granules are increased by 40–50% (Figure 12 *A*), consistent with prior experimental observations (Zhu et al., 2015). When all granules can anchor independently of microtubule binding, enrichment occurs in the absence of any microtubule perturbation, contrary to observations. Alternatively, when affinity is too high, enrichment becomes extreme and once again independent of microtubule dynamics. In short, when

anchoring is high affinity or all granules (microtubule bound and unbound) can anchor, microtubule properties have little effect on peripheral densities.

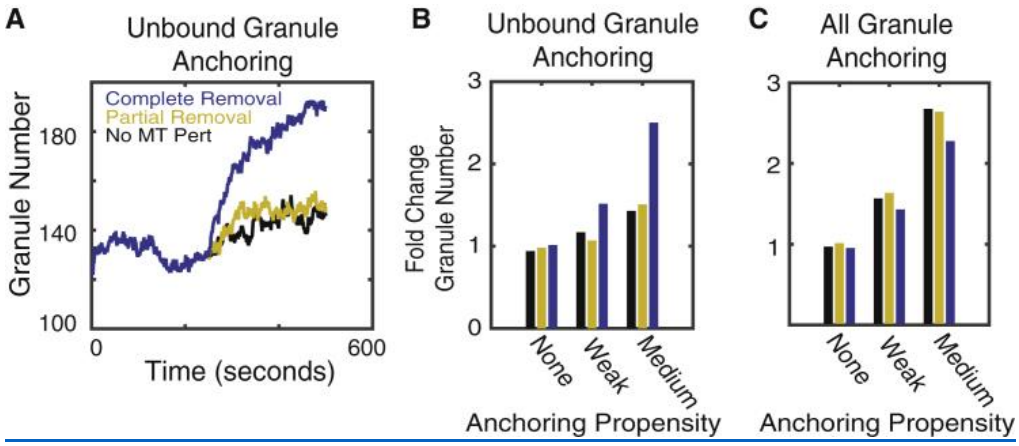

Figure 12. Influence of microtubule perturbations on peripheral granule density

Influence of microtubule perturbations on peripheral granule density**.** (*A*) The number of granules within 250 nm of the cell border as a function of time is shown in simulations in which only unbound granules are able to anchor to the membrane. This simulation shows the case for "weak" anchoring. The black curve indicates no microtubule perturbation is applied, red corresponds to removal of 1/3 of longer MTs, and blue indicates complete removal of all MTs (corresponding to glucose + NOC treatment). (*B* and *C*) Quantification of the fold change in peripheral granule density after MTs are perturbed is shown. The vertical axis shows the fold change in peripheral granule density after the relevant perturbation. The horizontal axis corresponds to different anchoring rates (none = 0, weak = 1:32, medium = 1:8). Slow microtubule dynamics are assumed so that the average lifetime is 1000 s. Alternative simulations were performed with short microtubule lifetimes (10 s; see Fig. S2 online). In (*B*), only MT-unbound granules are allowed to anchor to the membrane. In (*C*), all granules are assumed to be capable of anchoring. To see this figure in color, go online.

We thus conclude that anchoring is necessary to account for enrichment of peripheral granules upon glucose + NOC stimulation but that only unbound granules should anchor and with low affinity. These results suggest MTs may have a role in negatively regulating the availability of peripheral granules by binding them and making them unavailable for anchoring.

Discussion

Glucose homeostasis is tightly regulated at the systemic level in both the amount of insulin in circulation and the response of peripheral tissues to insulin (including liver, skeletal muscles, and fat). This study combines experimental tests and modeling to investigate how *beta* cells regulate the amount of insulin to secrete in response to a given stimulus. We focus on how MTs in beta cells regulate the localization and anchoring of insulin granules to the plasma membrane, a prerequisite for insulin secretion. Results here suggest that cytoskeletal factors contribute to the tight regulation of insulin at the level of individual beta cells.

Although individual beta cells can contain on the order of 10,000 individual insulin granules, only a relatively small population are secreted in response to glucose stimulation (Rorsman and Renstrom, 2003). Thus, at the cellular level, significant negative regulation of GSIS must be present. A well-established key negative factor is the actin cytoskeleton, which ensures that only a small portion of vesicles are available to break the cell cortex and secreted (Thurmond et al., 2003). Here, we have identified two potential alternative mechanisms by which microtubule dynamics contribute to this negative regulation (see Figure 13 for a schematic). First, MTs near the cell periphery actively transport insulin granules away from the cell membrane. Second, traction forces generated by MT-associated molecular motors prevent stable granule anchoring to the membrane, which is a precursor to exocytosis.

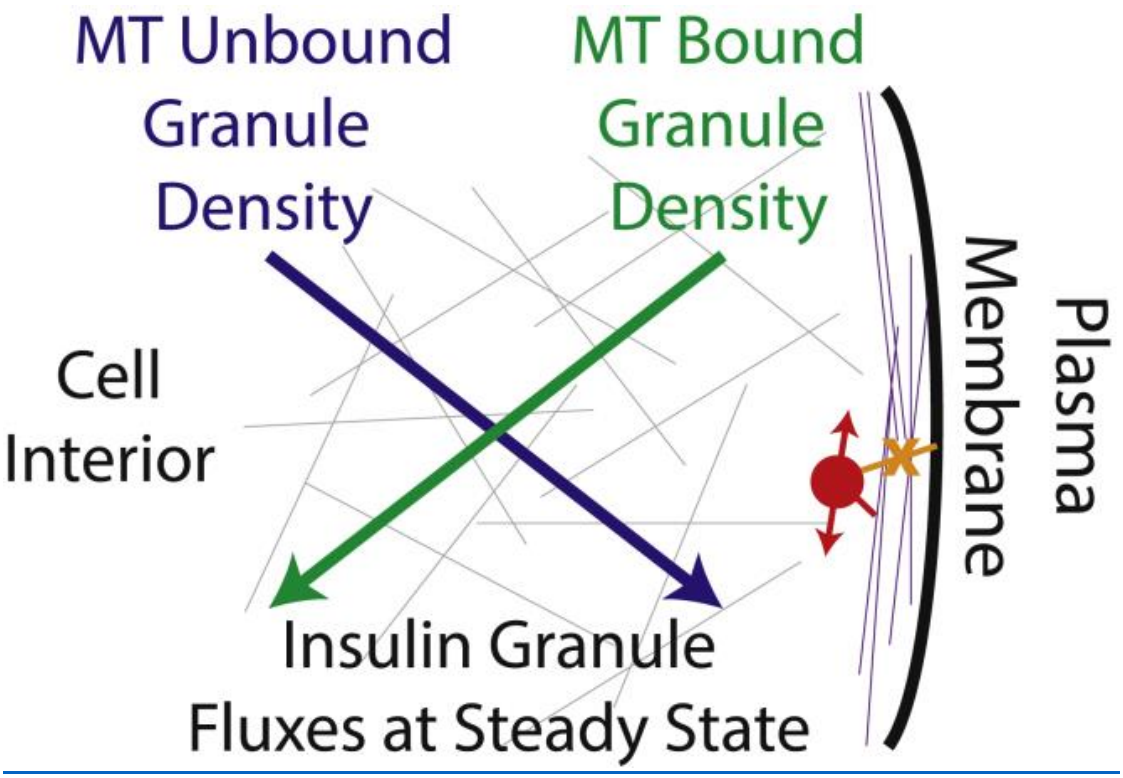

Figure 13. Cartoon schematic of the MT-network-induced counterpropagating insulin granule gradients.

Cartoon schematic of the MT-network-induced counterpropagating insulin granule gradients. The blue and green lines depict gradients of insulin that are unbound and bound, respectively, to the microtubule network. Slopes indicate the direction in which those gradients point (*blue* toward the plasma membrane and *green* away from it), and arrow heads depict the direction of flux of each of these insulin populations at steady state. At steady state, the flux of unbound granules toward the plasma membrane is balanced by the flux of bound granules away from it. Gray and purple lines in the background depict the randomly oriented and organized microtubule networks in the interior and peripheral regions of the cell. The red circle indicates an MT-bound granule that is prevented from docking to the membrane by motor-driven motions. To see this figure in color, go online.

Both mechanisms are supported by prior observations. First, prior imaging (Zhu et al., 2015) demonstrated that depolymerization of the microtubule cytoskeleton substantially inhibited the removal of insulin granules from the membrane, supporting the conclusion here that MTs predominantly serve to remove granules from the cells surface. Secondly, recent work (Gandasi et al., 2018) demonstrated that membrane docking of granules is substantially inhibited in human type 2 diabetes. This along with the observation that microtubule density is increased in diabetic mouse models supports the conclusion that MT-mediated transport prevents or inhibits anchoring of granules to the membrane (Zhu et al., 2015).

Interestingly, both phenotypes are consequences of an alteration in the microtubule structure near the cell membrane. Prior imaging has found that the microtubule network in *beta* cells is unusually unstructured and randomly oriented (Varadi and Rutter, 2002; Zhu et al., 2015). However, results here demonstrate that in peripheral regions within ~250 nm of the cell membrane, MTs are predominantly oriented parallel to the membrane. The two previously mentioned negative regulatory mechanisms are a direct consequence of this alteration in organization. As a result, the microtubule network acts like a sponge near the membrane that soaks up granules and transports them away from the periphery while preventing their membrane anchoring and stimulated release.

Coalignment of MTs at the cell periphery can arise as a result of microtubule capture at the cortex or cell-cell junctions, which prevents microtubule catastrophe (Fukata et al., 2002; Gundersen, 2002; Schmoranzer et al., 2009; Stehbens et al., 2014; Watanabe et al., 2004; Zaoui et al., 2010) and thus can promote their turning by the actin retrograde flow (Bicek et al., 2009; Gupton et al., 2002) and polymerization along the cortex. Alternatively, subcellular signals localized at the plasma membrane such as glycogen synthase kinase 3 beta (GSK3*β)* inactivation can locally increase microtubule coating by MAPs, which, in turn, can promote excessive microtubule growth along the cell periphery (Kumar et al., 2009; Nishimura et al., 2012; Zhu et al., 2016). Such mechanisms that promote microtubule turning must also increase their lifetimes and stability, which is consistent with the unusually high levels of stabilization that we observe in the peripheral microtubule arrays in beta cells. Thus, there are a number of potential regulatory mechanisms under the control of cell differentiation and metabolic signals that could produce this aligned peripheral mesh and, as a result, tune insulin availability for GSIS.

Interestingly, MT-mediated withdrawal of peripheral granules does not require directed (i.e., ballistic) motor-driven transport. That is, it does not appear to be the case that granules are

being ballistically transported away from the periphery by a plus- or minus-end-directed motor. This would be inconsistent with observations that both the microtubule network and granule motions on it are random. Instead, it is the topology of the microtubule network that influences cargo localization, not the specific motor dynamics (similar to (Ando et al., 2015; Maelfeyt et al., 2019)). Rather, the random but motor-driven granule motions observed in cells, coupled with the structured nature of the network near the membrane, are sufficient to generate directed motion of MT-bound granules away from the membrane. It is interesting that whereas most studies concentrate on kinesin-1 as the main MT-dependent motor that transports insulin granules (McDonald et al., 2009; Varadi and Rutter, 2002), the transport is likely driven by multiple motor transport involving both kinesin and dynein (Varadi et al., 2005). Furthermore, peripherally aligned microtubule arrays likely lack net polarity: there is no reason to anticipate that MTs growing along the cell periphery will be bundled or oriented in the same tangential directions. Furthermore, microtubule buckling at the periphery can produce MTs with “reversed” polarity, with their plus ends directed toward the cell periphery (Zhu et al., 2016). In such a complex network, even solely plus-end-directed molecular motors would promote nondirectional transport.

The effects of microtubule configuration on granule distribution are predicted to persist under glucose stimulation conditions as well. MTs coaligned with the cell membrane and, accordingly, their functional consequences on granule dynamics are observed in both steady state (low glucose levels) and stimulated conditions (high glucose levels). Glucose stimulation does have two important consequences, however. First, it leads to the activation of docking and exocytic machinery (Gandasi et al., 2018), which facilitates the secretion of those granules not interacting with the microtubule cytoskeleton. Secondly, it leads to depletion of stable long-lived MTs (Figure 8; (Zhu et al., 2015)) and replacement by new, dynamic MTs that are nucleated at the Golgi membrane (Sanders et al., 2017; Zhu et al., 2015) and are characterized by rapid polymerization rates (Heaslip et al., 2014). Although this does not lead to a gross reduction in microtubule density or readily detectable restructuring, it does reduce their lifetime. As our results suggest, this leads to increased interaction between granules and the membrane and, subsequently, to increased secretion. Another way to interpret the result of increased microtubule dynamics is that it creates a pool of transiently “unbound” granules, which we show here to be prone to accumulation at the cell periphery.

Here, we used imaging and modeling to assess the consequences of microtubule dynamics specifically on secretion. However, much work is still needed to investigate how the

biophysical properties of motors themselves as well as docking proteins influence secretion. One central hypothesis stemming from this work is that the motions and/or traction forces generated by the action of molecular motors on MTs parallel to the membrane inhibit stable membrane anchoring. Does this occur through the prevention of bond formation or the force-dependent breaking of those bonds? Furthermore, how does the nature of the multiple motor transport that these granules are likely subject to influence interactions with the membrane? Addressing these questions will require further experimental investigation of the biophysical interactions between the cytoskeleton, molecular motors, membrane docking proteins, and insulin granules.

These results do, however, suggest that there is a potential therapeutic merit in targeting the cytoskeleton to modulate *beta* cell function. Recent imaging demonstrated that increased microtubule density was found to correlate with decreased secretion in mouse models (Zhu et al., 2015). Although those results were correlative, our findings here indicate that in silico, a dense peripheral microtubule network interferes with the proper positioning of insulin granules for secretion. This result predicts that in fact, the link observed in mouse models may be causal, and interference with microtubule stability in *beta* cells might be used as an approach to increase insulin secretion efficiency. This idea is tempting because numerous MT-targeting small molecule compounds have already been considered or even used for cancer therapies. This potential must be approached very carefully, given the high toxicity of microtubule drugs on all cells and the likely negative effects of prolonged microtubule destabilization on insulin biogenesis in *beta* cells specifically. Nevertheless, one can envision that in the future, microtubule destabilizers could be applied to facilitate insulin secretion and overcome hyperinsulinemia in patients when locally delivered and released in a time-restricted manner. If proposing such an intervention is too bold, it is more realistic that future studies will identify specific MT-stabilizing MAPs, which are responsible for high microtubule density in diabetes models. Then, potential therapies could specifically target these MT-binding proteins.

Chapter 4
Glucose-stimulated KIF5B-driven microtubule sliding organizes microtubule networks in pancreatic beta cells

The precise level of glucose-stimulated insulin secretion from pancreatic beta cells is crucial for glucose homeostasis. On one hand, insufficient insulin secretion decreases glucose uptake by tissues, leading to diabetes. On the other hand, excessive secretion causes glucose depletion from the bloodstream and hypoglycemia. Not surprisingly, multiple levels of cellular regulation control the amount of secretory insulin granules (IGs) released on every stimulus. One level of this control is facilitated by microtubules (MTs), intracellular polymers which serve as tracks for intracellular transport of IGs and define how many IGs are positioned at the secretion sites (Desai and Mitchison, 1997; Heaslip et al., 2014; Varadi et al., 2002).

Microtubules have a dual role in availability of IGs for secretion. Microtubules are necessary for efficient IG generation at the trans Golgi network (TGN) and for their transportation throughout the cell (Trogden et al., 2019; Zhu et al., 2015), which includes non-directional, diffusion-like redistribution in the cytoplasm (Tabei et al., 2013b; Zhu et al., 2015) and directional runs of secretion-competent granules toward periphery (Hoboth et al., 2015; Muller et al., 2021). At the same time, peripheral IGs undergo MT-dependent withdrawal from secretion sites, which prevents IG docking and acute over-secretion following a given stimulus (Hu et al., 2021; Zhu et al., 2015). Such multi-faceted involvement of microtubule transport in secretion regulation is made possible by a complex architecture of microtubule networks in beta cells. Interior beta-cell MTs are twisted and interlocked (Varadi et al., 2003; Zhu et al., 2015), which makes them dramatically distinct from radially organized microtubule arrays well-studied in generic cultured cell models and explains the predominantly non-directional nature of IG transport (Bogan, 2021; Bracey et al., 2022). Importantly, withdrawal of IGs and secretion restriction is achieved by a prominent array of MTs underlying cell membrane (Bracey et al., 2020). Under basal conditions, IGs are robustly withdrawn from secretion sites along submembrane MTs, which are stabilized by MT-associated proteins (MAPs), including a well-known neuronal MAP tau (Ho et al., 2020). Upon a glucose stimulus, tau is phosphorylated and submembrane MTs become more dynamic (Ho et al., 2020) and fragmented, possibly via a MT-severing activity (Muller et al., 2021). Destabilization and partial depolymerization of submembrane MTs leads to IG docking and allows for secretion (Ho et al., 2020; Hu et al.,

2021), probably as a consequence of decreased IG withdrawal by MT-dependent transport. Thus, existing data provide at least initial understanding of the mechanisms whereby beta-cell microtubule architecture allows for fine-tuning of secretion levels.

However, it is yet unclear how the complex beta-cell microtubule network forms. As in many other eukaryotic cells, MTs in beta cells are nucleated at MT-organizing centers (MTOCs) in the cell interior, partially at the centrosome and to a large extent at the Golgi membranes (Trogden et al., 2019; Zhu et al., 2015). Conventionally, this should be followed by microtubule plus-end polymerization toward the cell periphery and result in a radial microtubule array with high microtubule density in the center rather than in the periphery. The beta cell lacks such well-characterized microtubule polarity (Bracey et al., 2022). Thus, it is puzzling that the actual resulting microtubule system is non-radial and consists of an interior mesh and a peripheral array (Bracey et al., 2020; Heaslip et al., 2014). How the beta cell organizes its cytoskeletal network for efficient trafficking of granules, and what factors contribute to the maintenance of the sub-membrane array, are important questions.

One of the established ways to modify the microtubule network without changing the location of MTOCs is to relocate already polymerized MTs by active motor-dependent transport. This phenomenon is called “microtubule sliding” (Straube et al., 2006). Several MT-dependent molecular motors have been implicated in driving microtubule sliding (Lu and Gelfand, 2017). In some cases, a motor facilitates microtubule sliding by walking along a microtubule while its cargo-binding domain is stationary being attached to a relatively large structure, e.g. plasma membrane. This causes sliding of a microtubule which served as a track for the stationary motor. This mechanism has been described for dynein-dependent microtubule sliding (Grabham et al., 2007; He et al., 2005). MTs can also be efficiently moved by motors which have two functional motor assemblies, such as a tetrameric kinesin-5/Eg5 (Acar et al., 2013; Vukusic et al., 2021), or which carry a microtubule as a cargo while walking along another MT. For the latter mechanism, a motor needs a non-motor domain with a capacity to bind either a microtubule itself, or a MT-associated protein as an adapter (Cao et al., 2020; Kurasawa et al., 2004; Vukusic et al., 2021).

Out of these MT-sliding factors, kinesin-1 is known to be critical for organizing unusual microtubule architecture in specialized cells. In oocytes, kinesin-1-dependent microtubule sliding empowers cytoplasmic streaming (Barlan et al., 2013). In differentiating neurons, kinesin-1 moves organelles and MTs into emerging neurites, which is a defining step in developing branched microtubule networks and long-distance neuronal transport (Jolly et al., 2010; Lu et

al., 2013). With these data in mind, kinesin-1 presents itself as the most attractive candidate for organizing MTs in beta cells. This motor highly expressed in beta cells and is well known to act as a major driving force in IG transport (Varadi et al., 2003).

Here, we show that KIF5B actively slides MTs in beta cells and that this phenomenon defines microtubule network morphology and supplies MTs for the submembrane array. Moreover, we find that microtubule sliding in beta cells is a glucose-dependent process and thus likely participates in metabolically driven cell reorganization during each secretion cycle.

Materials and Methods

1. Key reagents

Reagent type or resource	Designation	Source or reference	Additional information
Cell line	MIN6		RRID:CVCL_0431
Chemical compound, drug	Kinesore	Tocris, Cat#: 6664	Final concentration (50µm)
Chemical compound, drug	A/C Heterodimerizing Drug	Takara, Cat#: 635056	Final concentration (25µm)
Antibody	Anti-KIF5B antibody	Abcam, Cat#: Ab167429	(1:500 dilution)
Antibody	Anti-alpha-Tubulin antibody	Sigma-Aldrich, Cat#: T9026	(1:500 dilution)
Halo Dye-585, 647	HaloTag® Ligands	CS315105, GA1120	2ul/mL

2. Cell Lines

MIN6 cells between passage 40-60 were utilized (Ishihara et al., 1993; Miyazaki et al., 1990). Cells were maintained in 25 mM glucose Dulbecco's modified eagle medium (DMEM) (Life Technologies, Frederick, MD) supplemented with 10% fetal bovine serum (FBS), 0.001% beta-mercaptoethanol, 0.1 mg/ml penicillin, and 0.1 mg/ml streptomycin in 5% CO_2 at 37 degrees C.

3. Reagents and antibodies

Primary antibodies for immunofluorescence were: mouse anti-beta-tubulin (Sigma-Aldrich, 1:1000), rabbit anti-beta-tubulin (Sigma-Aldrich, 1:1000) and rabbit anti-KIF5B (Abcam), Alexa488-, Alexa568-, and Alexa647-conjugated highly cross-absorbed secondary antibodies (Invitrogen). Coverslips were mounted in Vectashield Mounting Medium (Vector Labaratories). Cells were treated with indicated drugs for three hours unless otherwise indicated. Drugs used were: Kinesore (Tocris Bioscience).

4. shRNA sequence

The Kif5b-targeting shRNA [shRNA Kif5b] #1, [TL510740B, 5'-ACTCTACGGAACACTATTCAGTGGCTGGA] and [shRNA Kif5b] #2, [TL51074CB 5' – AGACCGTAAACGCTATCAGCAAGAAGTAG] are in the plasmid backbone pGFP-C-shLenti and were from Origene (Rockville, MD). The non-targeting shRNA control, was pGFP-C-shLenti also from Origene.

5. DNA Constructs

Plasmid Construct	**Source**	**Catalog #**
SCR-TGFP	Origene	Custom
Kif5b shRNA#1-TGFP	Origene	Custom
Kif5b shRNA#2-TGFP	Origene	Custom
Scr shRNA mEmerald-Tubulin	This paper	Custom
Kif5b shRNA#1-mEmerald-tubulin	This paper	Custom
Kif5b shRNA#2-mEmerald-tubulin	This paper	Custom
mEmerald-Tubulin-C-18	Addgene	#54292
pcDNA4TO-K560-E236A-24xGCN4	Addgene	#60909
ScFv-GCN4-HaloTag-GB1-NLS	Addgene	#106303
FKBP-mCherry-KIF5B(568-964)	Kristen Verhey	(Ravindran et al., 2017)
p205ME_RnKIF5C(1-559)-TagBFP-FRB	Kristen Verhey	(Ravindran et al., 2017)
FKBP-mCherry-KIF5B(568-964)-AAAYA (MUT)	This paper	

6. Cloning

The Scr shRNA mEmerald-Tubulin, Kif5b shRNA#1-mEmerald-tubulin, Kif5b shRNA#2-mEmerald-tubulin were all generated from their respective TGFP containing constructs. Using the NotI and PmeI sites the TGFP was swapped for mEmerald-Tubulin.

The FKBP-mCherry-KIF5B(568-964) construct (gift from Kristen Verhey, University of Michigan), has previously been previously described (Ravindran et al., 2017).

By using site directed mutagenesis, we made 8 point mutations in the tail domain to change residues DRKRYQ to DAAAYA in the ATP independent microtubule binding domain. The point mutations were sufficient to rescue microtubule sliding in the cell. As previously published this disrupts the tail domain to bind to the acidic e hook of the microtubule tail (Lu et al., 2016;

Seeger and Rice, 2010). Point mutations were introduced using a site directed mutagenesis kit, In-Fusion® Snap Assembly (Takara).

7. Lentiviral Transduction and Transfection

Lentivirus production and infection followed standard methods (Huang et al., 2018). MIN6 were treated with a given shRNA expressing a mEmerald-tubulin/cytosolic pGFP marker for 96hrs prior to imaging to achieve KD efficiency.

For non-viral vectors, MIN6 cells were transfected using Amax Nucleofection (Lonza).

8. Western blotting

Cell lysates from MIN6 cells were lysed using 1% CHAPs buffer on ice for 5 minutes. For KIF5B knockdown, cells were first sorted for GFP expression. Protein lysate (20 µg) was loaded onto an SDS-PAGE gel under reducing conditions and transferred to nitrocellulose membranes. Membranes were probed with antibodies against KIF5B, and α-tubulin.

9. Image Acquisition

Immunofluorescence microscopy of fixed samples

Fixed samples were imaged using a laser scanning confocal microscope Nikon A1r based on a TiE Motorized Inverted Microscope using a 100X lens, NA 1.49, run by NIS Elements C software. Cells were imaged in 0.05 µm slices through the whole cell.

Live cell imaging

Cells were cultured on 4-chamber MatTek dishes coated with 10 µg/µl fibronectin and transduced 96hrs or transfected 48 h before experiment. For live-cell imaging of MICROTUBULE sliding, cells were transfected with Emerald-Tubulin and imaged using a Nikon TiE inverted microscope equipped with 488- and 568-nm lasers, a Yokogawa CSU-X1 spinning disk head, a PLAN APO VC 100x NA1.4 oil lens, intermediate magnification 1.5X, and CMOS camera (Photometrics Prime 95B), 405 Burker mini-scanner, all controlled by Nikon Elements software.

Photobleaching Assay

~1x10^6 MIN6 cells were transfected with 1 µg of mEmerald-tubulin or transduced with lentiviral KIF5B shRNA with mEmerald-tubulin as a reporter and attached to glass dishes coated with

fibronectin for up to 96 hrs. On the SDC microscope, the ROI tool in NIKON elements was used to place two ROI's ~5 µm apart at either end of the cell. These regions were assigned to be photobleached with the equipped 405nm mini scanner laser leaving a fluorescent patch over the middle which we termed the "fluorescent belt". After the regions were photobleached cells were then acquired for 5mins, across 7 optical slices (0.4 µm step size) in 10 second interval between frames.

Sun Tag Rigor Kinesin and Tracking of microtubule sliding

SunTag system for microtubule lattice fiducial marks was adapted from (Lu et al., 2016). ~1x10^6 MIN6 cells were co transfected with 1 µg of the ScFv-GCN4-HaloTag-GB1-NLS, and 0.5 µg of the pcDNA4TO-K560-E236A-24xGCN4 plasmid (K560Rigor^{E236A}-SunTag (Tanenbaum et al., 2014)). After 24 hours the cells were washed with 1x PBS and the media replaced with KRB containing 2.8 mM glucose for 1 hour, following a second incubation with HALO dye of choice (Promega) for 30 mins. Cells were imaged in 1 focal plane for 2 mins with 100 ms exposure time and no delay in acquisition. The acquired image was processed through Imaris Microscopy Image Analysis Software (Oxford Instruments), where the fiducial marks were tracked.

MATLAB Script: Microtubule Directionality

Oversampled images were deconvolved using the Richardson and Lucy Deconvolution algorithm. Images were masked and threshold (IsoData) in ImageJ. The MICROTUBULE directionality script was applied in MATLAB. Only the outer 1 µm of MTs were taken for binning and quantification purposes.

MATLAB Script: Msdanalyzer, Segmentation

The position of all tracked fiducial spots were exported from Imaris to excel. The MSDanalyzer was developed by Nadine Tarantino et al, and adapted by Kai Bracey, Pi'Illani Noguchi, and Alisa Cario (Vanderbilt University) to normalize the tracks in time. Tracks were segmented into displacements over 5s and binned as shown in the results.

10. Statistics and reproducibility

For all experiments, *n* per group is as indicated by the figure legend and the scatter dot plots indicate the mean of each group and error bars indicate the standard error of the mean. All graphs and statistical analyses were generated using Excel (Microsoft) and Prism software (Graphpad). Statistical significance for all *in vitro* and *in vivo* assays was analyzed using an

unpaired t-test, one-way ANOVA with Sidak's multiple comparisons test, Kolmogorov-Smirnov test as indicated in the figure legends. For each analysis $p < 0.05$ was considered statistically significant, and *$p < 0.05$, **$p < 0.01$, ***$p < 0.001$, ****$p < 0.0001$.

Author contributions

KMB performed most of the experiments and a large part of data analysis and wrote the manuscript. PN and AC provided scripts for data analysis and analyzed data. CE performed Western Blotting experiments. GG provided conceptual insight and molecular cloning strategy. I.K. supervised the study, provided conceptual insight and wrote the manuscript.

Results

Identification of Kif5B as a MT-sliding motor in beta cells

To address the factors that shape the configuration of microtubule networks in beta cells, we tested for a potential involvement of motors-dependent microtubule sliding. Not surprisingly, analysis of RNA-sequencing data in mouse islet beta cells highlighted kinesin-1 KIF5B as the highest expressing beta-cell motor protein (*Figure 14*A). Since this kinesin has been reported to have microtubule sliding activity in many types of interphase cells, we concentrated on testing its potential ability to slide MTs in beta cells.

Efficient depletion of KIF5B was achieved by utilizing two independent lentiviral-based shRNAs against mouse KIF5B in the mouse insulinoma cell line MIN6 (*Figure 14*B). To visualize microtubule sliding, shRNA-treated cells MIN6 cells expressing mEmerald-tubulin were imaged by live-cell spinning disk confocal microscopy. We photobleached MTs in two large cell regions leaving a thin unbleached band ("fluorescent belt") and analyzed relocation of MTs from the "fluorescent belt" into the bleached areas over time. To minimize the effects of plausible microtubule polymerization and to reduce photobleaching, MTs were imaged for short time periods (5 mins). Strikingly, in control cells (treated with scrambled control shRNA) MTs were efficiently translocated from the "fluorescent belt" into the photobleached area, indicating that microtubule sliding events are prominent in this cell type (*Figure 14*C,D). In contrast, MIN6 cells expressing either KIF5B shRNA variants displayed a significant loss of microtubule sliding ability (*Figure 14* C,E,F), indicating that the loss of KIFB leads to the loss of microtubule sliding.

While the assay described above provides an easy visualization of microtubule sliding, it allows for visualization of only a subset of the microtubule network. In addition, despite the careful optimization of our photobleaching conditions, it is important to confirm that the observed

phenomena are not biased by potential photodamaging effects in cells. Thus, we sought to implement a second system to visualize microtubule sliding that does not involve photobleaching and allows for evaluation of displacements within the whole MT network. To this end we applied a microtubule probe of fiducial marks, K560Rigor^{E236A}-SunTag (Tanenbaum et al., 2014) in MIN6 cells (*Figure 14*G-H). This probe contains the human kinesin-1 motor domain (residues 1–560) with a rigor mutation in the motor domain (K560Rigor^{E236A}) and fused to 24 copies of a GCN4 peptide. The rigor mutation in the motor domain causes it to bind irreversibly to microtubules (Rice et al., 1999). When co-expressed with a pHalo-tagged anti-GCN4 single-chain antibody (ScFv-GCN4-HaloTag-GB1-NLS), K560Rigor^{E236A} can recruit up to 24 of the Halo ligands to a single position on a microtubule. This enables visualization of microtubule sliding events via single molecule tracking of the fiducial marks along the microtubule lattice. The pHalo- tagged anti-GCN4 construct also contains a nuclear localization signal (NLS), which functions to reduce background of the unbound dye in the cytoplasm. This approach allowed us to visualize microtubule sliding behavior within the whole network with temporal and spatial resolution. Our data indicate that in cells treated with scrambled control shRNA, a subset of K560Rigor^{E236A}-SunTag fiducial marks underwent rapid directional movements, interpreted as microtubule sliding events (*Figure 14*G). In contrast, the vast majority of fiducial marks in cells expressing Kif5b-specific shRNAs were stationary (*Figure 14*H,I),(Quantification unavailable at this time) indicating the lack of microtubule sliding. Collectively, these results indicate that Kif5b is necessary for microtubule sliding in MIN6 cells.

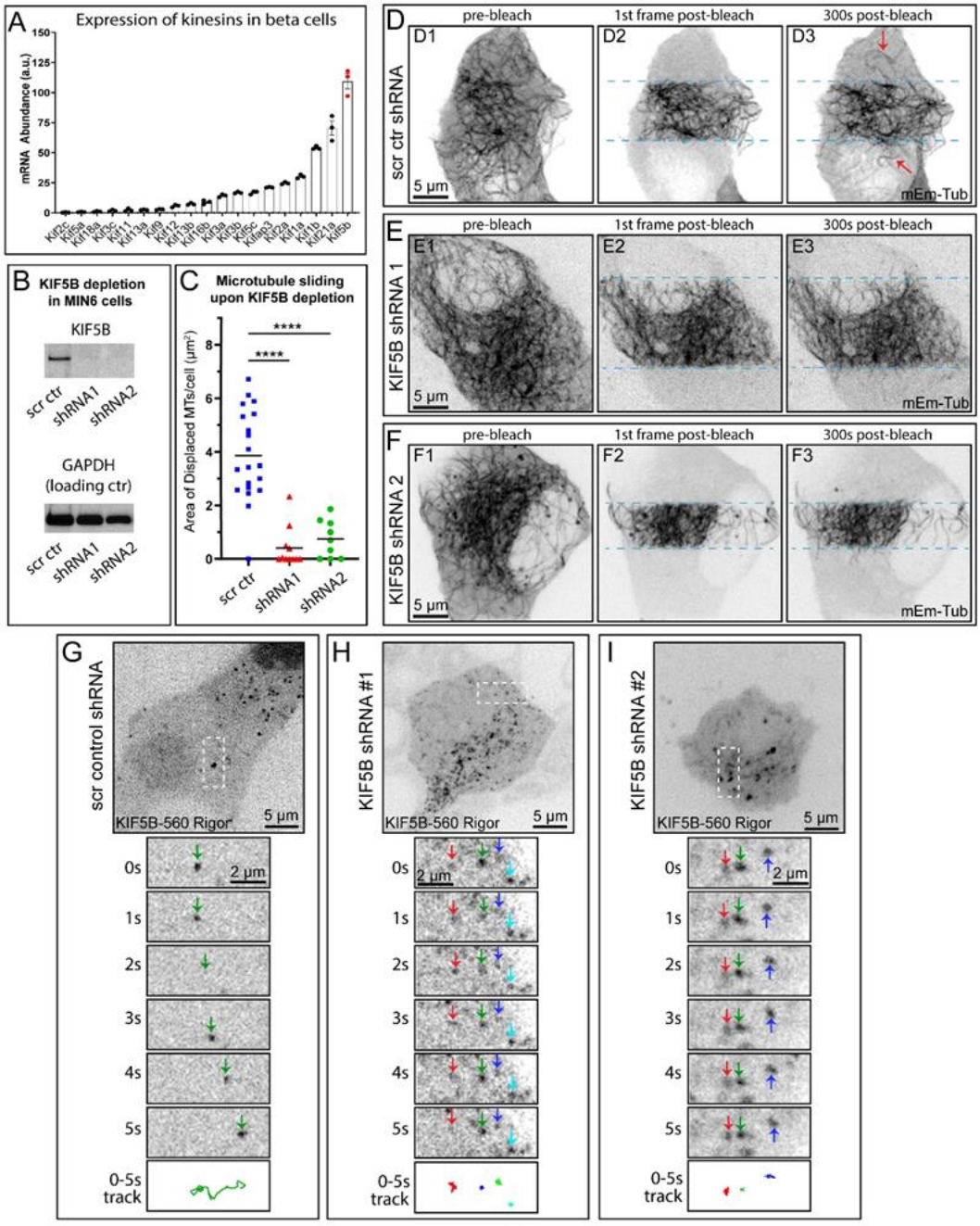

Figure legend on next page

Figure 14. MTs in pancreatic beta cells undergo extensive sliding driven by kinesin KIF5B. (**A**) A subset of RNA-sequencing data from primary mouse beta cells showing highly expressed kinesins as indicated by mRNA counts. KIF5B (most-right bar, red data points) is the most abundant kinesin motor in this cell type. N=3. Note that this is a subset of the RNA sequencing sets published (data unpublished). (**B**) Efficient depletion of KIF5B in MIN6 cells using two alternative shRNA sequences, as compared to a scrambled shRNA control. GAPDH, loading control. Relevant ROIs from a western blotting is shown. A representative example out of 3 repeats. (**C**) Quantification of MT sliding FRAP assay in cells treated with scrambled control or one of the two KIF5B-specific shRNAs (see representative data in D-F). MT displacement is shown as area of MTs displaced into the bleached area after 5 minutes of recovery. One-way ANOVA test was performed for statistical significance (p-value <0.0001). N=9-19 cells per set. (**D-F**) Frames from representative FRAP live-cell imaging sequences. mEmerald-tubulin-expressing MIN6 cells. Inverted grayscale images of maximum intensity projections over 1 µm-thick stacks by spinning disk confocal microscopy. (D1-F1) The last frame prior to photobleaching. (D2-F2) The first frame after photobleaching. (D3-F3) A frame 5 minutes (300 seconds) after photobleaching. Light-blue dotted lines indicate the edges of the photobleached areas. Red arrows indicate MTs displaced into the bleached area. Scale bars, 5 µm. (**G-I**) MIN6 cells featuring fiducial marks at MTs due to co-expression of SunTag-KIF5B-560Rigor construct and Halo-SunTag ligand. Representative examples for scrambled control shRNA-treated cell (G), KIF5B shRNA #1-treated cell (H) and KIF5B shRNA #2-treated cell (I) are shown. Single-slice spinning disk confocal microscopy. Halo-tag signal is shown as inverted gray-scale image. Top panels show cell overviews (scale bars 5µm). Below, boxed insets (scale bars 2 µm) are enlarged to show dynamics of fiducial marks (color arrows) at 1 second intervals (1-5 seconds). 0- to 5-second tracks of fiducial mark movement are shown in the bottom panel, each track color-coded corresponding to the arrows in the image sequences.

Beta-cell kinesin-1 drives microtubule sliding through the C-terminal MT-binding domain

While membrane cargo transport by KIF5s requires association of the heavy chain with the kinesin light chains (KLCs) and/or other adaptors, transportation of MTs as cargos occurs due to direct binding of KIF5 to MTs through the ATP-independent microtubule binding domain in heavy chain tail (C-terminus) (Jolly et al., 2010; Seeger and Rice, 2010).

To specifically evaluate the role of microtubule sliding by kinesin-1 in beta cells, we sought to evaluate the effects of suppressing the binding of KIF5B tail to MTs on microtubule binding. To this end we used a previously generated construct (Ravindran et al., 2017), which is a motor-less version of wild-type (WT) kinesin-1 motor KIF5B containing the cargo-binding and ATP independent microtubule binding domain and tagged with mCherry (mCh) at the amino terminus (Figure 15A). When overexpressed, this construct acts as a dominant-negative (DN) tool preventing association of the tail of endogenous KIF5B with MTs. This tool is referred to as KIFDN^{wt} (KIF5B dominant negative WT) moving forward (Figure 15A).

To confirm that the KIF5B tail domain binds to MTs in MIN6 cells and acts as a dominant negative, we co-expressed KIFDN^{wt} and mEmerald-tubulin. In the FRAP assay, we detected a significant loss of microtubule sliding events vs control (Figure 15B-D). To prevent tail engagement of the microtubule lattice through the ATP-independent binding domain, we changed residues 892-DRKRYQ to 892-DAAAYA in the tail domain, thus generating KIFDN^{MUT} (Figure 15A). The microtubule sliding phenotype was restored in cells co-expressing KIFDN^{MUT} with mEmerald-tubulin indicated that (Figure 15B,E), indicating that these amino acid residues are necessary for the tail domain to engage the lattice.

The DN constructs are also tagged with the FK506-rapamycin-binding protein (FKBP), as indicated in Figure 15 A. Additionally, the motor domain is fused with the FKBP-rapamycin binding (FRB) domain. This allows heterodimerization using A/C Heterodimerizer (rapalog) to reconstitute a functional motor (Inobe and Nukina, 2016). We restored kinesin-1 activity by connecting the motor-less KIF5B mutant, KIFDN^{wt}, to kinesin-1 motor domain as a way to rescue the effects of the DN approach of KIF5B tail overexpression. To this end, we co-expressed MIN6 cells with the tail domain, mEmerald-tubulin, and the KIF5C motor domain fused to FRB domain (Figure 15A). Once the tail and motor domain were dimerized with rapalog, we saw that the once blocked microtubule sliding events of the KIFDN^{wt} tail alone were now reversed (Figure 15B,F). In contrast, under conditions of heterodimerization of KIFDN^{MUT} with the motor, microtubule sliding was greatly impaired (Figure 15 B,G), indicating that the motor with a mutated ATP-independent binding domain cannot use MTs as cargos.

Interestingly, the endogenous motor in this case was unable to efficiently transport MTs, suggesting that the endogenous motor pool engaged in microtubule sliding was significantly smaller than the overexpressed non-functional motor.

Overall, the results of the DN approach confirm that microtubule sliding in beta cells is driven by KIF5B through direct kinesin-1 tail binding to cargo MTs.

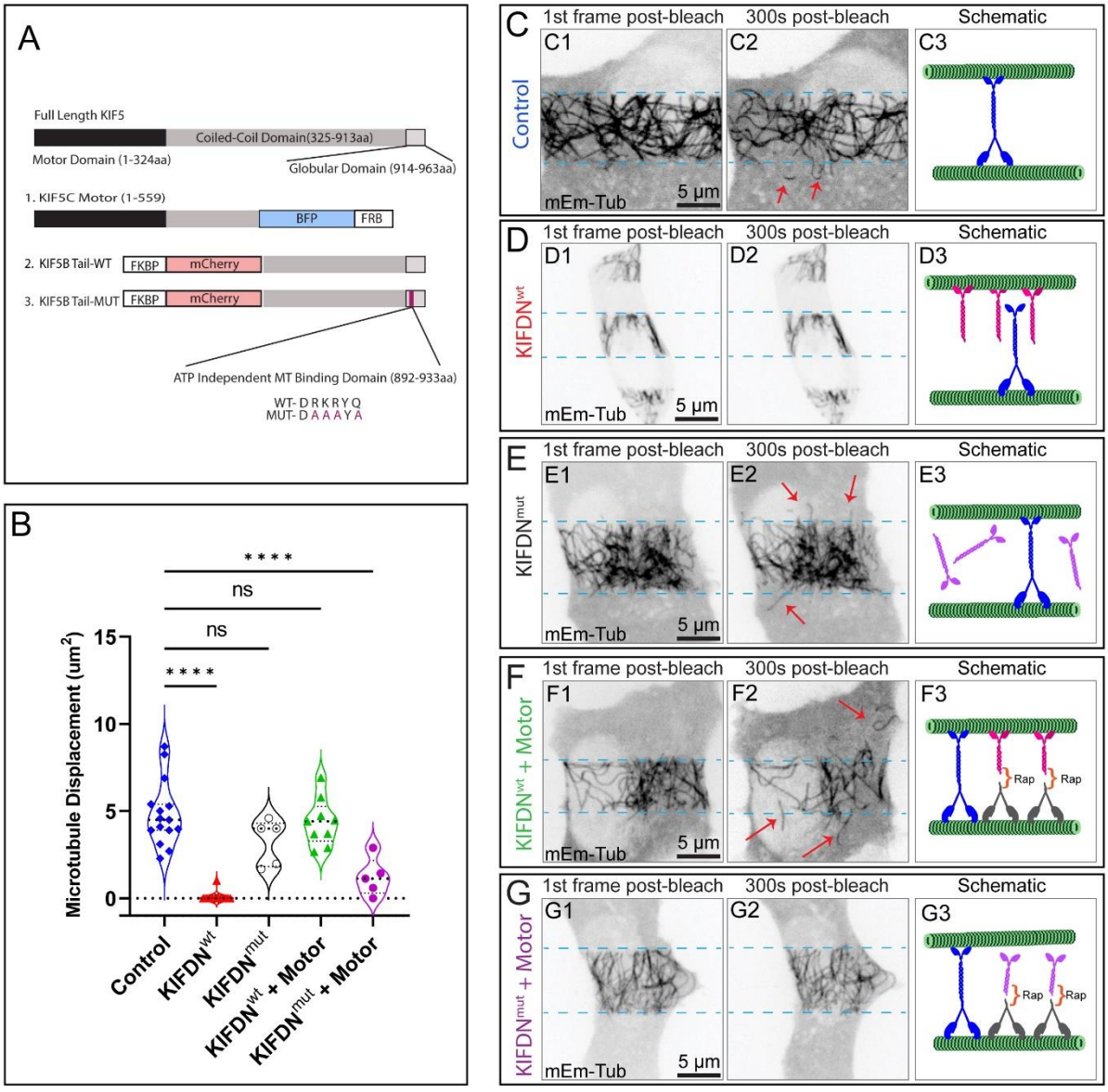

Figure legend on next page

Figure 15. Microtubule sliding is facilitated through the ATP-independent MT-binding domain of kinesin-1.

(**A**) Schematic of kinesin-1 (KIF5) and the Dominant Negative (KIFDN) and heterodimerization strategy. Top schematic shows full length KIF5s, consisting of the motor domain, stalk coil-coil domain and the tail. Three constructs utilized here include (1) The KIF5C motor domain tagged with a blue fluorescent protein (BFP) and the FRB for heterodimerization; (2) KIFDN^{wt} construct with KIF5B Tail domain tagged with the mCherry fluorescent protein and the FKBP for heterodimerization. (3) KIFDN^{mut} construct is the same as (2) but features a set of point mutations (magenta) making the ATP-independent MT-binding domain unable to bind MT lattice. (**B**) Quantification of MT sliding in FRAP assay in cells subjected to DN construct expression and heterodimerization (shown as area of displaced MTs). MT displacement is shown as area of MTs displaced into the bleached area after 5 minutes of recovery. See representative data (**C-G**). N= 5-25 per condition. One-way ANOVA test was performed for statistical significance (p-value <0.0001; ns, non-significant). **(C-G")** Frames from representative FRAP live-cell imaging sequences. mEmerald-tubulin-expressing MIN6 cells. Inverted grayscale images of maximum intensity projections over 1 µm-thick stacks by spinning disk confocal microscopy. (C1-G1) The first frame after photobleaching. (C2-G2) A frame 5 minutes (300 seconds) after photobleaching. Light-blue dotted lines indicate the edges of the photobleached areas. Red arrows indicate MTs displaced into the bleached area. Scale bars, 5 µm. (C3-G3) Schematics of experimental manipulation: green represents MTs, blue represents endogenous KIF5B, magenta represents KIFDN^{wt}, purple represents KIFDN^{mut}, gray represents KIF5C motor, orange bracket represents heterodimerizing agent (rap, rapalog). Conditions: (**C1-C3**) Untreated control. Only endogenous KIF5B is present. (**D1-D3**) KIFDN^{wt} overexpression. Endogenous KIF5B is unable to bind MTs. (**E1-E3**) KIFDN^{mut} overexpression. It does not bind MTs and does not interfere with endogenous KIF5B. (**F1-F3**) KIFDN^{wt} and KIF5C motor overexpression plus rapalog treatment. Heterodimerization creates a large pool of motors capable of MT sliding. (**G-G"**) KIFDN^{mut} and KIF5C motor overexpression plus rapalog treatment. Heterodimerization creates a large pool of the motor non-functional in MT sliding.

KIF5B is required for beta-cell microtubule organization

Because microtubule sliding mediated by KIF5B is a prominent phenomenon in beta cells, we sought to test whether it has functional consequences for microtubule networks in these cells. Tubulin immunostaining revealed striking differences in microtubule organization between MIN6 cells treated with scrambled control shRNA versus KIF5B-specific shRNAs. While control cells had convoluted non-radial MTs with a prominent sub-membrane array, typical for beta cells (Figure 16), KIF5B-depleted cells featured extra-dense MTs in the cell center and sparse reseeding MTs at the periphery (Figure 16B,C). Significant reduction of tubulin staining intensity at the cell periphery (Figure 16D) confirms the robustness of this phenotype. This indicated that loss of KIF5B leads to a strong defect in microtubule location to the cell periphery.

Keeping in mind that KIF5B has additional major functions in addition to microtubule sliding, we sought to test the consequence of microtubule sliding more directly by overexpression of the KIFDN constructs. We first transfected MIN6 cells with either the $KIFDN^{wt}$ or $KIFDN^{mut}$ tail domains either alone. We then co-expressed either tail domain and heterodimerized with the motor domain (*Figure 17* A-E). Cells were fixed and immunostained for tubulin to identify the microtubule network. Interestingly, over-expression combinations that led to impaired microtubule sliding (specifically, $KIFDN^{wt}$ and $KIFDN^{mut}$ heterodimerized with the motor, see Figure 15B,D,G) also resulted in decreased peripheral tubulin intensity (*Figure 17*A,D,E). Combined, these data indicate that KIF5B-driven microtubule sliding is critical for populating the beta cell periphery with MTs, likely via redistribution of centrally nucleated MTs.

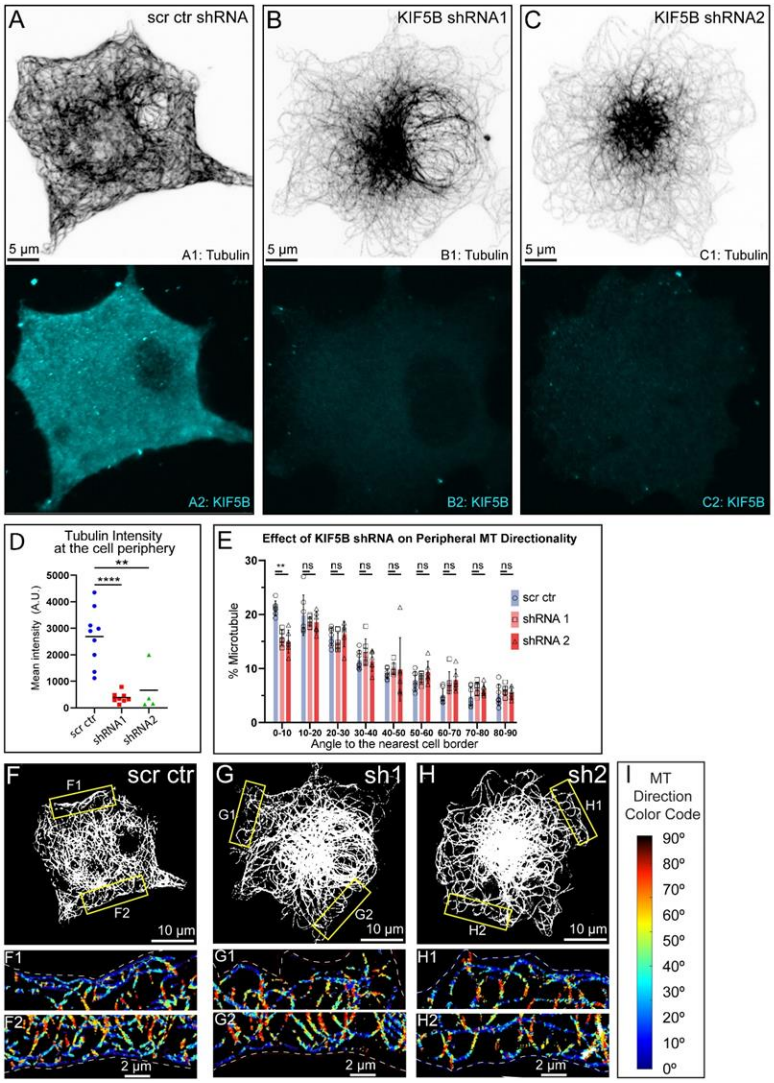

Figure legend on next page

Figure 16. Microtubule abundance and alignment at the cell periphery depend on KIF5B

(A-C) MT organization in MIN6 cells expressing scrambled control shRNA (A), KIF5B-targeting shRNA #1 (B), or KIF5B-targeting shRNA #2 (C). Top, immunofluorescence staining for tubulin (grayscale, inverted). Bottom, immunofluorescence staining for Kif5B (cyan). Laser scanning confocal microscopy maximum intensity projection of 1µm at the ventral side of the cell. N=12. Scale bars: 5um. (D) Quantification of mean tubulin intensity within the outer 2µm peripheral area of a cell, in data represented in (A-C). Mean values, black bars. One-way ANOVA, $p<0.0001$. N=5-11 cells. (E) Histograms of MT directionality within 1um of cell boundary using perfected thresholds (see Supplemental figure 3/1 for the analysis workflow) in cells treated with scrambled control versus KIF5B-targeting shRNA. Data are shown for the summarized detectable tubulin-positive pixels in the analyzed shRNA-treated cell population, as represented in (F-H). Unpaired t-test were performed across each bin for all cells, and a Kolmogorov-Smirnov test was performed on the overall distribution $p<0.01$. The share of MTs parallel to the edge (bin 0-10) is significantly higher in control as compared to KIF5B depletions. Pixel numbers in the analysis: SCR N=106,780 pixels across 9 cells, shRNA#1 N=71,243 pixels across 8 cells, shRNA#2 N=45,569 across 8 cells. (F-H) Representative examples of MT directionality analysis quantified in (E). (F) Scrambled control shRNA-treated cell. (G) KIF5B shRNA #1-treated cell. (H) KIF5B shRNA#1-treated cell. Overviews of cellular MT networks are shown as threshold to detect individual peripheral MTs (see Supplemental figure 3/1 panel A5). (F1-H2) Directionality analysis outputs of regions from yellow boxes in (F-H) are shown color-coded for the angles between MTs and the nearest cell border (see Supplemental figure 4/1 panel A8). (I) Color code for (F1-H2): MTs parallel to the cell edge, blue; MTs perpendicular to the cell edge, red.

KIF5B is required for beta-cell sub-membrane microtubule array alignment

Given the known significance of the peripheral microtubule array, which normally consists of well-organized MTs parallel to the cell membrane (Bracey et al., 2020), we have further analyzed directionally of MTs remaining at the cell periphery after KIF5B depletion. Previously we published a custom image analysis algorithm (Bracey et al., 2020) allowing for detailed quantitative characterization of MTs directionality in relation to the nearest cell border (Figure 19 Supplemental Fig. 1). Here we applied the same computational analysis to microtubule imaging data in MIN6 cells with perturbed KIF5B level and/or function. After deconvolution for increased signal-to-noise ratio, single 2D slices of microtubule images were subjected to thresholding and the directionality of MTs was determined with respect to the cell border. Every pixel of the image was analyzed with inconclusive pixels disregarded. Subsequently, microtubule directionality was quantified as a function of the distance from the cell border within 1 µm of the cell border. Our results indicate that in non-targeting control (Figure 16E,F) as well as in non-transfected cells (Figure 17F,G), the distribution of microtubule angles in the cell periphery are vastly parallel and co-aligned with the cell boundary, as previously reported for islet beta cells (Bracey et al. 2019). In contrast, the loss of KIF5B via shRNA depletion (Figure 16E,G,H) or block of microtubule sliding by overexpression of mutant heterodimerized kinesin-1 ($KIFDN^{mut}$ heterodimerized with the motor, Figure 17F,I) resulted in a significant loss of parallel MTs at the periphery. This indicated that microtubule sliding by KIF5B acts to align microtubule at the cell periphery in addition to delivering MTs to this cell location. Interestingly, overexpression of functional heterodimerized motor, which was capable of microtubule sliding and populating of the cell periphery with MTs ($KIFDN^{wt}$ heterodimerized with the motor, Figure 17F,H) also led to a deficient microtubule aligning at the periphery. This can be interpreted as a result of unregulated sliding in this experimental condition and suggests that proper organization of MTs within the sub-membrane array requires fine tuning of microtubule sliding activity.

Combined our data demonstrate a dramatic effect of KIF5B perturbation on both the distribution of MTs to the cell periphery and their orientation along the cell boundary. These data suggest that KIF5B-driven microtubule sliding is a decisive mechanism of the sub-membrane microtubule array generation, likely via redistribution of centrally nucleated MTs and subsequent aligning them at the cell edge. Thus, microtubule sliding is likely a critical component in functional microtubule organization in beta cells.

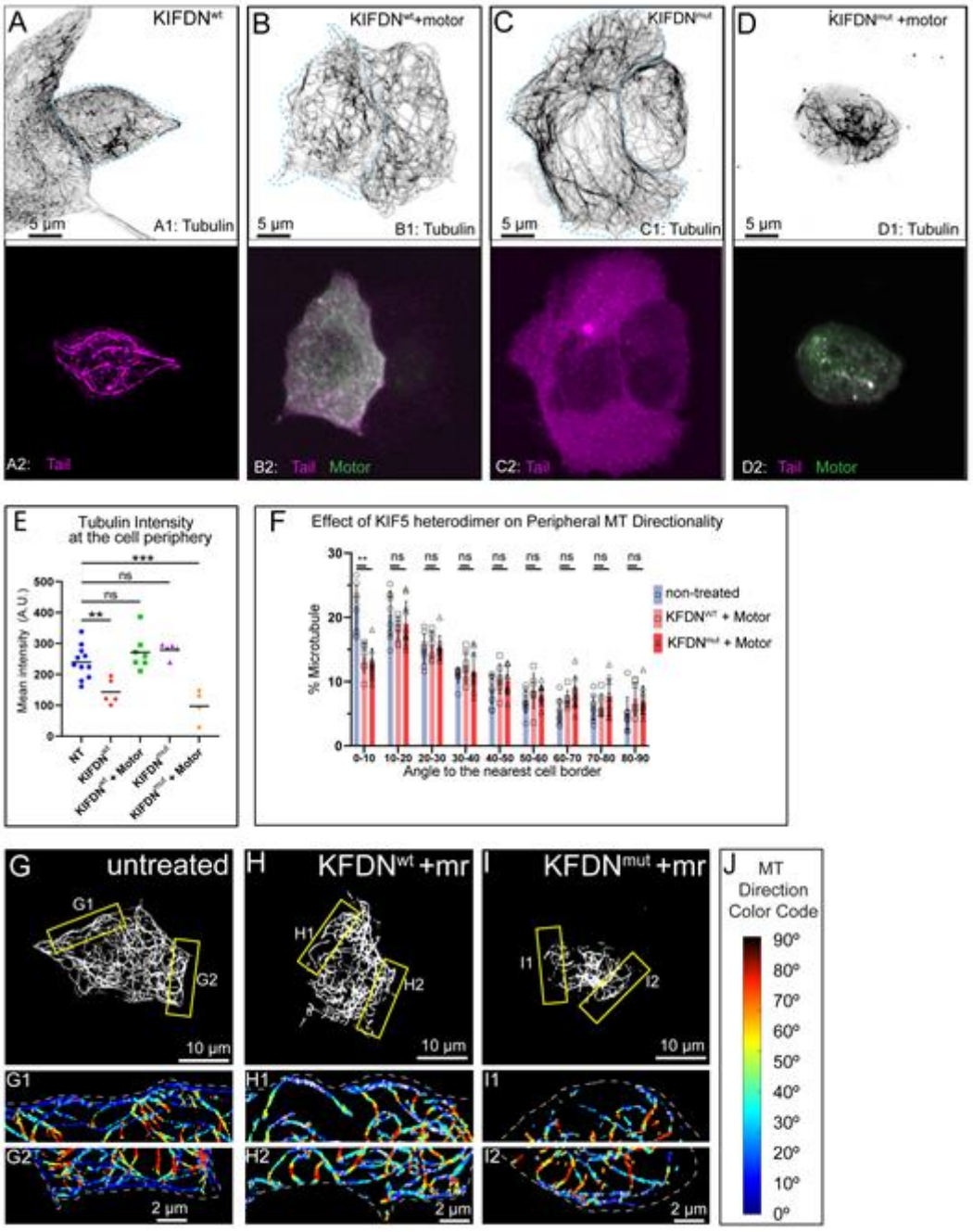

Figure legend on next page

Figure 17. Microtubule abundance and alignment at the cell periphery is impaired by dominant-negative perturbation of MT sliding.
(A-D) MT organization in MIN6 cells expressing (A) KIFDN^{wt}, (B) KIFDN^{mut}, (C) KIFDN^{wt} and KIF5C motor heterodimerized via rapalog treatment, (D) KIFDN^{mut} and KIF5C motor heterodimerized via rapalog treatment. Top, immunofluorescence staining for tubulin (grayscale, inverted). Blue dotted line indicates the borders of a cell expressing constructs of interest. Bottom, ectopically expressed mCherry-labeled KIFDN constructs (magenta) and BFP-labeled KIF5C motor (green). Laser scanning confocal microscopy maximum intensity projection of 1µm at the ventral side of the cell. Scale bars: 5um. (E) Quantification of mean tubulin intensity within the outer 2µm peripheral area of a cell, in data represented in (A-D). Mean values, black bars. One-way ANOVA, $p<0.0001$. N=4-12 (F) Histograms of MT directionality within 1um of cell boundary (see Supplemental figure 19/1 for the analysis workflow) in control cells compared to cells expressing heterodimerized KIFDN variants. Data are shown for the summarized detectable tubulin-positive pixels in the analyzed shRNA-treated cell population, as represented in (G-I). Unpaired t-test were performed across each bin for all cells. The share of MTs parallel to the edge (bin 0-10) is significantly higher in control as compared to the over-expressions. NT N=138,810 pixels across 9 cells, KIFDN^{wt} +motor N=41,553 pixels across 7 cells, KIFDN^{mut} N=40,832 pixels across 8 cells. (G-I) Representative examples of MT directionality analysis quantified in (F). (G) Control cell, no ectopic expressions. (H) Cell expressing KIFDN^{wt}+ Motor. (I) Cell expressing KIFDN^{mut}+ Motor. Overviews of cellular MT networks are shown as threshold to detect individual peripheral MTs (see Supplemental figure 19/1 panel A5). (G1-I2) Directionality analysis outputs of regions from yellow boxes in (G-I) are shown color-coded for the angles between MTs and the nearest cell border (see Supplemental figure 19/1 panel A8). (J) Color code for (G1-I2): MTs parallel to the cell edge, blue; MTs perpendicular to the cell edge, red.

Microtubule sliding in beta cells is activated by glucose stimulation

It has previously been reported that kinesin-1 switches activity level in the presence of glucose stimulation (Donelan et al., 2002). We predicted that as Kif5b activity changes in the cell so would the trafficking of various cargoes. Thus MT sliding would also change depending on the glucose concentration. To test this idea, we pre-incubated MIN6 cells with media containing a low concentration (2.8 mM) glucose (*Figure 18*A). We applied the photobleaching assay and detected little to no microtubule sliding events. However, at a high concentration of 20 mM glucose, microtubule sliding and remodeling events were significantly increased (*Figure 18*B). Quantification of sliding events demonstrated that MIN6 displaced MTs via microtubule sliding significantly more efficiently with high glucose stimulation (*Figure 18*). We then turned to single molecule tracking of microtubule lattice fiducial marks (K560Rigor^{E236A}-SunTag) to further investigate this observation. Consistent with the photobleaching assay, the fiducial marks were predominantly stationary in cells pre-incubated in 2.8 mM glucose (*Figure 18* D) but frequently underwent directed relocation events indicative of microtubule sliding in cells after stimulated with 20 mM glucose (*Figure 18* E). Normalized displacements of > 5 seconds showed an increase in cells treated with 20 mM glucose. We note that with 2.8 mM glucose, there were significantly more fiducial marks with < 0.15 um displacement in 5s intervals. In addition, the sub fraction of MTs that were displaced greater than 0.3 um were increased in high glucose conditions (Figure 18 H)

These data collectively demonstrate that glucose-stimulated remodeling of the microtubule network involves regulated microtubule sliding. Given the importance of microtubule sliding for peripheral microtubule organization (Figures 16, 17), this effect may be essential to restore peripheral microtubule array after glucose-dependent destabilization or regulate other aspects of MT-dependent tuning of GSIS.

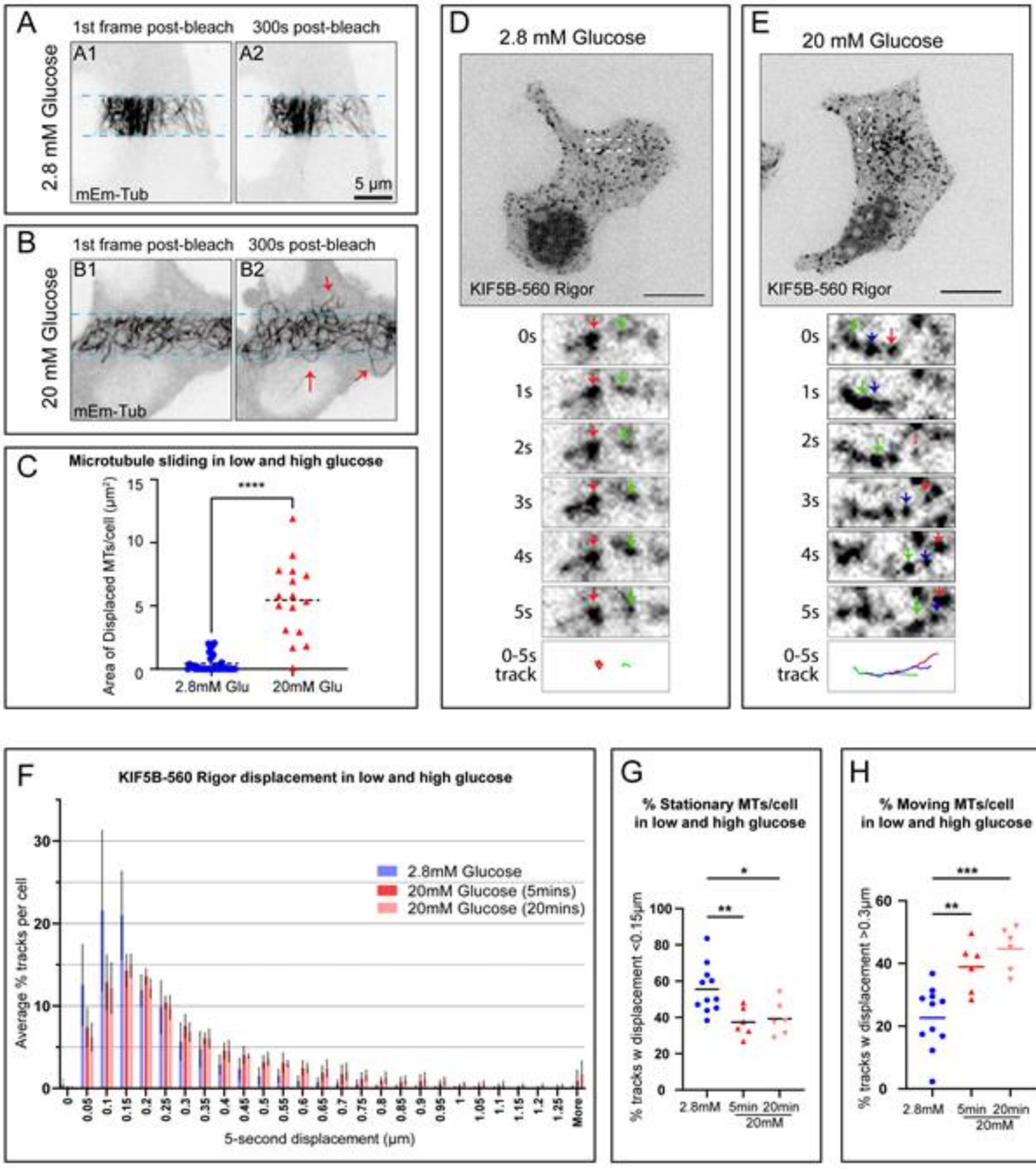

Figure legend on next page

Figure 18. MT sliding in beta cells is stimulated by glucose.

(**A-B**) Frames from representative FRAP live-cell imaging sequences of MT sliding response to glucose stimulation. mEmerald-tubulin-expressing MIN6 cells. Inverted grayscale images of maximum intensity projections over 1 µm-thick stacks by spinning disk confocal microscopy. (**A**) A cell pretreated with 2.8 mM glucose before the assay. (**B**) A cell pretreated with 2.8 mM glucose and stimulated with 20 mM glucose before the assay. (**A1-B1**) The first frame after photobleaching. (**A2-B2**) A frame 5 minutes (300 seconds) after photobleaching. Light-blue dotted lines indicate the edges of the photobleached areas. Red arrows indicate MTs displaced into the bleached area. Scale bars, 5 µm. (**C**) Quantification of MT sliding FRAP assay in cells in 2.8 mM versus 20 mM glucose (see representative data in A-B). MT displacement is shown as area of MTs displaced into the bleached area after 5 minutes of recovery. One-way ANOVA test was performed for statistical significance (p-value <0.0001). N=6-11 cells per set. (**D-E**) MIN6 cells featuring fiducial marks at MTs due to co-expression of SunTag-KIF5B-560Rigor construct and Halo-SunTag ligand. Representative examples for cells in 2.8 mM glucose (D) and a cell stimulated by 20 mM glucose (E) are shown. Single-slice spinning disk confocal microscopy. Halo-tag signal is shown as inverted gray-scale image. Top panels show cell overviews (scale bars 5µm). Below, boxed insets are enlarged to show dynamics of fiducial marks (color arrows) at 1 second intervals (1-5 seconds). 0- to 5-second tracks of fiducial mark movement are shown in the bottom panel, each track color-coded corresponding to the arrows in the image sequences.

Discussion

Since the first description of a convoluted microtubule network in MIN6 cells by the Rutter group (Varadi et al., 2003), our views on regulation, function, and dynamics of pancreatic beta cell microtubule network have been gradually evolving (Bracey et al., 2022). However, the field is still far from understanding the mechanisms underlying the network architecture. Here, we show that microtubule sliding is a prominent phenomenon in beta cells, that it is driven by kinesin KIF5B, that kinesin-1-dependent microtubule sliding is a critical mechanism needed for the formation and a long-term maintenance of beta cell microtubule network, especially the peripheral microtubule arrays, and that glucose stimulation facilitates microtubule sliding activity. Overall, our study establishes microtubule sliding as an essential regulator of beta cell architecture and function.

Our data indicate that microtubule sliding is activated on a short-term basis after stimulation. It is plausible to suggest that this is needed to replace MTs at the cell periphery that are destabilized in high glucose after MT-stabilizing protein tau is phosphorylated and detached from the sub-membrane MTs (Ho et al., 2020). However, the amount of microtubule polymer on every glucose stimulation changes only slightly, often undetectably (Muller et al., 2021; Zhu et al., 2015). In fact, we observe a prominent effect of peripheral microtubule loss only after a long-term kinesin depletion (three-four days). This is consistent with our observation that only a minor subset of microtubule is being moved at every stimulation. We assume that the loss of peripheral microtubule array in KIF5B-depleted cells in a manifestation of accumulated lack of sliding over an extended period.

Interestingly, blocking kinesin results in a striking accumulation of microtubules in the cell center where they are normally nucleated at MTOCs, which include the centrosome and the Golgi, in differentiated beta cells, the latter being the main MTOC. Thus, sliding MTs originate from the MTOC area. At the same time, FIB-SEM analysis did not detect many MTs associated with MTOCs in physiologically normal beta cells (Muller et al., 2021). This implicates that MTs are normally rapidly dissociated from MTOCs so that they become available for transport by sliding. It is worth mentioning that for long-distance transport by sliding, cargo MTs must be short, otherwise microtubule buckling and not long-distance transport will occur (Straube et al., 2006). Interestingly, shorter MTs have been observed in high glucose conditions (Muller et al., 2021), when microtubules are nucleated more actively (Trogden et al., 2019) and transported more frequently (this work). Possibly, nucleated MTs are detached from MTOCs before they achieve a length that would prevent their transport. There is a possibility suggested that MTs

are being severed by katanin in high glucose (Muller et al., 2021), which would generate microtubule fragments that can serve as cargos more easily. It is also possible that the sliding microtubule subpopulation has some additional, specific features that make them preferred cargos, since it is becoming increasingly clearer in the field that there is immense heterogeneity among MTs. Post-translational modifications and microtubule associated proteins, which vastly alter stability and coordination of motor proteins (Hammond et al., 2008; McKenney et al., 2016; Monroy et al., 2018; Yu et al., 2015), might also influence which MTs serve as cargos versus transportation tracks in beta cells.

On a final note, it is important to evaluate the phenomenon reported here in light of the dual role of KIF5B as IG transporter and microtubule transporter and the coordination of those two roles in IG transport and availability for secretion. Our results indicate that KIF5B is needed for the patterning of peripheral MTs which we have shown to restrict secretion (Bracey et al., 2020; Ho et al., 2020). At the same time, it is well established that KIF5B transports IGs (Varadi et al., 2002) and KIF5B loss of function impairs insulin secretion (Cui et al., 2011). After a prolonged KIF5B inactivation, a loss of peripheral readily-releasable IG should be expected due to two factors: because there is no microtubule bundle to prevent over-secretion and IG depletion, and because there are no new IGs being transported from the Golgi area. In contrast, physiological activation of kinesin by glucose (Donelan et al., 2002; Varadi et al., 2003) would both promote replenishment of IG through non-directional transport through the cytoplasm and restoration of peripheral microtubule array to prevent over-secretion on each stimulus.

In conclusion, here we add another very important cell type to the list of systems that employ KIF5-dependent microtubule sliding to build functional microtubule networks. This system is unique because in this case microtubule sliding is metabolically regulated and activated on a single-minute time scale by nutrition triggers.

Supplemental Figures

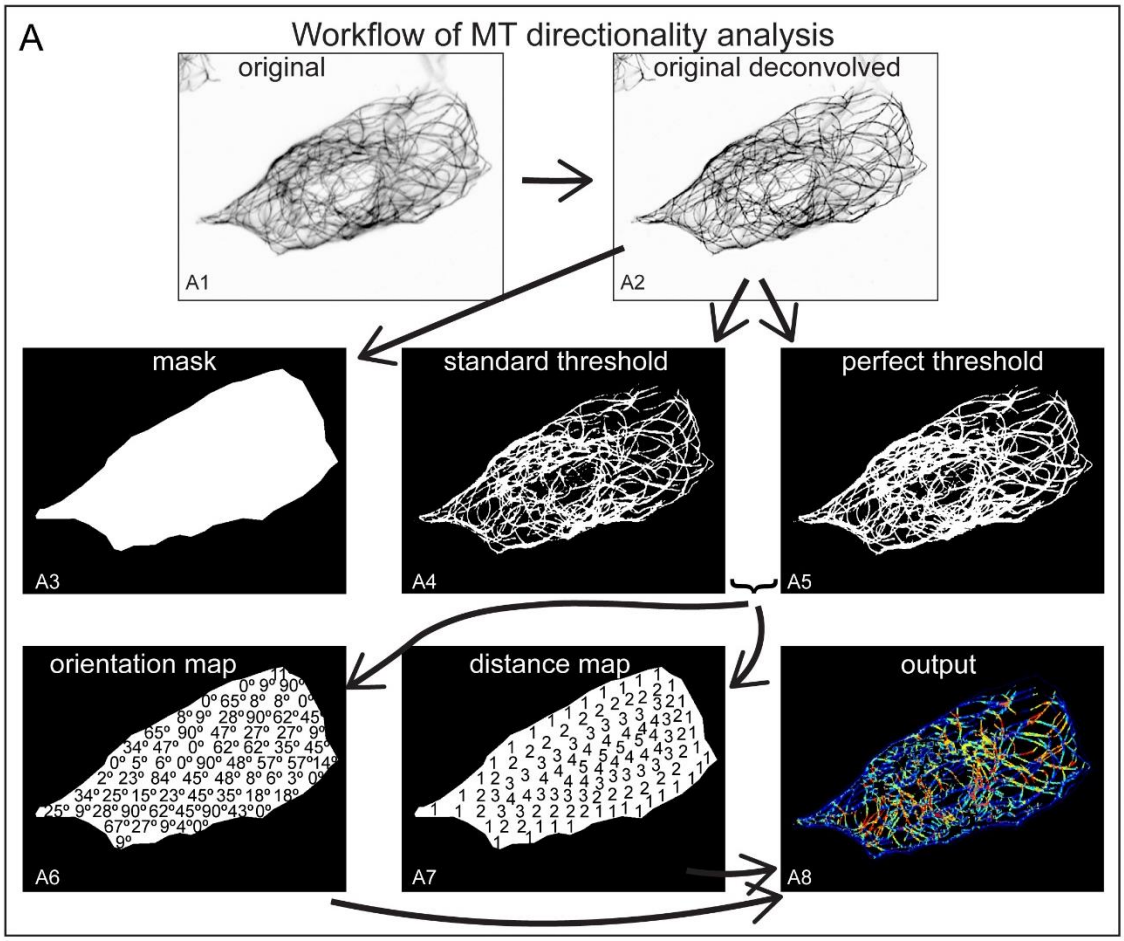

Figure 19. Supplemental Figure 1. Workflow of MT directionality analysis.

Supplemental Figure 1. Workflow of MT directionality analysis.

(**A**) Representation of the analysis workflow using a control DMSO-treated cell immunostained for tubulin as an example. (A1) An image of the original inverted grayscale confocal slice. (A2) A deconvolved image. (A3) Mask of the cell boundary. (A4) An image within the mask after application of standard % threshold. (A5) An image within the mask after application of a threshold optimizing detection of peripheral MTs for a particular cell. (A3-A5) are derivatives of (A2). (A6) A schematic illustrating map of angles per pixel (not to scale). (A7) A schematic illustrating map of distances from the nearest cell (mask) border per pixel (not to scale). A6 and A7 can be produced from A4 or A5. (A8) Color-coded output map of MT directionalities. A8 is a derivative of A6 and A7.

Chapter 5
Conclusion and future directions

The pancreatic beta cell is a widely studied model for regulated protein secretion and is of significant importance in the study of diabetes. In response to increased glucose concentrations, beta cells mobilize insulin-containing secretory vesicles to the cell surface, where they fuse with the plasma membrane to release insulin into the bloodstream. The delicate balance between GSIS from beta cells and insulin-stimulated effects on glucose metabolism in various cell types is essential for glucose homeostasis.

Beta cells contain a large number of insulin secretory granules, and acute glucose stimulation causes only a small percentage of these granules to undergo exocytosis. Both readily-releasable and reserve pools of granules contribute to insulin secretion. The readily-releasable pool has been classically considered as vesicles docked at the plasma membrane, while the reserve pool, which is important to replenish pools of IG is more abundant, and relies on microtubule-based transport to reach the cell surface. Microtubules play a crucial role in granule trafficking, although newly synthesized insulin is preferentially released, and aged insulin granules are targeted for degradation in lysosomes, suggesting that microtubules have a complicated role in granule trafficking.

Müller et al. used focused ion beam scanning electron microscopy (FIB-SEM) to study the effects of glucose stimulation on microtubules, IGs, and other organelles in whole primary mouse beta cells (Muller et al., 2021). The resulting 3D images supported the 2015 Zhu et al., finding that beta cell architecture is full of nonradial, and dense MTs. Additionally, the cytoskeleton was determined to be tortuous, and mostly not connected to either centrioles or the Golgi complex. This observation was interesting as the Golgi serves as the major MTOC in beta cells. We now know that the beta-cell microtubule network is built in a unique configuration. We also know that the microtubule network is remodeled downstream of glucose in such a way that both MT-dependent insulin biogenesis and secretion are allowed. Yet, mere microtubule presence serves as a negative regulator, adding to other “filter” mechanisms that prevent insulin over-secretion.

The FIB-SEM data indicate that the microtubule cytoskeleton negatively regulates insulin granule exocytosis in unstimulated cells. Glucose stimulation induced an approximately threefold increase in the number of microtubules and an approximately threefold decrease in the average length of each microtubule, indicating an important role for microtubules in positioning the granules for exocytosis. Although glucose did not cause any marked change in the

association of secretory granules with microtubules, the data suggest that glucose may promote budding of nascent secretory vesicles at the trans-Golgi network, which may be a direct effect or secondary to increased flux through the secretory pathway.

These studies do, however, suggest that there is a potential therapeutic merit in targeting the cytoskeleton to modulate *beta* cell function. Recent imaging demonstrated that increased microtubule density was found to correlate with decreased secretion in mouse models (Zhu et al., 2015). Additionally, in silico, a dense peripheral microtubule network interferes with the proper positioning of insulin granules for secretion. This result predicts that in fact, the link observed in mouse models may be causal, and interference with microtubule stability in *beta* cells might be used as an approach to increase insulin secretion efficiency. This idea is tempting because numerous MT-targeting small molecule compounds have already been considered or even used for cancer therapies.

Although individual beta cells can contain on the order of ~10,000 individual insulin granules, only a subset are secreted in response to glucose stimulation. Thus, at the cellular level, significant negative regulation of GSIS must be present. Alternative mechanisms by which microtubule dynamics contribute to this negative regulation are still to be discovered. As discussed in Chapter 2: there is the possibility of MTs near the cell periphery to actively transport IGs away from the cell membrane, or traction forces generated by MT-associated molecular motors prevent stable granule anchoring to the membrane, which is a precursor to exocytosis. Motor protein involvement of this higher order of regulation is of immediate interest as studies provided in Chapter 4 indicate that not only is Kinesin-1 is specifically activated by glucose to support GSIS (Donelan et al., 2002; Varadi et al., 2003), but is also involved in shaping the roadways necessary for secretion.

Microtubule sliding appears to be an essential regulator of beta cell architecture and function and our data indicate that MT sliding is activated on a short-term basis after stimulation. It is plausible to suggest that this is needed to replace MTs at the cell periphery that are destabilized in high glucose after MT-stabilizing protein tau is phosphorylated and detached from the sub-membrane MTs (Ho et al). However, the amount of microtubule polymer on every glucose stimulation changes only slightly, often undetectably (Muller et al., 2021; Zhu et al., 2015). Peripheral microtubule loss is observed only after a long-term depletion of kinesin (three to four days), indicating that only a minor subset of microtubules is being moved during each stimulation event. We propose that the loss of peripheral microtubule array in KIF5B-depleted cells is a manifestation of the accumulated lack of sliding over an extended period.

Exaggerated kinesin-dependent microtubule sliding has been shown to cause microtubule bundling and buckling into aberrant configurations (Straube et al., 2006). We predict the existence of a fine-tuning regulatory pathway that restricts the number of microtubule sliding events to meet the cell's needs.

Glucose stimulation remodels microtubule networks to promote insulin release, but the mechanisms underlying this process are not well understood. The observation that the majority of MTs are not attached to their MTOC suggests that MTs must be removed from their nucleation sites. The microtubule sliding hypothesis proposes that MT sliding allows beta cells to reshape their cytoskeleton. However, the mechanisms underlying the formation of smaller MT fragments remain a major point of discussion. Microtubule sliding events could be related to instances of dissociation from the MTOC.

Future Directions

These collective studies provide the framework for how beta cell architecture not only is structural but rather also functional. Additionally, this provides evidence for how motor proteins influence the cytoskeletal network. That being the case, a significant goal for future studies will be to determine how the sliding of microtubules is controlled by signaling pathways responsive to moment-by-moment challenges in the life of the beta cell. Also important is the need to develop new and better ways to image the sliding of microtubules, which remains a technical struggle given the three-dimensional shape of the beta cell and high density of microtubules. Finally, more needs to be done on the sliding and crosslinking of microtubules with actin filaments, which is of significant importance to many aspects of secretory machinery.

As further characterization of the beta cell architecture is pursued there are several questions that still remain elusive. Which microtubules are designated for MT sliding fates? As mentioned previously not all MTs are translocated, identifying the PTM(s) that prime this subpopulation is of interest. Not only are the PTM's on the microtubule important but also the PTMs that dictate the cargo load for Kineisin-1. Do certain PTMs prevent the KLC from associating and driving Kinesin into a MT sliding "mode". We also note that although previous work done by Donelan et al, 2009 supports this work we cannot rule out other signaling factors that influence MT sliding.

Kinesin-1 is the most highly expressed motor protein in these cells but additionally we would like to investigate if Kinesin-3, the second highest expressing motor protein, also plays a role in MT sliding in interphase.

Perhaps the most technically challenging question at hand is, “Does the length of the MT matter inside the cell?”. As MTs are being constantly reshaped and have so many dynamic properties one can’t help but ask if the length of the MT influences its ability to be transported. In beta cells we see that MTs are truncated in length upon glucose stimulation. Are these shorter MTs more actively transported? Lastly, how do the shorter MTs arise? Are MT severing enzymes such as katanin, involved?

Collectively, these work aides our understanding of MTs and how the formation of a specific microtubule network is mediated by at least one motor protein, Kif5b. To conclude, we are currently at an exciting nucleation point where increased understanding of microtubule organization and regulation will inform how GSIS is precisely tuned in endocrine islet beta cells. Future studies will illustrate how MT-regulators and motor proteins interact to maintain or alter the beta cell architecture which will lead to a better understanding of beta-cell function. As diabetic mice have previously been shown to have denser MT networks it is plausible that a similar phenomenon could be observed in human beta cells. This increased MT density could directly correlate with the loss of insulin secretion as the MT network can restrict insulin secretion. Overall the MT architecture is in a delicate balance to support proper beta cell structure of its roadways.

References:

Abderrahmani, A., G. Niederhauser, V. Plaisance, M.E. Roehrich, V. Lenain, T. Coppola, R. Regazzi, and G. Waeber. 2004. Complexin I regulates glucose-induced secretion in pancreatic beta-cells. *J Cell Sci*. 117:2239-2247.

Acar, S., D.B. Carlson, M.S. Budamagunta, V. Yarov-Yarovoy, J.J. Correia, M.R. Ninonuevo, W. Jia, L. Tao, J.A. Leary, J.C. Voss, J.E. Evans, and J.M. Scholey. 2013. The bipolar assembly domain of the mitotic motor kinesin-5. *Nat Commun*. 4:1343.

Akimoto, Y., G.W. Hart, L. Wells, K. Vosseller, K. Yamamoto, E. Munetomo, M. Ohara-Imaizumi, C. Nishiwaki, S. Nagamatsu, H. Hirano, and H. Kawakami. 2007. Elevation of the post-translational modification of proteins by O-linked N-acetylglucosamine leads to deterioration of the glucose-stimulated insulin secretion in the pancreas of diabetic Goto-Kakizaki rats. *Glycobiology*. 17:127-140.

Alejandro, E.U., B. Gregg, M. Blandino-Rosano, C. Cras-Meneur, and E. Bernal-Mizrachi. 2015. Natural history of beta-cell adaptation and failure in type 2 diabetes. *Mol Aspects Med*. 42:19-41.

Ananthanarayanan, V. 2016. Activation of the motor protein upon attachment: Anchors weigh in on cytoplasmic dynein regulation. *Bioessays*. 38:514-525.

Ando, D., N. Korabel, K.C. Huang, and A. Gopinathan. 2015. Cytoskeletal Network Morphology Regulates Intracellular Transport Dynamics. *Biophys J*. 109:1574-1582.

Arous, C., and P.A. Halban. 2015. The skeleton in the closet: actin cytoskeletal remodeling in beta-cell function. *Am J Physiol Endocrinol Metab*. 309:E611-620.

Avrahami, D., A. Klochendler, Y. Dor, and B. Glaser. 2017. Beta cell heterogeneity: an evolving concept. *Diabetologia*. 60:1363-1369.

Baas, P.W., and F.J. Ahmad. 1993. The transport properties of axonal microtubules establish their polarity orientation. *J Cell Biol*. 120:1427-1437.

Baas, P.W., and S. Lin. 2011. Hooks and comets: The story of microtubule polarity orientation in the neuron. *Dev Neurobiol*. 71:403-418.

Balasubramanian, N., D.W. Scott, J.D. Castle, J.E. Casanova, and M.A. Schwartz. 2007. Arf6 and microtubules in adhesion-dependent trafficking of lipid rafts. *Nat Cell Biol*. 9:1381-1391.

Balczon, R., K.A. Overstreet, R.P. Zinkowski, A. Haynes, and M. Appel. 1992. The identification, purification, and characterization of a pancreatic beta-cell form of the microtubule adenosine triphosphatase kinesin. *Endocrinology*. 131:331-336.

Barbier, P., O. Zejneli, M. Martinho, A. Lasorsa, V. Belle, C. Smet-Nocca, P.O. Tsvetkov, F. Devred, and I. Landrieu. 2019. Role of Tau as a Microtubule-Associated Protein: Structural and Functional Aspects. *Front Aging Neurosci*. 11:204.

Barlan, K., and V.I. Gelfand. 2017. Microtubule-Based Transport and the Distribution, Tethering, and Organization of Organelles. *Cold Spring Harb Perspect Biol*. 9.

Barlan, K., W. Lu, and V.I. Gelfand. 2013. The microtubule-binding protein ensconsin is an essential cofactor of kinesin-1. *Curr Biol*. 23:317-322.

Benninger, R.K.P., and V. Kravets. 2022. The physiological role of beta-cell heterogeneity in pancreatic islet function. *Nat Rev Endocrinol*. 18:9-22.

Bicek, A.D., E. Tuzel, A. Demtchouk, M. Uppalapati, W.O. Hancock, D.M. Kroll, and D.J. Odde. 2009. Anterograde microtubule transport drives microtubule bending in LLC-PK1 epithelial cells. *Mol Biol Cell*. 20:2943-2953.

Bogan, J.S. 2021. Granular detail of beta cell structures for insulin secretion. *J Cell Biol*. 220.

Bonnet, C., D. Boucher, S. Lazereg, B. Pedrotti, K. Islam, P. Denoulet, and J.C. Larcher. 2001. Differential binding regulation of microtubule-associated proteins MAP1A, MAP1B, and MAP2 by tubulin polyglutamylation. *J Biol Chem*. 276:12839-12848.

Bouchet, B.P., and A. Akhmanova. 2017. Microtubules in 3D cell motility. *J Cell Sci*. 130:39-50.

Boyd, A.E., 3rd, W.E. Bolton, and B.R. Brinkley. 1982. Microtubules and beta cell function: effect of colchicine on microtubules and insulin secretion in vitro by mouse beta cells. *J Cell Biol*. 92:425-434.
Bracey, K.M., G. Gu, and I. Kaverina. 2022. Microtubules in Pancreatic beta Cells: Convoluted Roadways Toward Precision. *Front Cell Dev Biol*. 10:915206.
Bracey, K.M., K.H. Ho, D. Yampolsky, G. Gu, I. Kaverina, and W.R. Holmes. 2020. Microtubules Regulate Localization and Availability of Insulin Granules in Pancreatic Beta Cells. *Biophys J*. 118:193-206.
Brissova, M., M. Shiota, W.E. Nicholson, M. Gannon, S.M. Knobel, D.W. Piston, C.V. Wright, and A.C. Powers. 2002. Reduction in pancreatic transcription factor PDX-1 impairs glucose-stimulated insulin secretion. *J Biol Chem*. 277:11225-11232.
Brouhard, G.J., and L.M. Rice. 2018. Microtubule dynamics: an interplay of biochemistry and mechanics. *Nat Rev Mol Cell Biol*. 19:451-463.
Bryantseva, S.A., and O.N. Zhapparova. 2012. Bidirectional transport of organelles: unity and struggle of opposing motors. *Cell Biol Int*. 36:1-6.
Byers, H.R., K. Fujiwara, and K.R. Porter. 1980. Visualization of microtubules of cells in situ by indirect immunofluorescence. *Proc Natl Acad Sci U S A*. 77:6657-6661.
Canty, J.T., and A. Yildiz. 2020. Activation and Regulation of Cytoplasmic Dynein. *Trends Biochem Sci*. 45:440-453.
Cao, Y., J. Lipka, R. Stucchi, M. Burute, X. Pan, S. Portegies, R. Tas, J. Willems, L. Will, H. MacGillavry, M. Altelaar, L.C. Kapitein, M. Harterink, and C.C. Hoogenraad. 2020. Microtubule Minus-End Binding Protein CAMSAP2 and Kinesin-14 Motor KIFC3 Control Dendritic Microtubule Organization. *Curr Biol*. 30:899-908 e896.
Chatterjee Bhowmick, D., M. Ahn, E. Oh, R. Veluthakal, and D.C. Thurmond. 2021. Conventional and Unconventional Mechanisms by which Exocytosis Proteins Oversee beta-cell Function and Protection. *Int J Mol Sci*. 22.
Chaudhary, A.R., F. Berger, C.L. Berger, and A.G. Hendricks. 2018. Tau directs intracellular trafficking by regulating the forces exerted by kinesin and dynein teams. *Traffic*. 19:111-121.
Corthesy-Theulaz, I., A. Pauloin, and S.R. Pfeffer. 1992. Cytoplasmic dynein participates in the centrosomal localization of the Golgi complex. *J Cell Biol*. 118:1333-1345.
Cui, J., Z. Wang, Q. Cheng, R. Lin, X.M. Zhang, P.S. Leung, N.G. Copeland, N.A. Jenkins, K.M. Yao, and J.D. Huang. 2011. Targeted inactivation of kinesin-1 in pancreatic beta-cells in vivo leads to insulin secretory deficiency. *Diabetes*. 60:320-330.
Dean, P.M. 1973. Ultrastructural morphometry of the pancreatic -cell. *Diabetologia*. 9:115-119.
DeFronzo, R.A., E. Ferrannini, L. Groop, R.R. Henry, W.H. Herman, J.J. Holst, F.B. Hu, C.R. Kahn, I. Raz, G.I. Shulman, D.C. Simonson, M.A. Testa, and R. Weiss. 2015. Type 2 diabetes mellitus. *Nat Rev Dis Primers*. 1:15019.
Desai, A., and T.J. Mitchison. 1997. Microtubule polymerization dynamics. *Annu Rev Cell Dev Biol*. 13:83-117.
Devis, G., E. Van Obberghen, G. Somers, F. Malaisse-Lagae, L. Orci, and W.J. Malaisse. 1974. Dynamics of insulin release and microtubular-microfilamentous system. II. Effect of vincristine. *Diabetologia*. 10:53-59.
Dixit, R., J.L. Ross, Y.E. Goldman, and E.L. Holzbaur. 2008. Differential regulation of dynein and kinesin motor proteins by tau. *Science*. 319:1086-1089.
Dogterom, M., and T. Surrey. 2013. Microtubule organization in vitro. *Curr Opin Cell Biol*. 25:23-29.
Dominguez, R., and K.C. Holmes. 2011. Actin structure and function. *Annu Rev Biophys*. 40:169-186.
Donelan, M.J., G. Morfini, R. Julyan, S. Sommers, L. Hays, H. Kajio, I. Briaud, R.A. Easom, J.D. Molkentin, S.T. Brady, and C.J. Rhodes. 2002. Ca2+-dependent dephosphorylation of

kinesin heavy chain on beta-granules in pancreatic beta-cells. Implications for regulated beta-granule transport and insulin exocytosis. *J Biol Chem*. 277:24232-24242.
Efimov, A., A. Kharitonov, N. Efimova, J. Loncarek, P.M. Miller, N. Andreyeva, P. Gleeson, N. Galjart, A.R. Maia, I.X. McLeod, J.R. Yates, 3rd, H. Maiato, A. Khodjakov, A. Akhmanova, and I. Kaverina. 2007. Asymmetric CLASP-dependent nucleation of noncentrosomal microtubules at the trans-Golgi network. *Dev Cell*. 12:917-930.
Forth, S., and T.M. Kapoor. 2017. The mechanics of microtubule networks in cell division. *J Cell Biol*. 216:1525-1531.
Friedman, D.S., and R.D. Vale. 1999. Single-molecule analysis of kinesin motility reveals regulation by the cargo-binding tail domain. *Nat Cell Biol*. 1:293-297.
Fritsch, C.C., and J. Langowski. 2012. Kinetic lattice Monte Carlo simulation of viscoelastic subdiffusion. *J Chem Phys*. 137:064114.
Fu, J., X. Dai, G. Plummer, K. Suzuki, A. Bautista, J.M. Githaka, L. Senior, M. Jensen, D. Greitzer-Antes, J.E. Manning Fox, H.Y. Gaisano, C.B. Newgard, N. Touret, and P.E. MacDonald. 2017. Kv2.1 Clustering Contributes to Insulin Exocytosis and Rescues Human beta-Cell Dysfunction. *Diabetes*. 66:1890-1900.
Fu, Z., E.R. Gilbert, and D. Liu. 2013. Regulation of insulin synthesis and secretion and pancreatic Beta-cell dysfunction in diabetes. *Curr Diabetes Rev*. 9:25-53.
Fukata, M., T. Watanabe, J. Noritake, M. Nakagawa, M. Yamaga, S. Kuroda, Y. Matsuura, A. Iwamatsu, F. Perez, and K. Kaibuchi. 2002. Rac1 and Cdc42 capture microtubules through IQGAP1 and CLIP-170. *Cell*. 109:873-885.
Gaisano, H.Y. 2017. Recent new insights into the role of SNARE and associated proteins in insulin granule exocytosis. *Diabetes Obes Metab*. 19 Suppl 1:115-123.
Galbraith, J.A., T.S. Reese, M.L. Schlief, and P.E. Gallant. 1999. Slow transport of unpolymerized tubulin and polymerized neurofilament in the squid giant axon. *Proc Natl Acad Sci U S A*. 96:11589-11594.
Gandasi, N.R., P. Yin, M. Omar-Hmeadi, E. Ottosson Laakso, P. Vikman, and S. Barg. 2018. Glucose-Dependent Granule Docking Limits Insulin Secretion and Is Decreased in Human Type 2 Diabetes. *Cell Metab*. 27:470-478 e474.
Gao, N., P. White, N. Doliba, M.L. Golson, F.M. Matschinsky, and K.H. Kaestner. 2007. Foxa2 controls vesicle docking and insulin secretion in mature Beta cells. *Cell Metab*. 6:267-279.
Garnham, C.P., and A. Roll-Mecak. 2012. The chemical complexity of cellular microtubules: tubulin post-translational modification enzymes and their roles in tuning microtubule functions. *Cytoskeleton (Hoboken)*. 69:442-463.
Ghiasi, S.M., T. Dahlby, C. Hede Andersen, L. Haataja, S. Petersen, M. Omar-Hmeadi, M. Yang, C. Pihl, S.E. Bresson, M.S. Khilji, K. Klindt, O. Cheta, M.J. Perone, B. Tyrberg, C. Prats, S. Barg, A. Tengholm, P. Arvan, T. Mandrup-Poulsen, and M.T. Marzec. 2019. Endoplasmic Reticulum Chaperone Glucose-Regulated Protein 94 Is Essential for Proinsulin Handling. *Diabetes*. 68:747-760.
Glater, E.E., L.J. Megeath, R.S. Stowers, and T.L. Schwarz. 2006. Axonal transport of mitochondria requires milton to recruit kinesin heavy chain and is light chain independent. *J Cell Biol*. 173:545-557.
Goodson, H.V., and E.M. Jonasson. 2018. Microtubules and Microtubule-Associated Proteins. *Cold Spring Harb Perspect Biol*. 10.
Grabham, P.W., G.E. Seale, M. Bennecib, D.J. Goldberg, and R.B. Vallee. 2007. Cytoplasmic dynein and LIS1 are required for microtubule advance during growth cone remodeling and fast axonal outgrowth. *J Neurosci*. 27:5823-5834.
Gundersen, G.G. 2002. Evolutionary conservation of microtubule-capture mechanisms. *Nat Rev Mol Cell Biol*. 3:296-304.

Gundersen, G.G., S. Khawaja, and J.C. Bulinski. 1987. Postpolymerization detyrosination of alpha-tubulin: a mechanism for subcellular differentiation of microtubules. *J Cell Biol*. 105:251-264.
Gupton, S.L., W.C. Salmon, and C.M. Waterman-Storer. 2002. Converging populations of f-actin promote breakage of associated microtubules to spatially regulate microtubule turnover in migrating cells. *Curr Biol*. 12:1891-1899.
Hammond, J.W., D. Cai, and K.J. Verhey. 2008. Tubulin modifications and their cellular functions. *Curr Opin Cell Biol*. 20:71-76.
Harada, A., Y. Takei, Y. Kanai, Y. Tanaka, S. Nonaka, and N. Hirokawa. 1998. Golgi vesiculation and lysosome dispersion in cells lacking cytoplasmic dynein. *J Cell Biol*. 141:51-59.
He, Y., F. Francis, K.A. Myers, W. Yu, M.M. Black, and P.W. Baas. 2005. Role of cytoplasmic dynein in the axonal transport of microtubules and neurofilaments. *J Cell Biol*. 168:697-703.
Heaslip, A.T., S.R. Nelson, A.T. Lombardo, S. Beck Previs, J. Armstrong, and D.M. Warshaw. 2014. Cytoskeletal dependence of insulin granule movement dynamics in INS-1 beta-cells in response to glucose. *PLoS One*. 9:e109082.
Herrmann, H., and U. Aebi. 2016. Intermediate Filaments: Structure and Assembly. *Cold Spring Harb Perspect Biol*. 8.
Hillen, T., D. White, G. de Vries, and A. Dawes. 2017. Existence and uniqueness for a coupled PDE model for motor-induced microtubule organization. *J Biol Dyn*. 11:294-315.
Hinnen, D. 2017. Glucagon-Like Peptide 1 Receptor Agonists for Type 2 Diabetes. *Diabetes Spectr*. 30:202-210.
Hirokawa, N., Y. Noda, Y. Tanaka, and S. Niwa. 2009. Kinesin superfamily motor proteins and intracellular transport. *Nat Rev Mol Cell Biol*. 10:682-696.
Ho, K.H., X. Yang, A.B. Osipovich, O. Cabrera, M.L. Hayashi, M.A. Magnuson, G. Gu, and I. Kaverina. 2020. Glucose Regulates Microtubule Disassembly and the Dose of Insulin Secretion via Tau Phosphorylation. *Diabetes*. 69:1936-1947.
Hoboth, P., A. Muller, A. Ivanova, H. Mziaut, J. Dehghany, A. Sonmez, M. Lachnit, M. Meyer-Hermann, Y. Kalaidzidis, and M. Solimena. 2015. Aged insulin granules display reduced microtubule-dependent mobility and are disposed within actin-positive multigranular bodies. *Proc Natl Acad Sci U S A*. 112:E667-676.
Hofling, F., and T. Franosch. 2013. Anomalous transport in the crowded world of biological cells. *Rep Prog Phys*. 76:046602.
Hollenbeck, P.J., and J.A. Swanson. 1990. Radial extension of macrophage tubular lysosomes supported by kinesin. *Nature*. 346:864-866.
Holmes, W.R. 2019. Subdiffusive Dynamics Lead to Depleted Particle Densities near Cellular Borders. *Biophys J*. 116:1538-1546.
Hou, J.C., L. Min, and J.E. Pessin. 2009. Insulin granule biogenesis, trafficking and exocytosis. *Vitam Horm*. 80:473-506.
Hu, R., X. Zhu, M. Yuan, K.H. Ho, I. Kaverina, and G. Gu. 2021. Microtubules and Galphao-signaling modulate the preferential secretion of young insulin secretory granules in islet beta cells via independent pathways. *PLoS One*. 16:e0241939.
Huang, C., E.M. Walker, P.K. Dadi, R. Hu, Y. Xu, W. Zhang, T. Sanavia, J. Mun, J. Liu, G.G. Nair, H.Y.A. Tan, S. Wang, M.A. Magnuson, C.J. Stoeckert, Jr., M. Hebrok, M. Gannon, W. Han, R. Stein, D.A. Jacobson, and G. Gu. 2018. Synaptotagmin 4 Regulates Pancreatic beta Cell Maturation by Modulating the Ca(2+) Sensitivity of Insulin Secretion Vesicles. *Dev Cell*. 45:347-361 e345.
Huang, X.F., and P. Arvan. 1995. Intracellular transport of proinsulin in pancreatic beta-cells. Structural maturation probed by disulfide accessibility. *J Biol Chem*. 270:20417-20423.

Hudish, L.I., J.E. Reusch, and L. Sussel. 2019. beta Cell dysfunction during progression of metabolic syndrome to type 2 diabetes. *J Clin Invest*. 129:4001-4008.
Idevall-Hagren, O., and A. Tengholm. 2020. Metabolic regulation of calcium signaling in beta cells. *Semin Cell Dev Biol*. 103:20-30.
Inobe, T., and N. Nukina. 2016. Rapamycin-induced oligomer formation system of FRB-FKBP fusion proteins. *J Biosci Bioeng*. 122:40-46.
Ishihara, H., T. Asano, K. Tsukuda, H. Katagiri, K. Inukai, M. Anai, M. Kikuchi, Y. Yazaki, J.I. Miyazaki, and Y. Oka. 1993. Pancreatic beta cell line MIN6 exhibits characteristics of glucose metabolism and glucose-stimulated insulin secretion similar to those of normal islets. *Diabetologia*. 36:1139-1145.
Janke, C., and M.M. Magiera. 2020. The tubulin code and its role in controlling microtubule properties and functions. *Nat Rev Mol Cell Biol*. 21:307-326.
Jolly, A.L., and V.I. Gelfand. 2010. Cytoplasmic microtubule sliding: An unconventional function of conventional kinesin. *Commun Integr Biol*. 3:589-591.
Jolly, A.L., H. Kim, D. Srinivasan, M. Lakonishok, A.G. Larson, and V.I. Gelfand. 2010. Kinesin-1 heavy chain mediates microtubule sliding to drive changes in cell shape. *Proc Natl Acad Sci U S A*. 107:12151-12156.
Jordens, I., M. Fernandez-Borja, M. Marsman, S. Dusseljee, L. Janssen, J. Calafat, H. Janssen, R. Wubbolts, and J. Neefjes. 2001. The Rab7 effector protein RILP controls lysosomal transport by inducing the recruitment of dynein-dynactin motors. *Curr Biol*. 11:1680-1685.
Kahn, S.E., M.E. Cooper, and S. Del Prato. 2014. Pathophysiology and treatment of type 2 diabetes: perspectives on the past, present, and future. *Lancet*. 383:1068-1083.
Kalwat, M.A., and D.C. Thurmond. 2013. Signaling mechanisms of glucose-induced F-actin remodeling in pancreatic islet beta cells. *Exp Mol Med*. 45:e37.
Kapitein, L.C., and C.C. Hoogenraad. 2011. Which way to go? Cytoskeletal organization and polarized transport in neurons. *Mol Cell Neurosci*. 46:9-20.
Kasai, K., T. Fujita, H. Gomi, and T. Izumi. 2008. Docking is not a prerequisite but a temporal constraint for fusion of secretory granules. *Traffic*. 9:1191-1203.
Khawaja, S., G.G. Gundersen, and J.C. Bulinski. 1988. Enhanced stability of microtubules enriched in detyrosinated tubulin is not a direct function of detyrosination level. *J Cell Biol*. 106:141-149.
Kliuchnikov, E., E. Klyshko, M.S. Kelly, A. Zhmurov, R.I. Dima, K.A. Marx, and V. Barsegov. 2022. Microtubule assembly and disassembly dynamics model: Exploring dynamic instability and identifying features of Microtubules' Growth, Catastrophe, Shortening, and Rescue. *Comput Struct Biotechnol J*. 20:953-974.
Kumar, P., K.S. Lyle, S. Gierke, A. Matov, G. Danuser, and T. Wittmann. 2009. GSK3beta phosphorylation modulates CLASP-microtubule association and lamella microtubule attachment. *J Cell Biol*. 184:895-908.
Kurasawa, Y., W.C. Earnshaw, Y. Mochizuki, N. Dohmae, and K. Todokoro. 2004. Essential roles of KIF4 and its binding partner PRC1 in organized central spindle midzone formation. *EMBO J*. 23:3237-3248.
Lacy, P.E. 1972. The secretion of insulin. *Diabetes*. 21:510.
Lacy, P.E. 1975. Endocrine secretory mechanisms. A review. *Am J Pathol*. 79:170-188.
Lappalainen, P., T. Kotila, A. Jegou, and G. Romet-Lemonne. 2022. Biochemical and mechanical regulation of actin dynamics. *Nat Rev Mol Cell Biol*. 23:836-852.
Li, G., E. Rungger-Brandle, I. Just, J.C. Jonas, K. Aktories, and C.B. Wollheim. 1994. Effect of disruption of actin filaments by Clostridium botulinum C2 toxin on insulin secretion in HIT-T15 cells and pancreatic islets. *Mol Biol Cell*. 5:1199-1213.

Li, X., O.A. Itani, L. Haataja, K.J. Dumas, J. Yang, J. Cha, S. Flibotte, H.J. Shih, C.E. Delaney, J. Xu, L. Qi, P. Arvan, M. Liu, and P.J. Hu. 2019. Requirement for translocon-associated protein (TRAP) alpha in insulin biogenesis. *Sci Adv*. 5:eaax0292.
Lindwall, G., and R.D. Cole. 1984. Phosphorylation affects the ability of tau protein to promote microtubule assembly. *J Biol Chem*. 259:5301-5305.
Lu, W., P. Fox, M. Lakonishok, M.W. Davidson, and V.I. Gelfand. 2013. Initial neurite outgrowth in Drosophila neurons is driven by kinesin-powered microtubule sliding. *Curr Biol*. 23:1018-1023.
Lu, W., and V.I. Gelfand. 2017. Moonlighting Motors: Kinesin, Dynein, and Cell Polarity. *Trends Cell Biol*. 27:505-514.
Lu, W., M. Lakonishok, and V.I. Gelfand. 2015. Kinesin-1-powered microtubule sliding initiates axonal regeneration in Drosophila cultured neurons. *Mol Biol Cell*. 26:1296-1307.
Lu, W., M. Winding, M. Lakonishok, J. Wildonger, and V.I. Gelfand. 2016. Microtubule-microtubule sliding by kinesin-1 is essential for normal cytoplasmic streaming in Drosophila oocytes. *Proc Natl Acad Sci U S A*. 113:E4995-5004.
Luini, A., A.A. Mironov, E.V. Polishchuk, and R.S. Polishchuk. 2008. Morphogenesis of post-Golgi transport carriers. *Histochem Cell Biol*. 129:153-161.
Lutz, E. 2001. Fractional Langevin equation. *Phys Rev E Stat Nonlin Soft Matter Phys*. 64:051106.
Maelfeyt, B., S.M.A. Tabei, and A. Gopinathan. 2019. Anomalous intracellular transport phases depend on cytoskeletal network features. *Phys Rev E*. 99:062404.
Malaisse-Lagae, F., M. Amherdt, M. Ravazzola, A. Sener, J.C. Hutton, L. Orci, and W.J. Malaisse. 1979. Role of microtubules in the synthesis, conversion, and release of (pro)insulin. A biochemical and radioautographic study in rat islets. *J Clin Invest*. 63:1284-1296.
Marx, A., A. Hoenger, and E. Mandelkow. 2009. Structures of kinesin motor proteins. *Cell Motil Cytoskeleton*. 66:958-966.
McDonald, A., S. Fogarty, I. Leclerc, E.V. Hill, D.G. Hardie, and G.A. Rutter. 2009. Control of insulin granule dynamics by AMPK dependent KLC1 phosphorylation. *Islets*. 1:198-209.
McKenney, R.J., W. Huynh, R.D. Vale, and M. Sirajuddin. 2016. Tyrosination of alpha-tubulin controls the initiation of processive dynein-dynactin motility. *EMBO J*. 35:1175-1185.
Meng, Y.X., G.W. Wilson, M.C. Avery, C.H. Varden, and R. Balczon. 1997. Suppression of the expression of a pancreatic beta-cell form of the kinesin heavy chain by antisense oligonucleotides inhibits insulin secretion from primary cultures of mouse beta-cells. *Endocrinology*. 138:1979-1987.
Miranda, M.A., J.F. Macias-Velasco, and H.A. Lawson. 2021. Pancreatic beta-cell heterogeneity in health and diabetes: classes, sources, and subtypes. *Am J Physiol Endocrinol Metab*. 320:E716-E731.
Mitchison, T., and M. Kirschner. 1984. Dynamic instability of microtubule growth. *Nature*. 312:237-242.
Miyazaki, J., K. Araki, E. Yamato, H. Ikegami, T. Asano, Y. Shibasaki, Y. Oka, and K. Yamamura. 1990. Establishment of a pancreatic beta cell line that retains glucose-inducible insulin secretion: special reference to expression of glucose transporter isoforms. *Endocrinology*. 127:126-132.
Monroy, B.Y., D.L. Sawyer, B.E. Ackermann, M.M. Borden, T.C. Tan, and K.M. Ori-McKenney. 2018. Competition between microtubule-associated proteins directs motor transport. *Nat Commun*. 9:1487.
Morfini, G., N. Schmidt, C. Weissmann, G. Pigino, and S. Kins. 2016. Conventional kinesin: Biochemical heterogeneity and functional implications in health and disease. *Brain Res Bull*. 126:347-353.

Mourad, N.I., M. Nenquin, and J.C. Henquin. 2011. Metabolic amplification of insulin secretion by glucose is independent of beta-cell microtubules. *Am J Physiol Cell Physiol*. 300:C697-706.
Muller, A., D. Schmidt, C.S. Xu, S. Pang, J.V. D'Costa, S. Kretschmar, C. Munster, T. Kurth, F. Jug, M. Weigert, H.F. Hess, and M. Solimena. 2021. 3D FIB-SEM reconstruction of microtubule-organelle interaction in whole primary mouse beta cells. *J Cell Biol*. 220.
Muroyama, A., and T. Lechler. 2017. Microtubule organization, dynamics and functions in differentiated cells. *Development*. 144:3012-3021.
Nasri, H., and M. Rafieian-Kopaei. 2014a. Metformin and diabetic kidney disease: a mini-review on recent findings. *Iran J Pediatr*. 24:565-568.
Nasri, H., and M. Rafieian-Kopaei. 2014b. Metformin: Current knowledge. *J Res Med Sci*. 19:658-664.
Nasteska, D., and D.J. Hodson. 2018. The role of beta cell heterogeneity in islet function and insulin release. *J Mol Endocrinol*. 61:R43-R60.
Nekooki-Machida, Y., and H. Hagiwara. 2020. Role of tubulin acetylation in cellular functions and diseases. *Med Mol Morphol*. 53:191-197.
Nessa, A., S.A. Rahman, and K. Hussain. 2016. Hyperinsulinemic Hypoglycemia - The Molecular Mechanisms. *Front Endocrinol (Lausanne)*. 7:29.
Nishimura, Y., K. Applegate, M.W. Davidson, G. Danuser, and C.M. Waterman. 2012. Automated screening of microtubule growth dynamics identifies MARK2 as a regulator of leading edge microtubules downstream of Rac1 in migrating cells. *PLoS One*. 7:e41413.
Odde, D.J., L. Ma, A.H. Briggs, A. DeMarco, and M.W. Kirschner. 1999. Microtubule bending and breaking in living fibroblast cells. *J Cell Sci*. 112 (Pt 19):3283-3288.
Oddoux, S., K.J. Zaal, V. Tate, A. Kenea, S.A. Nandkeolyar, E. Reid, W. Liu, and E. Ralston. 2013. Microtubules that form the stationary lattice of muscle fibers are dynamic and nucleated at Golgi elements. *J Cell Biol*. 203:205-213.
Ohara-Imaizumi, M., K. Aoyagi, and T. Ohtsuka. 2019. Role of the active zone protein, ELKS, in insulin secretion from pancreatic beta-cells. *Mol Metab*. 27S:S81-S91.
Olofsson, C.S., S.O. Gopel, S. Barg, J. Galvanovskis, X. Ma, A. Salehi, P. Rorsman, and L. Eliasson. 2002. Fast insulin secretion reflects exocytosis of docked granules in mouse pancreatic B-cells. *Pflugers Arch*. 444:43-51.
Olokoba, A.B., O.A. Obateru, and L.B. Olokoba. 2012. Type 2 diabetes mellitus: a review of current trends. *Oman Med J*. 27:269-273.
Omar-Hmeadi, M., and O. Idevall-Hagren. 2021. Insulin granule biogenesis and exocytosis. *Cell Mol Life Sci*. 78:1957-1970.
Palmer, K.J., P. Watson, and D.J. Stephens. 2005. The role of microtubules in transport between the endoplasmic reticulum and Golgi apparatus in mammalian cells. *Biochem Soc Symp*:1-13.
Pellegrini, F., and D.R. Budman. 2005. Review: tubulin function, action of antitubulin drugs, and new drug development. *Cancer Invest*. 23:264-273.
Pellinen, T., A. Arjonen, K. Vuoriluoto, K. Kallio, J.A. Fransen, and J. Ivaska. 2006. Small GTPase Rab21 regulates cell adhesion and controls endosomal traffic of beta1-integrins. *J Cell Biol*. 173:767-780.
Polishchuk, E.V., A. Di Pentima, A. Luini, and R.S. Polishchuk. 2003. Mechanism of constitutive export from the golgi: bulk flow via the formation, protrusion, and en bloc cleavage of large trans-golgi network tubular domains. *Mol Biol Cell*. 14:4470-4485.
Portran, D., L. Schaedel, Z. Xu, M. Thery, and M.V. Nachury. 2017. Tubulin acetylation protects long-lived microtubules against mechanical ageing. *Nat Cell Biol*. 19:391-398.
Proks, P., F. Reimann, N. Green, F. Gribble, and F. Ashcroft. 2002. Sulfonylurea stimulation of insulin secretion. *Diabetes*. 51 Suppl 3:S368-376.

Ramos, L.S., J.H. Zippin, M. Kamenetsky, J. Buck, and L.R. Levin. 2008. Glucose and GLP-1 stimulate cAMP production via distinct adenylyl cyclases in INS-1E insulinoma cells. *J Gen Physiol*. 132:329-338.
Ravindran, M.S., M.F. Engelke, K.J. Verhey, and B. Tsai. 2017. Exploiting the kinesin-1 molecular motor to generate a virus membrane penetration site. *Nat Commun*. 8:15496.
Reck-Peterson, S.L., W.B. Redwine, R.D. Vale, and A.P. Carter. 2018a. The cytoplasmic dynein transport machinery and its many cargoes. *Nat Rev Mol Cell Biol*. 19:382-398.
Reck-Peterson, S.L., W.B. Redwine, R.D. Vale, and A.P. Carter. 2018b. Publisher Correction: The cytoplasmic dynein transport machinery and its many cargoes. *Nat Rev Mol Cell Biol*. 19:479.
Renstrom, E., L. Eliasson, and P. Rorsman. 1997. Protein kinase A-dependent and -independent stimulation of exocytosis by cAMP in mouse pancreatic B-cells. *J Physiol*. 502 (Pt 1):105-118.
Rice, S., A.W. Lin, D. Safer, C.L. Hart, N. Naber, B.O. Carragher, S.M. Cain, E. Pechatnikova, E.M. Wilson-Kubalek, M. Whittaker, E. Pate, R. Cooke, E.W. Taylor, R.A. Milligan, and R.D. Vale. 1999. A structural change in the kinesin motor protein that drives motility. *Nature*. 402:778-784.
Rios, R.M. 2014. The centrosome-Golgi apparatus nexus. *Philos Trans R Soc Lond B Biol Sci*. 369.
Roll-Mecak, A. 2019. How cells exploit tubulin diversity to build functional cellular microtubule mosaics. *Curr Opin Cell Biol*. 56:102-108.
Roll-Mecak, A., and R.D. Vale. 2006. Making more microtubules by severing: a common theme of noncentrosomal microtubule arrays? *J Cell Biol*. 175:849-851.
Rorsman, P., and F.M. Ashcroft. 2018. Pancreatic beta-Cell Electrical Activity and Insulin Secretion: Of Mice and Men. *Physiol Rev*. 98:117-214.
Rorsman, P., and E. Renstrom. 2003. Insulin granule dynamics in pancreatic beta cells. *Diabetologia*. 46:1029-1045.
Roux, A., S. Gilbert, A. Loranger, and N. Marceau. 2016. Impact of keratin intermediate filaments on insulin-mediated glucose metabolism regulation in the liver and disease association. *FASEB J*. 30:491-502.
Sanchez, A.D., and J.L. Feldman. 2017. Microtubule-organizing centers: from the centrosome to non-centrosomal sites. *Curr Opin Cell Biol*. 44:93-101.
Sanders, A., K. Chang, X. Zhu, R.J. Thoppil, W.R. Holmes, and I. Kaverina. 2017. Nonrandom gamma-TuNA-dependent spatial pattern of microtubule nucleation at the Golgi. *Mol Biol Cell*. 28:3181-3192.
Sanders, A.A., and I. Kaverina. 2015. Nucleation and Dynamics of Golgi-derived Microtubules. *Front Neurosci*. 9:431.
Schmoranzer, J., J.P. Fawcett, M. Segura, S. Tan, R.B. Vallee, T. Pawson, and G.G. Gundersen. 2009. Par3 and dynein associate to regulate local microtubule dynamics and centrosome orientation during migration. *Curr Biol*. 19:1065-1074.
Seeger, M.A., and S.E. Rice. 2010. Microtubule-associated protein-like binding of the kinesin-1 tail to microtubules. *J Biol Chem*. 285:8155-8162.
Shang, Z., K. Zhou, C. Xu, R. Csencsits, J.C. Cochran, and C.V. Sindelar. 2014. High-resolution structures of kinesin on microtubules provide a basis for nucleotide-gated force-generation. *Elife*. 3:e04686.
Somers, G., E. Van Obberghen, G. Devis, M. Ravazzola, F. Malaisse-Lagae, and W.J. Malaisse. 1974. Dynamics of insulin release and microtubular-microfilamentous system. III. Effect of colchicine upon glucose-induced insulin secretion. *Eur J Clin Invest*. 4:299-305.
Song, Y., and S.T. Brady. 2015. Post-translational modifications of tubulin: pathways to functional diversity of microtubules. *Trends Cell Biol*. 25:125-136.

Spurlin, B.A., and D.C. Thurmond. 2006. Syntaxin 4 facilitates biphasic glucose-stimulated insulin secretion from pancreatic beta-cells. *Mol Endocrinol*. 20:183-193.
Stehbens, S.J., M. Paszek, H. Pemble, A. Ettinger, S. Gierke, and T. Wittmann. 2014. CLASPs link focal-adhesion-associated microtubule capture to localized exocytosis and adhesion site turnover. *Nat Cell Biol*. 16:561-573.
Stokes, A., and S.H. Preston. 2017. Deaths Attributable to Diabetes in the United States: Comparison of Data Sources and Estimation Approaches. *PLoS One*. 12:e0170219.
Straube, A., G. Hause, G. Fink, and G. Steinberg. 2006. Conventional kinesin mediates microtubule-microtubule interactions in vivo. *Mol Biol Cell*. 17:907-916.
Suter, B. 2018. RNA localization and transport. *Biochim Biophys Acta Gene Regul Mech*. 1861:938-951.
Swisa, A., B. Glaser, and Y. Dor. 2017. Metabolic Stress and Compromised Identity of Pancreatic Beta Cells. *Front Genet*. 8:21.
Tabei, S.M., S. Burov, H.Y. Kim, A. Kuznetsov, T. Huynh, J. Jureller, L.H. Philipson, A.R. Dinner, and N.F. Scherer. 2013a. Intracellular transport of insulin granules is a subordinated random walk. *Proc Natl Acad Sci U S A*. 110:4911-4916.
Tabei, S.M.A., S. Burov, H.Y. Kim, A. Kuznetsov, T. Huynh, J. Jureller, L.H. Philipson, A.R. Dinner, and N.F. Scherer. 2013b. Intracellular transport of insulin granules is a subordinated random walk. *Proceedings of the National Academy of Sciences of the United States of America*. 110:4911-4916.
Tan, R., A.J. Lam, T. Tan, J. Han, D.W. Nowakowski, M. Vershinin, S. Simo, K.M. Ori-McKenney, and R.J. McKenney. 2019. Microtubules gate tau condensation to spatially regulate microtubule functions. *Nat Cell Biol*. 21:1078-1085.
Tanenbaum, M.E., L.A. Gilbert, L.S. Qi, J.S. Weissman, and R.D. Vale. 2014. A protein-tagging system for signal amplification in gene expression and fluorescence imaging. *Cell*. 159:635-646.
Teitelman, G. 2019. Heterogeneous Expression of Proinsulin Processing Enzymes in Beta Cells of Non-diabetic and Type 2 Diabetic Humans. *J Histochem Cytochem*. 67:385-400.
Thurmond, D.C., and H.Y. Gaisano. 2020. Recent Insights into Beta-cell Exocytosis in Type 2 Diabetes. *J Mol Biol*. 432:1310-1325.
Thurmond, D.C., C. Gonelle-Gispert, M. Furukawa, P.A. Halban, and J.E. Pessin. 2003. Glucose-stimulated insulin secretion is coupled to the interaction of actin with the t-SNARE (target membrane soluble N-ethylmaleimide-sensitive factor attachment protein receptor protein) complex. *Mol Endocrinol*. 17:732-742.
Trogden, K.P., J. Lee, K.M. Bracey, K.H. Ho, H. McKinney, X. Zhu, G. Arpag, T.G. Folland, A.B. Osipovich, M.A. Magnuson, M. Zanic, G. Gu, W.R. Holmes, and I. Kaverina. 2021. Microtubules regulate pancreatic beta-cell heterogeneity via spatiotemporal control of insulin secretion hot spots. *Elife*. 10.
Trogden, K.P., X. Zhu, J.S. Lee, C.V.E. Wright, G. Gu, and I. Kaverina. 2019. Regulation of Glucose-Dependent Golgi-Derived Microtubules by cAMP/EPAC2 Promotes Secretory Vesicle Biogenesis in Pancreatic beta Cells. *Curr Biol*. 29:2339-2350 e2335.
Tseng, C.W., C. Masuda, R. Chen, and D.M. Hartung. 2020. Impact of Higher Insulin Prices on Out-of-Pocket Costs in Medicare Part D. *Diabetes Care*. 43:e50-e51.
Tsuboi, Y., T. Mishima, and S. Fujioka. 2021. Perry Disease: Concept of a New Disease and Clinical Diagnostic Criteria. *J Mov Disord*. 14:1-9.
Vale, R.D. 2003. The molecular motor toolbox for intracellular transport. *Cell*. 112:467-480.
van Obberghen, E., G. Somers, G. Devis, G.D. Vaughan, F. Malaisse-Lagae, L. Orci, and W.J. Malaisse. 1973. Dynamics of insulin release and microtubular-microfilamentous system. I. Effect of cytochalasin B. *J Clin Invest*. 52:1041-1051.

Varadi, A., E.K. Ainscow, V.J. Allan, and G.A. Rutter. 2002. Involvement of conventional kinesin in glucose-stimulated secretory granule movements and exocytosis in clonal pancreatic beta-cells. *J Cell Sci*. 115:4177-4189.
Varadi, A., and G.A. Rutter. 2002. Dynamic imaging of endoplasmic reticulum Ca2+ concentration in insulin-secreting MIN6 Cells using recombinant targeted cameleons: roles of sarco(endo)plasmic reticulum Ca2+-ATPase (SERCA)-2 and ryanodine receptors. *Diabetes*. 51 Suppl 1:S190-201.
Varadi, A., T. Tsuboi, L.I. Johnson-Cadwell, V.J. Allan, and G.A. Rutter. 2003. Kinesin I and cytoplasmic dynein orchestrate glucose-stimulated insulin-containing vesicle movements in clonal MIN6 beta-cells. *Biochem Biophys Res Commun*. 311:272-282.
Varadi, A., T. Tsuboi, and G.A. Rutter. 2005. Myosin Va transports dense core secretory vesicles in pancreatic MIN6 beta-cells. *Mol Biol Cell*. 16:2670-2680.
Veluthakal, R., and D.C. Thurmond. 2021. Emerging Roles of Small GTPases in Islet beta-Cell Function. *Cells*. 10.
Verhage, M., and J.B. Sorensen. 2008. Vesicle docking in regulated exocytosis. *Traffic*. 9:1414-1424.
Vershinin, M., B.C. Carter, D.S. Razafsky, S.J. King, and S.P. Gross. 2007. Multiple-motor based transport and its regulation by Tau. *Proc Natl Acad Sci U S A*. 104:87-92.
Vinogradova, T., P.M. Miller, and I. Kaverina. 2009. Microtubule network asymmetry in motile cells: role of Golgi-derived array. *Cell Cycle*. 8:2168-2174.
Vukusic, K., I. Ponjavic, R. Buda, P. Risteski, and I.M. Tolic. 2021. Microtubule-sliding modules based on kinesins EG5 and PRC1-dependent KIF4A drive human spindle elongation. *Dev Cell*. 56:1253-1267 e1210.
Wang, S., J.N. Jensen, P.A. Seymour, W. Hsu, Y. Dor, M. Sander, M.A. Magnuson, P. Serup, and G. Gu. 2009. Sustained Neurog3 expression in hormone-expressing islet cells is required for endocrine maturation and function. *Proc Natl Acad Sci U S A*. 106:9715-9720.
Wang, X., and T.L. Schwarz. 2009. The mechanism of Ca2+ -dependent regulation of kinesin-mediated mitochondrial motility. *Cell*. 136:163-174.
Wang, Z., and D.C. Thurmond. 2009. Mechanisms of biphasic insulin-granule exocytosis - roles of the cytoskeleton, small GTPases and SNARE proteins. *J Cell Sci*. 122:893-903.
Watanabe, T., S. Wang, J. Noritake, K. Sato, M. Fukata, M. Takefuji, M. Nakagawa, N. Izumi, T. Akiyama, and K. Kaibuchi. 2004. Interaction with IQGAP1 links APC to Rac1, Cdc42, and actin filaments during cell polarization and migration. *Dev Cell*. 7:871-883.
White, D., G. de Vries, J. Martin, and A. Dawes. 2015. Microtubule patterning in the presence of moving motor proteins. *J Theor Biol*. 382:81-90.
Wieczorek, M., S. Bechstedt, S. Chaaban, and G.J. Brouhard. 2015. Microtubule-associated proteins control the kinetics of microtubule nucleation. *Nat Cell Biol*. 17:907-916.
Wloga, D., E. Joachimiak, and H. Fabczak. 2017. Tubulin Post-Translational Modifications and Microtubule Dynamics. *Int J Mol Sci*. 18.
Woehlke, G., and M. Schliwa. 2000. Walking on two heads: the many talents of kinesin. *Nat Rev Mol Cell Biol*. 1:50-58.
Wu, J., and A. Akhmanova. 2017. Microtubule-Organizing Centers. *Annu Rev Cell Dev Biol*. 33:51-75.
Wu, J., C. de Heus, Q. Liu, B.P. Bouchet, I. Noordstra, K. Jiang, S. Hua, M. Martin, C. Yang, I. Grigoriev, E.A. Katrukha, A.F.M. Altelaar, C.C. Hoogenraad, R.Z. Qi, J. Klumperman, and A. Akhmanova. 2016. Molecular Pathway of Microtubule Organization at the Golgi Apparatus. *Dev Cell*. 39:44-60.
Yan, C., J. Jiang, Y. Yang, X. Geng, and W. Dong. 2022. The function of VAMP2 in mediating membrane fusion: An overview. *Front Mol Neurosci*. 15:948160.

Yang, W., Y. Tanaka, M. Bundo, and N. Hirokawa. 2014. Antioxidant signaling involving the microtubule motor KIF12 is an intracellular target of nutrition excess in beta cells. *Dev Cell*. 31:202-214.
Yarmola, E.G., T. Somasundaram, T.A. Boring, I. Spector, and M.R. Bubb. 2000. Actin-latrunculin A structure and function. Differential modulation of actin-binding protein function by latrunculin A. *J Biol Chem*. 275:28120-28127.
Yoon, S.O., S. Shin, and A.M. Mercurio. 2005. Hypoxia stimulates carcinoma invasion by stabilizing microtubules and promoting the Rab11 trafficking of the alpha6beta4 integrin. *Cancer Res*. 65:2761-2769.
Yu, I., C.P. Garnham, and A. Roll-Mecak. 2015. Writing and Reading the Tubulin Code. *J Biol Chem*. 290:17163-17172.
Yuan, T., L. Liu, Y. Zhang, L. Wei, S. Zhao, X. Zheng, X. Huang, J. Boulanger, C. Gueudry, J. Lu, L. Xie, W. Du, W. Zong, L. Yang, J. Salamero, Y. Liu, and L. Chen. 2015a. Diacylglycerol Guides the Hopping of Clathrin-Coated Pits along Microtubules for Exo-Endocytosis Coupling. *Dev Cell*. 35:120-130.
Yuan, T., J. Lu, J. Zhang, Y. Zhang, and L. Chen. 2015b. Spatiotemporal detection and analysis of exocytosis reveal fusion "hotspots" organized by the cytoskeleton in endocrine cells. *Biophys J*. 108:251-260.
Zaoui, K., K. Benseddik, P. Daou, D. Salaun, and A. Badache. 2010. ErbB2 receptor controls microtubule capture by recruiting ACF7 to the plasma membrane of migrating cells. *Proc Natl Acad Sci U S A*. 107:18517-18522.
Zhao, A., M. Ohara-Imaizumi, M. Brissova, R.K. Benninger, Y. Xu, Y. Hao, J. Abramowitz, G. Boulay, A.C. Powers, D. Piston, M. Jiang, S. Nagamatsu, L. Birnbaumer, and G. Gu. 2010. Galphao represses insulin secretion by reducing vesicular docking in pancreatic beta-cells. *Diabetes*. 59:2522-2529.
Zhu, X., N. Efimova, C. Arnette, S.K. Hanks, and I. Kaverina. 2016. Podosome dynamics and location in vascular smooth muscle cells require CLASP-dependent microtubule bending. *Cytoskeleton (Hoboken)*. 73:300-315.
Zhu, X., R. Hu, M. Brissova, R.W. Stein, A.C. Powers, G. Gu, and I. Kaverina. 2015. Microtubules Negatively Regulate Insulin Secretion in Pancreatic beta Cells. *Dev Cell*. 34:656-668.
Zhu, X., and I. Kaverina. 2013. Golgi as an MTOC: making microtubules for its own good. *Histochem Cell Biol*. 140:361-367.